University of Maribor

Faculty of Chemistry and
Chemical Engineering

Doctoral dissertation

FORMATION, CHARACTERIZATION AND APPLICATION OF POLYSACCHARIDE AEROGELS

March 2018

Gabrijela Horvat

University of Maribor

Faculty of Chemistry and Chemical Engineering

Gabrijela Horvat

FORMATION, CHARACTERIZATION AND APPLICATION OF POLYSACCHARIDE AEROGELS

Doctoral dissertation

Maribor, 2018

University of Maribor

Faculty of Chemistry and Chemical Engineering

FORMATION, CHARACTERIZATION AND APPLICATION OF POLYSACCHARIDE AEROGELS

Doctoral dissertation

Student: Gabrijela Horvat

Mentor: Prof Dr Željko Knez

Co-mentor: Prof Dr Zoran Novak

Maribor, 2018

CONTENTS

ACKNOWLEDGMENTS

During the last four years while working and then writing my PhD, a lot of people stood by my side. Here I would like to say a special thanks to all of those who participated and contributed to this work and without whom this thesis wouldn't exist.

Firstly, I am grateful to the Slovenian Research Agency for financial support and also to L'Oréal UNESCO, For Women in Science for a one-year scholarship.

A huge thank you goes to Prof Dr Željko Knez. Thank you for this opportunity, for believing in me before I even started and for your invaluable advice and help during this research.

I will be forever grateful to my co-mentor Prof Dr Zoran Novak, firstly, for introducing me to aerogel science and then for all the questions, concerns and doubts through which my knowledge has grown. Thank you for all the suggestions, for all the remarks, corrections and advice. Most of all, thank you for believing in me and for passing on your knowledge to me.

Many thanks to all of my co-workers from the Laboratory for Separation Processes and Product Design and others from the Faculty of Chemistry and Chemical Engineering. Thank you all for all the coffee breaks, much needed talks and jokes to enlighten my day, to cheer me up when I needed it most and, most important, for your support when it was the hardest. Milica, Alejandro, Nina, Amra, Roman, Tanja, Daša, Nina and Janja, Marko, Igor and Neven and everyone else - thank you!

There are not enough beautiful words in the world to describe how thankful I am for and to my family. My parents helped me through the years of my studies, as much financially as emotionally. They raised me into the person I am today, and for that I will be forever thankful. Thanks to my older sister Tanja and to Matej, and especially to Sofia and Aria for making my days easier and for cheering me up.

Thanks to all of my friends for every coffee, every walk, every talk and every laugh. I wouldn’t be who I am today without all of you.

The last words are for my husband, who has been there for me every day for the past 11 years. Thank you for supporting me, for always finding the right words, for encouraging me and most of all, for believing in me. Thank you for accepting me for who I am, with all my mistakes and weaknesses. Thank you for making my life wonderful.

And for you, the littlest of our family. For showing me the love I couldn’t know even existed. Forever.

If I have seen further than others,
it is by standing upon the
shoulders of giants.
-*Newton*

ABSTRACT

The aim of this PhD dissertation was to describe and analyze the preparation and characterization of polysaccharide aerogels and their future pharmaceutical and medical application. For the research, we used four types of polysaccharides: pectin, alginate, xanthan and guar. We used two types of pectin, high-methoxyl and low-methoxyl pectin, because of their different gelation mechanisms. The first part of the dissertation describes the preparation and characterization of pure polysaccharide aerogels. First, we prepared pectin spherical aerogels, cross-linked with three different ions, and we investigated their final properties. Later, we developed a new method for the preparation of alginate, pectin, xanthan and guar aerogels. We used only ethanol and no other cross-linkers. Ethanol was removed in the later processes of supercritical drying, and the remaining final material was thus only porous polysaccharide. By this method, we were able to prepare pure xanthan and guar aerogels. Prior to this study, xanthan and guar aerogels were prepared only as composites. Pectin aerogels prepared by the new method have amazing properties. On the other hand, alginate aerogels show poor characteristics, and thus the methods need to be optimised. We tried different alginate viscosities, different alcohols (methanol, ethanol, 1-propanol and 1-butanol), and we investigated longer (24h) and shorter (1h) gel setting times.

The second part of this dissertation describes the pharmaceutical and medical applications of prepared aerogels. The release of diclofenac sodium from spherical pectin aerogels was investigated *in vitro*. Calcium cross-linked aerogels were not able to retain the drug, and its release was immediate. In order to achieve controlled release of diclofenac sodium, zinc ions had to be used as cross-linkers. Later, a low water-soluble drug, nifedipine, was used as a model drug for the monolithic aerogels prepared by the new method. The release of nifedipine from pectin and alginate aerogels was highly increased, compared to the crystalline drug. This result is promising for future evaluation of these materials for increasing the bioavailability of poorly water-soluble drugs. Nifedipine release from xanthan and guar aerogels was prolonged up to two weeks. This result reveals a new perspective on such materials for their potential use in

medicine as implants and local drug delivery. According to these results, we then developed a new coating material for medical-grade stainless steel from xanthan and pectin. An aerogel coating was loaded with diclofenac sodium and indomethacin, and their release profiles were investigated *in vitro*. Electrochemical analysis and cell tests proved the safety of such materials for use in medicine. Using aerogel coatings, the drug can be introduced locally into the body; therefore, the need for intravenous, post-operational treatment is greatly reduced.

KEYWORDS: polysaccharides, aerogels, supercritical drying, drug carriers

UDK: 544.774.2:54-139(043.3)

POVZETEK

Cilj doktorske dizertacije je priprava, karakterizacija in aplikacija polisaharidnih aerogelov. Za pripravo aerogelov smo uporabili štiri polisaharide: pektin, alginat, ksantan in guar. Uporabili smo dve vrsti pektina, visokometilirani in nizkometilirani pektin, ki se med seboj razlikujeta po stopnji esterifikacije ter s tem tudi po načinu geliranja. V prvem delu raziskave smo se osredotočili na pripravo in karakterizacijo polisaharidnih aerogelov. Najprej smo pripravili pektinske aerogele ter preiskovali vpliv ionov na geliranje ter končne lastnosti materialov. Razvili smo enotno metodo za pripravo alginatnih, pektinskih, ksantan in guar aerogelov z dodatkom etanola ter brez dodatnih zamreževalcev. Prvič smo opisali pripravo čistih ksantan in guar aerogelov, ki so do sedaj bili pripravljeni samo kot kompoziti. Z novo metodo smo dosegli izjemne lastnosti pektinskih aerogelov. Pripravo alginatnih aerogelov smo zaradi slabših strukturnih lastnosti optimizirali. Tako smo uporabili tri različne viskoznosti alginata, metanol, etanol, 1-propranol in 1-butanol ter primerjali krajši (1 h) ter daljši (24 h) čas geliranja.

V drugem delu doktorske dizertacije smo raziskovali uporabo pripravljenih aerogelov kot nosilcev aktivnih učinkovin. Primerjali smo sproščanje doklofenak natrija iz pektinskih aerogelov, zamreženih z različnimi ioni in ugotovili, da je zamreževanje s kalcijem primerno, če želimo doseči takojšnje sproščanje učinkovine. Če želimo doseči podaljšano sproščanje, je primernejše zamreženje pektina s cinkovimi ioni. V nadaljevanju študije smo uporabili v vodi slabo topno učinkovino, nifedipin, ter jo vezali v monolitne polisaharidne aerogele, pripravljene po novi metodi. Ti nosilci so primerni za farmacevtske aplikacije, saj so pripravljeni samo iz polisaharida, brez dodatnih zamreževalcev. Tako je potencialni nosilec samo polisaharid v obliki visoko porozne strukture. Ugotovili smo, da se sproščanje nifedipina znatno poviša z vezavo na pektinske in alginatne aerogele v primerjavi s čisto učinkovino. Tako lahko dosežemo dosti višjo učinkovitost v vodi slabo topnih aktivnih učinkovin. Z vezavo na ksantan in guar aerogele je bilo sproščanje te učinkovine podaljšano do dveh tednov. Ta rezultat daje priložnost za aplikacijo takih aerogelov v medicini, morebiti za implantate ali za lokalno dostavo zdravil. V zadnjem delu smo pripravili kompozitni ksantan-pektin aerogel v obliki

prevleke na jeklo. Primerjali smo sproščanje dveh aktivnih učinkovin, indometacina ter diklofenak natrija. Elektrokemijske ter celične študije so potrdile varnost uporabe takih nosilcev v medicini. Z aerogelnimi prevlekami dosežemo direktni vnos zdravila na željeno mesto v telesu ter tako preprečimo kasnejša vnetja in bolečine, predvsem pa znižamo potrebo po intravenskem vnosu zdravil po operativnih posegih. Sproščanje obeh učinkovin iz ksantan-pektin aerogelov je bilo podaljšano do 6 h.

KLJUČNE BESEDE: polisaharidi, aerogeli, superkritično sušenje, nosilci zdravilnih učinkovin

UDK: 544.774.2:54-139(043.3)

TABLES

FIGURES

SYMBOLS

T_c	critical temperature
P_c	critical pressure
ρ_c	critical density
P/P_0	relative pressure
C_p	heat capacity
T_g	glass transition temperature
w_o	initial sample weight
w_1	sample weight after predetermined time
w_2	final drug weight
c	concentration of the drug after the selected time interval
V	volume of the release medium
m_t	final drug amount within the releasemedia
S_{BET}	specific surface area, determined by the BET method
ε	porosity
ρ_B	bulk density
ρ_T	true density
S	slope
Φ	heat flow

ΔT	the difference between the temperature of the sample at time t and the melting point of the metal (T_{onset}).
h	the sample height
A	the cross-sectional area
λ	thermal conductivity

ABBREVIATIONS

Al - Alginate

API - active pharmaceutical ingredient

AS - amplitude sweep

BET - Brunnauer-Emmet-Teller

BJH - Barrett-Joyner-Halenda

BTCA - butanetetracarboxylic dianhydride

CP - cyclic polarization

DCF - diclofenac sodium

DL - drug loading

DSC - differential scanning calorimetry

EE - entrapment efficiency

FESEM - field emission scanning electron microscopy

G - galuronate

G'' - loss modulus

G' - elastic modulus

GC - gas chromatography

GIT - gastrointestinal tract

Gu - Guar

H1 - hysteresis type 1

H2 - hysteresis type 2

H3 - hysteresis type 3

H4 - hysteresis type 4

hmP - high-methoxyl pectin

HPLC - high performance liquid chromatography

HS - headspace

IND - indomethacin

IUPAC - International Union of Pure and Applied Chemistry

lmP - low-methoxyl pectin

M - mannuronate

NSAID - non-steroidal anti-inflammatory drug

PBS - phosphate buffer solution

SEM - scanning electron microscope

SC - supercritical

SCF - supercritical fluid

SCI - supercritical impregnation

SD - standard deviation

SR - swelling ratio

TG - thermogravimetry

USP - United State Pharmacopoeia

Xa - Xanthan

DECLARATION OF ACADEMIC ACHIEVEMENT

The majority of the work described in this thesis was conceived, conducted, interpreted and written by the author of this thesis, with the following exceptions:

1. In Chapter 3, aerogels were prepared with the help of student Mitja Štumpf.
2. In Chapter 4 – optimisation process-- aerogels were prepared with the help of student Jan Štos.
3. In Chapter 4, the rheological measurements were performed by Anton Paar Ljubljana, Slovenia.
4. In Chapter 5, the release experiments of diclofenac sodium were performed with the help of student Mitja Štumpf, and the release experiments of nifedipine were performed with the help of student Maja Gračnar.
5. In Chapter 5, all electrochemical analyses were performed by Dr Matjaž Finšgar and Dr. Klodian Xhanari.
6. In Chapter 5, cell toxicity was performed by Dr Uroš Maver and Lidija Gradišnik.
7. All TGA and DSC analyses were performed with the help of Tanja Fajfar or Dr Maša Knez Hrnčič.
8. Bulk densities of aerogels were measured by Dr Muzafera Peljevac.
9. FE-SEM analyses were performed by Dr Tonica Bončina.
10. Mettler Toledo, Slovenia, provided help in developing the method for measuring thermal conductivity of aerogels.

AIMS OF THE THESIS

The research is based on optimising the method for the preparation of polysaccharide aerogels in order to achieve optimal properties for their later drug delivery application. The research is focused on the gelation mechanism of polysaccharides, mainly pectins but also alginate, xanthan and guar. The well-known gelation mechanism of pectin is first investigated and optimised by different cross-linking ions. The development of a new gelation method is essential for the fast and cost-effective production of various polysaccharide aerogels. The gelation mechanisms of pectin, alginate, xanthan and guar are studied in order to develop a new approach to the gelation of various water-soluble polysaccharides. Production of alcogels instead of hydrogels is crucial for the fast production of polysaccharide aerogels. Gelation parameters such as viscosity of the solution, gelation time, cross-linking agents, etc. are investigated. Structural properties of polysaccharides are essential for their application in drug delivery systems. Among those, swelling, available surface areas, pore volume and thermal stability have the greatest effect on drug encapsulation and release.

However, there are several limitations regarding polysaccharide gelation. Some of them (xanthan and guar) are known to produce gels only by co-bonding with other polysaccharides. The production of alcogels is limited on account of the water-solubility of the chosen polysaccharides. Supercritical drying is effective only if the water is almost completely removed from the gel; if not, structural collapse follows.

PUBLICATIONS

The work being described in this thesis is based on the following published articles:

1. HORVAT, Gabrijela, PANTIČ, Milica, KNEZ, Željko, NOVAK, Zoran. Encapsulation and drug release of poorly water soluble nifedipine from bio-carriers. *Journal of Non-Crystalline Solids*, 2018, 481, 486-493, 1A1, IF=2.124

2. HORVAT, Gabrijela, XHANARI, Klodian, FINŠGAR, Matjaž, GRADIŠNIK, Lidija, MAVER, Uroš, KNEZ, Željko, NOVAK, Zoran. Novel ethanol-induced pectin-xanthan aerogel coatings for orthopaedic applications. *Carbohydrate Polymers*, 2017, 166, 365-376, 1A1, IF=4.811

3. HORVAT, Gabrijela, KRANVOGL, Roman, PERVA-UZUNALIĆ, Amra, KNEZ, Željko, NOVAK, Zoran. Optimisation of critical parameters during alginate aerogels' production. *Journal of Non-Crystalline Solids*, 2016, 443, 112-117, 1A1, IF= 2.124

4. TKALEC, Gabrijela, FAJFAR, Tanja, PERVA-UZUNALIĆ, Amra, KNEZ, Željko, NOVAK, Zoran. Thermal properties of polysaccharide aerogels. *Journal of Thermal Analysis and Calorimetry*, 2016, 1-8, 1A2, IF=1.953

5. TKALEC, Gabrijela, KNEZ, Željko, NOVAK, Zoran. PH sensitive mesoporous materials for immediate or controlled release of NSAID. *Microporous and Mesoporous Materials*, 2016, vol. 224, 190-200, 1A1, IF=3.615

6. TKALEC, Gabrijela, KNEZ, Željko, NOVAK, Zoran. Encapsulation of pharmaceuticals into pectin aerogels for controlled drug release. *Advanced Technologies*, 2015, 4, 2, 49-52, 1NK

7. TKALEC, Gabrijela, KNEZ, Željko, NOVAK, Zoran. Fast production of high-methoxyl pectin aerogels for enhancing the bioavailability of low-soluble drugs. *The Journal of Supercritical Fluids*, 2015, 106, 16-22, 1A1, IF=2.579

8. TKALEC, Gabrijela, KNEZ, Željko, NOVAK, Zoran. Formation of polysaccharide aerogels in ethanol. *RSC Advances*, 2015, 5, 94, 77362-77371, 1A2, IF=3.289

9. VERONOVSKI, Anja, TKALEC, Gabrijela, KNEZ, Željko, NOVAK, Zoran. Characterisation of biodegradable pectin aerogels and their potential use as drug carriers. *Carbohydrate Polymers*, 2014, 113, 272-278, 1A1, IF=4.074

10. TKALEC, Gabrijela, PANTIČ, Milica, NOVAK, Zoran, KNEZ, Željko. Supercritical impregnation of drugs and supercritical fluid deposition of metals into aerogels. *Journal of Materials Scienc*e, 2015, 50, 1, 1-12, 1A2, IF=2.302

1 INTRODUCTION

The opening chapter of this dissertation provides an introduction into the world of aerogels. Aerogels are outstanding materials with high porosity and large surface areas. These materials can be roughly divided into two groups: inorganic and organic. Most organic aerogels are prepared from polysaccharides that have incredible gelling ability and are thus capable of forming a gel, which is further transformed into aerogel by a process called supercritical drying.

This introduction is based on the theory of polysaccharides, their gelation and transformation into advanced materials - aerogels. The focus is placed on pectin, alginate, xanthan and guar, which were used in the later research.

Polysaccharides are complex polymeric carbohydrate molecules. They are composed of monosaccharide units arranged in chains. Periodic units are bound together by glycosidic linkages. Polysaccharides belong to a class of biopolymers and are present in different forms, from linear to highly branched.

Table 1.1 Sources of food polysaccharides [1].

Polysaccharide	**Main sources**
Starch (amylose)	Cereal grains, tubers
Starch 8amylopectin)	Cereal, tubers
Modified starches	Corn kernels
Maltodextrins	Corn and potato starches
Carboxymethylcellulose	Cotton cellulose
Galactomannans	Seeds of guar, locust bean, tara
Carragenans	Red seaweeds
Agars	Red seaweeds
Gum Arabic	Stem exudate of Acacia Senegal
Gum Tragacanth	Astragalus spp.
Pectins	Citrus, apple, and other fruits
Alginates	Brown seaweeds
Xanthan gum	Xanthomonas campestris
Chitin, chitosan	Invertebrates, lower forms of plants, shells of crustaceans
Inulins	Chicory, Jerusalem artichokes

Polysaccharides can have animal, vegetal (algae, plants, seeds, and exudates), and microbial/fungal origins. Therefore, they hold a wide range of different functions. Polysaccharides can also be roughly divided into groups according to their two main functions: energy storage (starch, glycogen and polysaccharides of some plant seed) and their contributions to the structural components of cells. Polysaccharides can also contribute to the structural integrity and mechanical strength of plant tissues by forming a hydrated, cross-linked,

three-dimensional network, as in the case of pectins in land plants and carrageenan, agar and alginate in marine species.

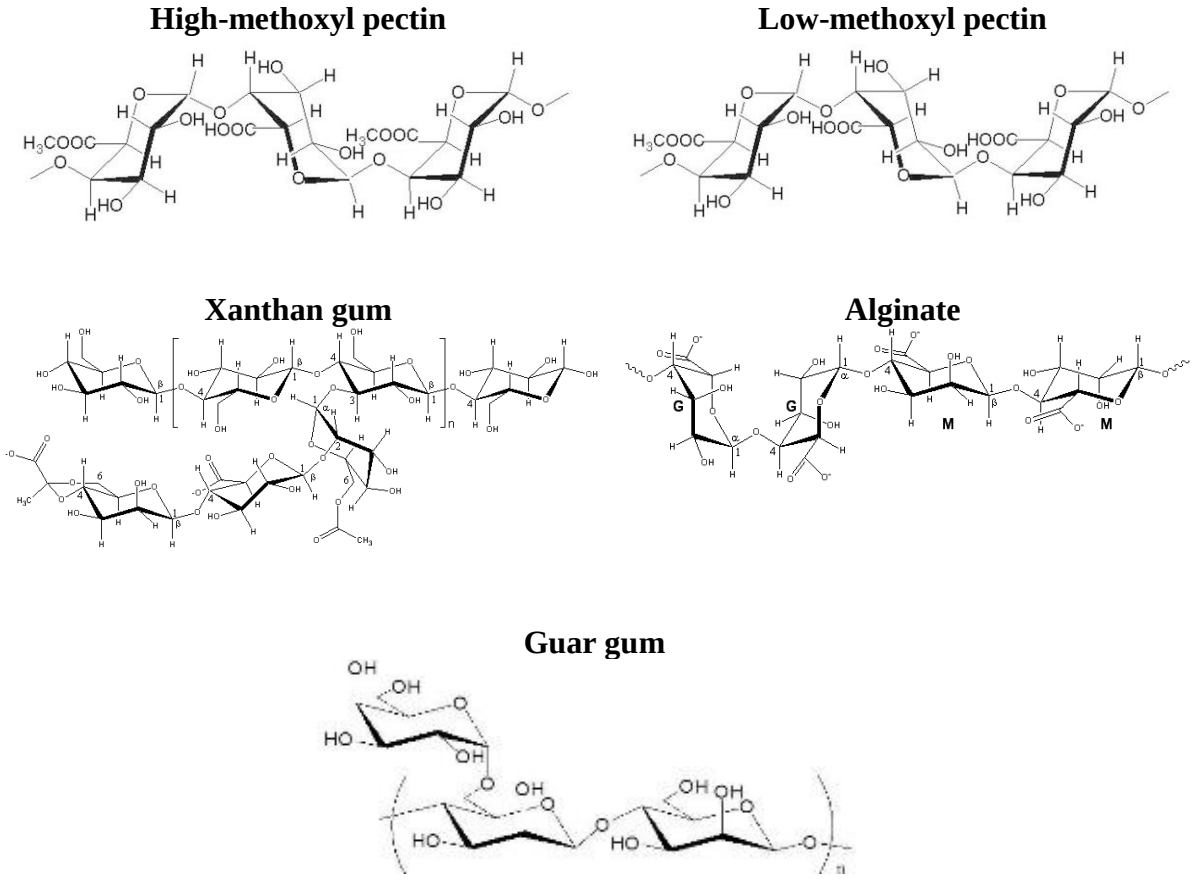

Figure 1.1 Structural formula of polysaccharides, used in the doctoral research

Plant foods are by far the commonest source of polysaccharides (Table 1.1). The polysaccharides that were used in the research work for this doctoral thesis will be thoroughly described deeply in the following subchapters. These are high- and low-methoxyl pectin, alginate, xanthan gum and guar gum, the structural formulas of which are presented in the Figure 1.1.

1.1 Pectin

Pectin was first described by Henri Braccannot in the year of 1825. The definition of pectins was later established in 1944, but since then it has been changed and modified. Nowadays the following definition is used for commercial use: 'Pectic acids are galacturonoglycans [poly(α-D-galactopyranosyluronic acids)] without or with only a negligible content of methyl ester groups. Pectic acids may have varying degrees of neutralization. Salts of pectin acids are called pectates.'… 'Pectins are mixtures of polysaccharides that originate from plants, contain pectinic acids as major component, are water soluble and are able to form gel under suitable conditions'[2].

Pectins are a family of complex polysaccharides, composed of 1,4-linked α-D-galactosyluronic acid residues. Many of those residues are esterified to form methyl esters. Depending on the isolation conditions, the remaining free carboxylic acid groups may be partially or fully neutralized. The ratio of esterified D-galacturonic acid units to total D-galacturonic acid units is called the degree of esterification and strongly influences the solubility, gel forming ability, conditions required for the gelation, gelling temperature and gel properties of the preparation. The degree of esterification can theoretically range from 0 to 100%. Based on the degree of esterification, pectins are then divided into two main groups. High-methoxyl pectin (hmP) has a degree of esterification higher than 50%; consequently low-methoxyl pectin (lmP) has a degree of esterification lower than 50 %. However, the pectin's structure is still not fully known [3], although it was discovered over 200 years ago. Three pectin polysaccharides have been isolated by now: homogalacturonan, rhamnogalacturonan-I and substituted galacturonans. The neutral sugars found in the pectin molecule are mainly D-galactose, L-arabinose and D-xylose. The total content of neutral sugars varies with the source, the extraction conditions and subsequent treatments. Pectin is both, polymolecular and polydisperse, i.e., it is heterogeneous with respect to both chemical structure and molecular weight.

Pectin constitutes approximately one-third of the dry weight of higher primary plant cell walls [4]. The amount, structure and chemical composition of the pectin differs between plants,

within a plant over time and in different parts of a single plant. In particular, it can be found in fruit cell walls, such as in citrus fruit and apple pomace. However, pectin is present not only in the primary cell walls but also in the middle lamella between plant cells, where it helps to bind the cells together (Figure 1.2). For commercial manufacture, the sources of pectin are limited, mostly owing to the ability of pectin to form a gel, which depends mainly on the molecular size and degree of esterification. Consequently, the high amount of pectin in a fruit is not enough to qualify that fruit as a source of commercial pectin.

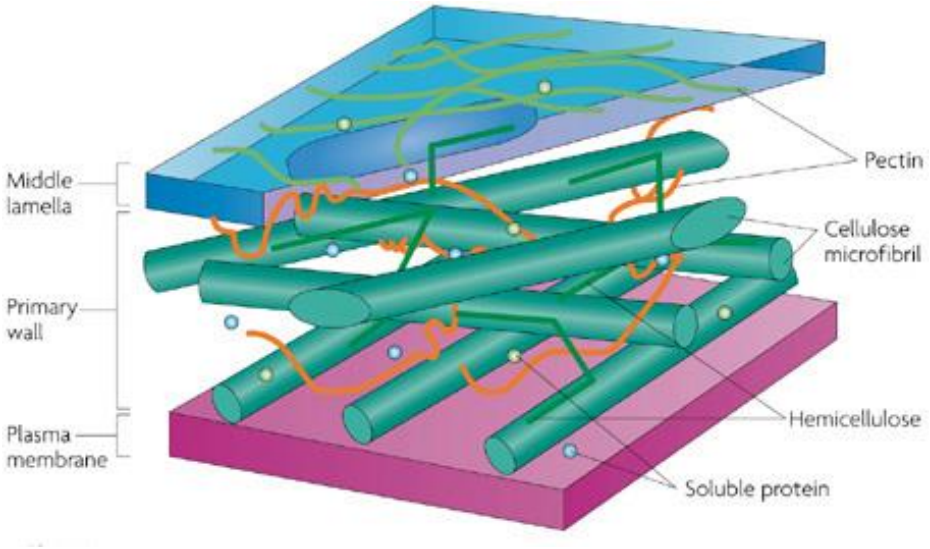

Figure 1.2. The main source of pectin in the cell wall [5].

For commercial use, nowadays pectins are almost exclusively derived from citrus peel or apple pomace. Both are by-products of juice manufacturing units. In applications, often both citrus and apple pectins act in a similar manner and are therefore often equally used. The physical appearance of apple and citrus pectin differs. Citrus pectins are light cream, whereas apple pectins are darker.

Pectin is soluble in water, but it is insoluble in aqueous solutions, in which they would gel at the same temperature if dissolved at a higher temperature. However, if dry powdered pectin is added to water, it has a tendency to hydrate very rapidly. This causes the formation of clumps, which consist of semi-dry packets of pectin contained in an envelope of highly hydrated outer

coating. Any further process of solubilisation is therefore highly restricted. In order to prevent the formation of such clumps, the dry powdered pectin should be added to water very slowly. Additionally, the dry pectin powder could be mixed with water-soluble carrier material. At lower concentrations, pectin solutions are Newtonian; at a moderate concentration, they exhibit pseudo plastic behaviour characteristics. As with the solubility, viscosity is also related to the molecular weight and degree of esterification.

Maximum stability of pectin solution or gel is found at pH 4. The presence of sugar also acts protectively, while elevated temperature increases the rate of degradation. With an increase in temperature or pH, chain cleavage is observed, which results in the rapid loss of viscosity and gelling properties. In an alkaline medium, pectin is rapidly de-esterified and degraded, even at room temperature [6]. Pectin is digested in the human body mainly in the large intestine (up to 80%) and in the small intestine (up to 40%). In the faeces, 0 – 25% of pectin has been recovered. Pectin is digested by increased bacterial action [7].

1.2 Alginate

Alginate is another type of biomaterial, natural polysaccharide that has found numerous applications in biomedical science and engineering, owing to its favourable properties. Like pectin, alginate also has a high tendency to form a gel. Alginate is present in brown seaweed, hence his high abundance in nature and its relatively low cost. It is non-toxic and biocompatible.

Commercially available alginate is typically extracted from brown algae (*Phaeophyceae*), including *Laminaria hyperborea*, *Laminaria digitata*, *Laminaria japonica*, *Ascophyllum nodosum*, and *Macrocystis pyrifera*.

Alginates are block copolymers between guluronate and mannuronate. The ratio varies depending on the natural source. Alginate is now known to be a whole family of linear copolymers containing blocks of (1,4)-linked β-D-mannuronate (M) and α-L-guluronate (G)

residues. Alginates extracted from different sources differ in M and G content, as well as in the length of each block, and more than 200 different alginates are currently being manufactured.

Only the G-blocks of alginate are believed to participate in intermolecular cross-linking with divalent cations (e.g., Ca^{2+}) to form hydrogels [8]. The composition (i.e., M/G ratio), sequence, G-block length and molecular weight are thus critical factors affecting the physical properties of alginate and its resultant hydrogels. The mechanical properties of alginate gels typically are enhanced by increasing the length of the G-block and molecular weight. Physical properties significantly control the stability of the gels, the rate of drug release from gels, and the phenotype and function of cells encapsulated in alginate gels.

The molecular weight of commercially available sodium alginates ranges between 32,000 and 400,000 g/mol. The viscosity of alginate solutions increases as the pH decreases, and reaches a maximum around pH = 3–3.5, as carboxylate groups in the alginate backbone become protonated and form hydrogen bonds.

Alginate hydrogels can be prepared by various cross-linking methods, and their structural similarity to extracellular matrices of living tissues allows wide application in wound healing, delivery of bioactive agents such as small chemical drugs and proteins, and cell transplantation. Alginate wound dressings maintain a physiologically moist microenvironment, minimize bacterial infection at the wound site, and facilitate wound healing. Drug molecules, from small chemical drugs to macromolecular proteins, can be released from alginate gels in a controlled manner, depending on the cross-linker types and cross-linking methods. In addition, alginate gels can be orally administered or injected into the body in a minimally invasive manner, which allows extensive applications in the pharmaceutical area.

1.3 Xanthan

Xanthan gum is a natural polysaccharide and an important industrial biopolymer. It was discovered in the 1950s. The polysaccharide, produced by the bacterium Xanthomonas

campestris, was extensively studied because of its properties, which allowed it to supplement other known natural and synthetic water-soluble gums [9].

Xanthan gum is a heteropolysaccharide with a primary structure consisting of repeated pentasaccharide units formed by two glucose units, two mannose units and one glucuronic acid unit, in the molar ratio 2.8:2.0:2.0. Its main chain consists of β-D-glucose units linked at the 1 and 4 positions. The chemical structure of the main chain is identical to that of cellulose. Trisaccharide side chains contain a D-glucuronic acid unit between two D-mannose units linked at the O-3 position of every other glucose residue in the main chain. Approximately one-half of the terminal D-mannose contains a pyruvic acid residue linked via keto group to the 4 and 6 positions, with an unknown distribution. The D-Mannose unit linked to the main chain contains an acetyl group at position O-6. The presence of acetic and pyruvic acids produces an anionic polysaccharide type. The molecular weight distribution ranges from 2×106 to 20×10^6 Da. This molecular weight distribution depends on the association between chains, forming aggregates of several individual chains. Variations in the fermentation conditions used in production are factors that can influence the molecular weight of xanthan [10].

Xanthan is non-toxic and does not inhibit growth. It is non-sensitizing and does not cause skin or eye irritation. It could be safely used as a food additive. Xanthan gum has been used in a wide variety of foods for a number of important reasons, including emulsion stabilization, temperature stability, compatibility with food ingredients, and its pseudoplastic rheological properties. Because of its properties in thickening aqueous solutions, as a dispersing agent, and stabilizer of emulsions and suspensions, xanthan gum is used in pharmaceutical formulations, cosmetics and agricultural products. It is used in textile printing pastes, ceramic glazes, slurry explosive formulations and rust removers. The high viscosity of solutions and water solubility of the polymer have created important applications for xanthan in the petroleum industry, where it is commonly used in drilling fluids and in enhanced oil recovery processes [9].

Xanthan gum is highly soluble in both cold and hot water, and this behavior is related to the polyelectrolyte nature of the xanthan molecule. Xanthan solutions are highly viscous even at low polymer concentrations [9].

1.4 Guar

Guar gum, also called guaran, is a galactomannan. It is primarily the ground endosperm of guar beans. The guar gum which can be obtained from the seed of the legume Cyamopsis tetragonalobus is a functional polysaccharide composed of a linear chain of D-mannose residues connected by (1→4)-β-glycosidic linkages. Pendant from the D-mannose are randomly attached D-galactose residues via (1→6)-α-glycosidic linkage units. The ratio of D-mannose to D-galactose is ca. 1.6–1.8:1 Among naturally occurring water-soluble polysaccharides, guar gum is known to have one of the highest molecular weights, reported [11] as $\sim 2.8 \times 10^7$ g mol^{-1}.

Guar gum is known for its low cost, nontoxicity, biodegradability, biocompatibility, high viscosity and high water-solubility. Thus, it is used in many industries as a sizing and finishing agent in the textile and paper industries; as a binder, stabilizer and thickener in the cosmetics and food industries; and as a fracturing fluid additive in mining and hydraulic fracturing processes. Guar gum is used as a thickener in cosmetics, sauces and salad dressings and as an agent in ice cream that prevents formation of ice crystals [12]. In the pharmaceutical sector, its functional properties are of primary importance for controlling the release of drugs in the gastrointestinal tract: as a carrier for colon targeted drugs, for anticancer drugs in the treatment of colorectal cancer and for oral rehydration solutions in the treatment of cholera in adults [13]. In pharmaceutical formulations, guar gum is used as a binder and disintegrant in solid dosage forms and as a suspending, thickening and stabilizing agent in liquid formulations [12]. Guar gum is a potential hydrophilic matrix carrier for oral controlled delivery of drugs with varying solubility [14]. On exposure to dissolution fluids, guar gum becomes hydrated and forms a viscous gel layer that slows down further seeping-in of dissolution fluids towards the core of the matrix tablet.

Several cross-linking methods have been proposed for the gelation of guar gum e.g. cross-linking with glutaraldehyde [15] and phosphating agents [16] in combination with polyacrylic

acid [17], or recently by using 1,2,3,4-butanetetracarboxylic dianhydride as a cross-linking agent [13].

1.5 Polysaccharide gelation

The sol-gel process is a well-known method for producing solid materials and has been extensively reviewed in books [18–23] and research articles [24–27].

The sol is a colloidal dispersion of particles with diameters in the range of 1 ± 1000 nm in a liquid [28]. When particles collide and polymerisation occurs, the molecule reaches macroscopic dimensions. The resulting structure is termed a gel. In summary, the gel is a substance that contains a continuous solid skeleton in which the liquid phase is enclosed. By Henisch [29], a gel has been defined as a "two-component system of a semisolid nature, rich in liquid".

The simplest way to understand the gelation process is to imagine the collision of clusters due to condensation or aggregation of particles. After the complete collision, one big cluster is formed, which is called a gel.

Gelation is a process where homogenous dispersion of a sol rigidifies. The sol or solution is transformed into a gel by going through a gel-point, meaning that the sol goes from a liquid state to a viscous state and then transforms to a solid state, which is called a gel. Formation of a gel occurs if and when the molecules interact to form a three-dimensional network that entraps a solvent. Junction zones are formed on account of the chain interactions. Those junction zones should not be too large, because the solute would precipitate rather than forming a gel [2]. The definition of the sol and the gel is stated in the book Introduction to Sol-Gel Processing [20] : 'A sol is a stable suspension of colloidal solid particles within a liquid. … A gel is a porous 3-dimensionally interconnected solid network that expand in a stable fashion throughout a liquid medium and is only limited by the size of the container.' The solid particles must be small enough for the dispersion forces to be greater than those of gravity. Solid particles in the

colloidal sol should range between 2 nm – 0.2 μm. The most commonly used solvent for the dispersion of solid particles is pure water; nevertheless, other organic solvents could be used.

The gel is composed of a solid network and a liquid medium, which have to be in thermodynamic equilibrium. Consequently, the liquid does not flow out of a gel. If the liquid in the gel is water, the corresponding gel is a hydrogel. These materials are usually very soft and can be easily cut with a knife. In contrast, if the liquid is alcohol, the gel is an alcogel. Eventually the liquid is removed from the gel, and only the solid network remains. Depending on the drying method, the resulting gel is then called a xerogel, aerogel or cryogel.

Polysaccharides, including hydrocolloids, are strongly hydrated in an aqueous medium, but they tend to have less ordered structures. The mechanism of gelation depends on the nature of the gelling agent(s) and on the conditions of gel formation, like the temperature, the presence of ions, the pH, and the concentration of gelling agents. [30]. Based on their cross-linked nature, (polysaccharides) hydrogels can be defined as chemical or physical. In the first case, crosslinks between different chains are strong, permanent and punctual, since they are due to covalent bonds. Conversely, in the second case, crosslinks are due to either polymer chain topological entanglement or physical interaction (this being typical of glucans and xanthan), such as H-bonds, ionic, van der Waals, dipole–dipole and hydrophobic interactions [31].

Pectin has been used for many years as a gelling agent. The earliest known research on the gelation of pectin goes back to 1933 [32], and since then, considerable research has been done in this field. Many of the findings have recently been published in the book ‘The Chemistry and Technology of Pectin’ [33]. To outline just a few important findings, the gelation mechanism of pectin is dependent on its degree of esterification. Thus, lmP can interact with divalent ions to form a three-dimensional gelled network. HmP requires a minimum amount of soluble solids and a pH within a narrow range, around 3.0, in order to form gels [34,35]. Apparent pK values vary with the degree of esterification. Pectins with a higher degree of esterification will gel at a higher pH because they have fewer carboxylate anions at any given pH. LmP forms thermoreversible gels at low pH (3-4.5), whereas hmP forms thermally irreversible gels in the presence of sugars, e.g. sucrose. If the methoxyl content is lower, the gelation is slower. The

main use of pectin still remains as a gelling agent, thickening agent and stabilizer in food. Because the commercial importance of pectin is predominantly the result of its unique ability to form spreadable gels in the presence of a dehydrating agent at a pH at or near 3 or in the presence of calcium ions, that is the property most often studied and focused upon. The factors that determine whether gelation can occur and that influence gel characteristics are pH, concentration of cosolutes (sugars), concentration and type of cations, temperature and pectin concentration. The way in which these factors influence gelation depends on the following molecular properties of the specific pectin: molecular weight, degree of esterification, degree of amidation, presence of acetate esters and heterogeneity. All these parameters are interdependent.

Alginate can form a gel by ionic cross-linking, covalent cross-linking, thermal gelation and cell cross-linking [8]. Cross-linking with ions is still considered the most common method to prepare hydrogels from an alginate aqueous solution. The ions that are usually used are divalent cations (such as calcium). The most widely employed cross-linking agent in the case of alginate is calcium chloride. The gelation is usually rapid and poorly controlled, owing to its high solubility in aqueous solutions. To slow down the gelation process and consequently have more control over the outcome, researchers are recommending the use of a buffer, containing phosphate, sulphate or carbonate. These groups compete with carboxylate groups of alginate in the reaction with calcium, and thus the gelation process is retarded. For example, when calcium carbonate is used for cross-linking the alginate, glucono – δ – lactone should be added to the mixture in order to dissociate calcium by lowering the pH of the solution. To improve the physical properties of alginate gel, covalent cross-linking could be employed. The use of poly(ethylene glycol)-diamines of various molecular weights for hydrophilic cross-linking can compensate for the loss of the hydrophilic character of the hydrogel. The mechanical properties and swelling of alginate hydrogels could be strongly tuned by using different cross-linking molecules. The alginate can be covalently cross-linked with 1,6-diaminohexane bridges, which are expected to improve the mechanical strength and resistance to chemical and microbial degradation, without a change in adsorption property [36]. Photo cross-linking is another promising approach to stable alginate gels. Alginate modified with methacrylate and cross-

linked by exposure to a laser forms clear, flexible hydrogels. However, covalent cross-linking may be toxic, and the unreacted chemicals may need to be removed thoroughly from the gels. Also, photo cross-linking reactions involve the use of light sensitizer or the release of acid, both of which may be harmful in the body. Thus, such prepared gels could rarely be used for biomedical applications. For the use of alginate gels in drug delivery applications, thermal gelation is one option. This is mostly because of their adjustable swelling properties in response to temperature changes. However, since alginate is not inherently thermo-sensitive, there have been only a few systems reporting thermal gelation of alginate [37]. Cell cross-linking of alginate is unfortunately the most often ignored method; however, it has been proven that the resulting gels might be ideal for cell delivery in tissue engineering. Cells added to a modified alginate solution form a uniform dispersion within the solution, and this system subsequently generates the cross-linked network structure [38]. If the alginate solution is not modified, the cells aggregate and form a non-uniform structure [8].

Xanthan solution can form a gel by the addition of trivalent chromic ions. It has been found that the rate of gel formation is strongly dependent on the Cr^{3+} concentration, but to a much smaller extent on the xanthan concentration [39]. Xanthan gum usually does not gel by itself, but shows curious rheological characteristics [40], and forms a gel in a mixture solution with galactomannan [41,42] and glucomannan [43–45].

The **Guar** gelation mechanism has not yet been investigated to the extent of pectin or alginate. Guar gum is readily soluble in cold water. There have been a few studies on the preparation of guar hydrogels; however, the vast majority of other studies are based on the gelation of guar together with other polysaccharides, or even inorganic substances. The gel is formed on cooling in the presence of salts [30]. Guar gum hydrogels were prepared via esterification with 1,2,3,4-butanetetracarboxylic dianhydride (BTCA). BTCA contains two acid anhydrides in its structure, and each readily reacts with certain functional groups such as isocyanates, amines and hydroxyl groups to undergo crosslinking. Thus, the merit of BTCA is to convert nonionic polysaccharides to the chemically cross-linked anionic hydrogels by a one-step reaction [13].

1.6 From wet gels to aerogels

A gel consists of a spongelike, three-dimensional solid network whose pores are usually filled with a liquid. The pore liquid mainly consists of water and/or alcohol. The resulting wet gels are therefore called hydrogels or alcogels.

Wet gels are broadly classified into two categories:

Permanent / chemical gel: covalently cross-linked (replacing the hydrogen bond by a stronger and stable covalent bond) networks. They attain an equilibrium swelling state which depends on the polymer-water interaction parameter and the crosslink density.

Reversible / physical gel: networks are held together by molecular entanglement, and / or secondary forces including ionic, hydrogen bonding or hydrophobic interactions. In physically cross-linked gels, dissolution is prevented by the physical interactions that exist between different polymer chains. All of these interactions are reversible, and can be disrupted by changes in physical conditions or application of stress [46].

When the pore liquid is replaced by air without decisively altering the network structure or the volume of the gel body, aerogels are obtained (or cryogels when the pore liquid is removed by freeze-drying). A xerogel is formed upon conventional drying of the wet gels, that is, by an increase in temperature or a decrease in pressure, with concomitant major shrinkage (and mostly destruction) of the initially uniform gel body [28] (Figure 1.3).

Therefore, the most common ways to dry wet gels are evaporative drying, freeze drying and supercritical drying. By evaporative drying, the microstructure collapses, mostly owing to capillary forces, and therefore some shrinkage of the solid occurs [47]. In the first stage of evaporative drying, the gel shrinks by the volume that was previously occupied by the liquid. The liquid flows/diffuses from the interior of the gel body to its surface. By continuing the drying process, the gel network becomes increasingly stiffer. The surface tension in the liquid rises, because the pore radii become smaller. Then, at some critical point in the drying process, the surface tension is no longer capable of deforming the network of the gel. The gel becomes

too stiff for further shrinkage. Since there is still liquid at the pore wall, this liquid film evaporates from the exterior surface of the gel body. Finally, the liquid that remains in isolated pockets of the gel leaves the gel by diffusion [28].

In evaporative drying, the collapse of the network happens because of a pressure gradient inside the gel and because of the different sizes of the pores, which are subjected to uneven stress and crack. To minimize those capillary forces that are causing the network collapse, the size of the pores should be larger; the capillary force is inversely proportional to the pore radius; the gel should be aged so that the network can become stiffer, or some tensides or chemical additives should be added.

Freeze-drying is a drying method where phase boundaries between liquid and gas phases are avoided. First, the liquid in the pores is frozen and then sublimed under vacuum. To achieve good network stability, aging periods have to be long enough, and the solvent must be exchanged for one with a lower expansion coefficient. A serious disadvantage of this process is that the network is often destroyed by the crystallization of the solvent in the pores. Cryogels are therefore often obtained in the form of a powder [28].

However, by supercritical drying, the fluid is a single phase. The liquid-gas interface is circumvented, and therefore collapse of the network is prevented [48]. The resulting materials retain most of the structure of the wet gel and possess interesting properties, such as high porosity, large surface area, low thermal and electrical conductivity and low density.

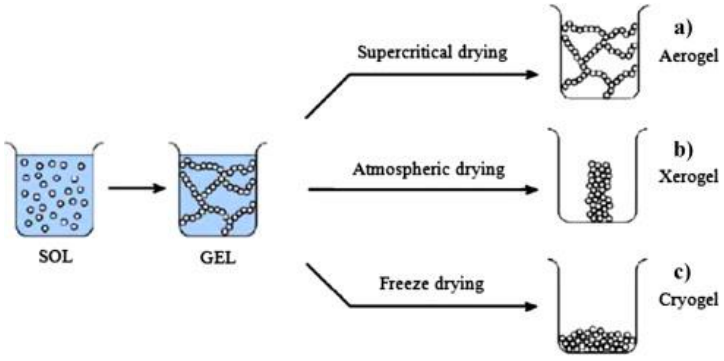

Figure 1.3. Methods of drying of a wet gel to give an (a) aerogel, (b) xerogel and (c) cryogel [49].

Three types of supercritical drying can be performed to produce aerogels. The first and most commonly used method is low temperature drying. Supercritical carbon dioxide is used for extraction of an organic solvent at low temperatures. In the second method, liquid carbon dioxide displaces an organic solvent, with subsequent supercritical CO_2 venting. Another possible way to dry wet gels is high temperature drying, where the wet gel is brought to the supercritical state of the organic solvent. In this method, the wet gel is placed in an autoclave with a sufficient amount of the solvent. By slowly raising the temperature above the critical point for the solvent, the pressure is also increased. These conditions are maintained for a certain time, after which the fluid is vented at a constant temperature. The pressure is therefore decreased, and the vessel is cooled to room temperature. The main disadvantage of high temperature drying is the high pressures and/or temperatures needed to reach the supercritical state. Supercritical drying depends on the solubility and diffusivity of the solvents in supercritical fluid. By increasing pressure, the solubility of organic materials or water increases, and therefore high pressures are used when the quantity of those substances is great.

As seen in Table 1.2, most solvents have high critical temperatures (400-650 K) and higher critical pressures up to 220 bars. Many of them are flammable and potentially explosive under those conditions. Another concern with high temperature drying is that organic polymer aerogels cannot be prepared by this method. Indeed, many of them degrade or react at higher temperatures.

Table 1.2. Critical data for the fluids used in the supercritical drying process.

Fluid	**T_c**	**P_c**	**ρ_c**
	K	bar	kgm^{-3}
Carbon dioxide (CO_2)	304.2	73.75	468
Water (H_2O)	647.3	220.6	322
Methanol (MeOH)	513.7	80.92	272
Ethanol (EtOH)	516.3	61.37	276
Acetone	508.2	46.6	273
Ammoniac (NH_3)	405.6	113.5	235

To summarize, carbon dioxide is the most desirable fluid in aerogel production. The physical properties of carbon dioxide have been known since the 1930s [50,51]. It is considered 'green' as it is relatively non-toxic, non-flammable and relatively inert. Its low price and relatively low critical conditions make it a highly desired solvent in the laboratory as well as on the industrial scale. Supercritical CO_2 is more environmentally friendly than traditional organic solvents. In addition, CO_2 occurs naturally, it is inexpensive, non-flammable and recyclable, while also having a low critical point (31.1°C and 73.8 bar) [52]. Supercritical fluids (SCF) have diffusivities like gases and densities like liquids.

The materials obtained after supercritical drying are termed aerogels. Aerogels are very low-density materials with high porosity and large surface areas. The term was first used by Kistler in 1931, who defined them as porous materials with stable network structures after solvent exchange [53]. Aerogel production starts with a traditional sol-gel synthesis, which has been reviewed in many research papers and books [18–22,26]. First, a precursor is added to a solution to form the sol. After polymerisation, a wet gel (hydrogel/alcogel) is formed. This wet gel is then supercritically dried.

Initially, silica aerogels were used in cosmetics [54]. Over the last decade, organic aerogels have been proposed for use in medical applications, especially within drug delivery systems [55]. Given their outstanding properties, today's aerogels have become interesting materials for a variety of applications [56]. To name just a few, aerogels are used in microelectronics [57], as catalysts [58], insulators [59], capacitors [60,61] or carriers of active substances in the food or pharmaceutical industries [62]. Silica aerogels have been used as additives in toothpastes or cosmetics since the 1960s. In 1995 Berg et al [55] proposed the use of organic aerogels in medical applications and also in drug delivery. This research was the beginning of increased interest in the use of inorganic and organic aerogels in the area of drug delivery.

2 METHODS

Chapter 2 briefly describes the methods that were used in the research, including supercritical drying of wet gels, characterization methods, supercritical impregnation, swelling and erosion and *in vitro* dissolution testing. Characterization methods are used for observing, measuring and describing the properties of an aerogel. There are many different ways of characterizing the materials. To characterize polysaccharide aerogels, most common and attractive methods include nitrogen adsorption, scanning electron microscopy, differential scanning calorimetry, thermogravimetry and thermal conductivity.

2.1 Supercritical drying with CO_2

Polysaccharide gels are prepared by mixing the precursors in water. Prior to supercritical drying, the water in the resulting gels should be replaced by an appropriate organic solvent e.g. ethanol or acetone. The reason involves the solubility of CO_2 in water and/or in this organic solvent. For instance, experiments showed [63] that the solubility of ethanol in supercritical CO_2 is much higher than the solubility of water. Inorganic aerogels, such as silica, are prepared by mixing the precursors in alcohol. Thus, the step of water/alcohol exchange is not needed. In order to prevent the formation of a liquid-vapour meniscus, which recedes during the emptying of the pores in wet gel, only one phase can be present during drying. Transformation of a liquid in SCF is one way of doing so. In supercritical drying, there is no capillary pressure gradient in the pore walls [64]. Thus, there is very low shrinkage and no surface tension; hence, the structure of the gel is almost unaffected [65]. However, organic polysaccharide aerogels are often prepared in water. Hence, the solvent (water) cannot be eliminated only by the supercritical CO_2. The solvent exchange step is performed prior to supercritical drying [62].

Supercritical drying with CO_2 can be performed in two ways:

A widely used method in the literature is the extraction of alcohol by liquid CO_2. The extraction is performed under 25°C and 67 bars. The time required for exchanging the original pore liquid for liquid CO_2 is determined by the diffusion of carbon dioxide into the gel, and is therefore dependent on the dimensions of the gel body [28]. Another requirement is the miscibility of the pore liquid with carbon dioxide. After final extraction, the extractor is heated to the critical point of CO_2. Consequently, the pressure also increases above the critical point.

Another method is the extraction of ethanol by supercritical CO_2. The temperature is first raised above the critical temperature, and then the pressure in the extractor is increased above the critical pressure. After complete extraction of alcohol, the system is slowly depressurized. In this step, the temperature has to stay above the critical point to avoid the liquid state of carbon

dioxide. CO_2 has to go from the supercritical state directly to the gas. Once atmospheric pressure in the extractor has been reached, the system can be cooled down.

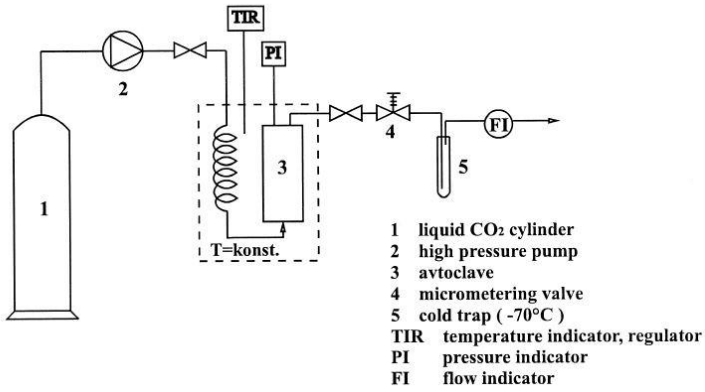

Figure 2.1. Experimental apparatus [66].

The process for drying wet gels in this research work is as follows (Figure 2.1): wet gels are placed into an autoclave, which is filled with the same solvent as in the gel pores. The solvent in the autoclave prevents the evaporation of solvent from the gel pores during the heating and pressure elevating steps, hence avoiding pore collapse. CO_2 is then heated above its critical temperature and pumped into the autoclave. CO_2 extracts the solvent from the wet gel. The CO_2 flow should be constant during the drying process. The solvent is then separated from the CO_2 in the separator. After few hours, the solvent is completely extracted from the gel, and supercritical CO_2 is the only substance remaining in the pores. Now is the time to slowly depressurize the system. After reaching atmospheric pressure, the system is left to cool down, and then the samples (aerogels) are withdrawn from the autoclave. It is difficult to predict the appropriate time for the drying of aerogels. Hence, mathematical modelling of the supercritical drying procedure could provide important information about optimization of the process.

2.2 Nitrogen adsorption

Nitrogen adsorption is a great tool for the characterisation of a variety of porous materials. Langmuir worked on monolayer adsorption, and his model predicted that the amount of

adsorbed gas at the plateau of a Type I isotherm corresponds to complete monolayer coverage. Later, it was proven that multilayer nitrogen adsorption is possible at a temperature of 77 K (temperature of liquid nitrogen) [67]. Brunauer and Emmett conducted those studies for the determination of surface area, and in 1938 Brunauer-Emmett-Teller (BET) published the theory providing theoretical support for determining the surface area [68].

Surface tension, like gas adsorption, is the result of surface energy. Except on the surface, the molecules of all solids are surrounded by and bound to neighbouring molecules. Surface molecules are bound on one side to inner molecules, and the surface is thus exposed to attract gas or liquid molecules. Those attractions are called van der Waals forces and are responsible for physisorption, surface tension and condensation in liquids.

From the specific surface area, it can be determined how solids burn, dissolve or react with other substances. To determine surface area, the solid material is first treated by a combination of heat, vacuum and/or gas to remove adsorbed substances (water and CO_2). Under vacuum, the sample is cooled to cryogenic temperatures (77K, -195°C). An adsorbent (usually nitrogen) is introduced in specific amounts into the sample tube. After each dosage, pressure equilibrium is reached, and the amount of adsorbed gas is then calculated. The amount of adsorbed gas at each temperature and pressure defines the adsorption isotherm. The amount of gas required to form a monolayer (one molecule thick) is calculated from the adsorption isotherm. BET is used to calculate the specific surface area.

Surface area determination requires special conditions for forming a monolayer of gas molecules on the surface of the sample. Continuing this process, gas condenses in the pores, and in this way porosity can be determined. By increasing the pressure, gas first condenses in smaller pores. Pressure then increases until all pores are filled with liquid. Pressure is immediately decreased to remove condensed gas from the system. Analysis of the adsorption and desorption branch of this curve, as well as its hysteresis, gives us information about pore size, pore volume and surface area.

Most reactions in solids take place on their surface. The porous structure, size and shape of an adsorbent determines whether the adsorbent reaches an active site in the sample. The IUPAC system divides pores according to adsorption mechanisms. Micropores (<2nm) have higher enthalpies of adsorption than meso- (2-50nm) or macropores (>50nm). Gas adsorption is an important characterization method for a wide range of porous materials [69]. Of all the gases, nitrogen is the one most commonly used in these analyses [70].

For interpretation of the adsorption isotherm, we first have to determine its type. IUPAC [71] divides isotherms into 6 groups, presented in Figure 2.2. Type 1 is typical of materials with very small pores, and types 2 and 4 characterize nonporous materials or materials with relatively wide pores. Types 3 and 5 appear under conditions when adsorbent molecules have a higher affinity for one another than for the sample. The type 6 isotherm is quite rare and represents nonporous solids with an almost completely uniform structure. Adsorption isotherms for organic aerogels a have typical hysteresis loop, determining a meso- and microporous structure [64].

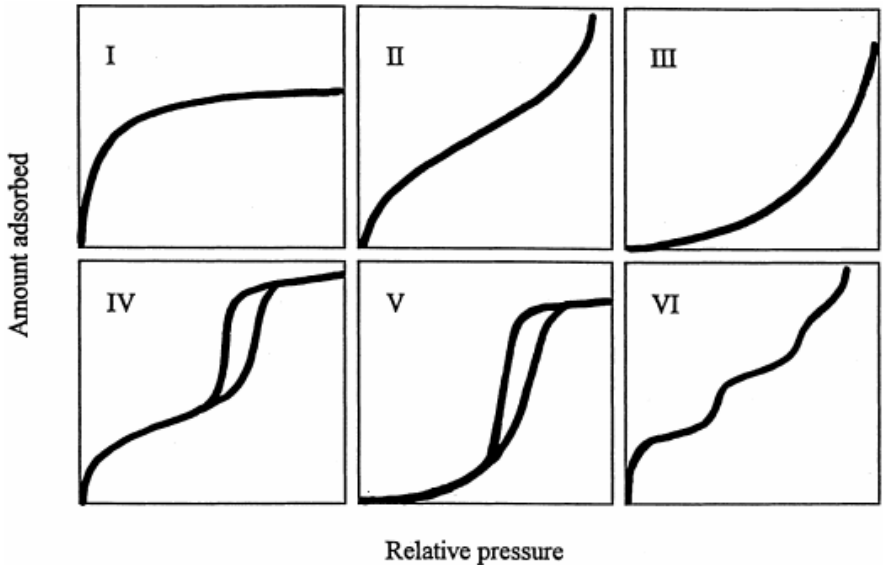

Figure 2.2. IUPAC classification: adsorption isotherms [72].

Before analysis, the sample should first be outgassed by evacuation or by sparging the adsorbed gas to remove all impurities from the air. The temperature is then decreased to cryogenic

temperature. The quantity of adsorbed gas vs. relative pressure at a specific temperature is presented as an adsorption isotherm. The resulting data are calculated according to gas adsorption theories. Results for surface area are given in m^2g^{-1} [72]. Gas adsorption is a volumetric method. It is calculated as the difference between the number of molecules introduced and the number of un-adsorbed molecules at equilibrium pressure. Assuming both molecules have the same size, and the absorption pressure (molecule number) is 50 Pa, we have to measure pressure change for 0.16% (N2) and 38% (Kr) at relative pressure (P/P0 = 0.3, N2 = 30400 Pa, Kr = 80 Pa). As it is easier to measure higher-pressure changes, accuracy is obviously better. To summarize, the lower the vapour pressure at adsorption temperature, the greater the accuracy in measuring lower surface areas of the sample.

Table 2.1 presents the properties of various gases used in gas adsorption. Krypton adsorption is usually used to determine very low specific surface areas. The cross-sectional area figures for krypton and nitrogen are 0.202 nm^2 and 0.162 nm^2, respectively. This means that the krypton molecule is larger than nitrogen by around 25%. To conclude, the krypton molecule is not suitable for measuring lower surface areas, owing to its greater cross-sectional area. However, the reason for using krypton lies in its adsorption temperature and its vapour pressure.

Gas adsorption is a volumetric method. It is calculated as the difference between the number of molecules introduced and the number of un-adsorbed molecules at equilibrium pressure. Assuming both molecules have the same size, and the absorption pressure (molecule number) is 50 Pa, we have to measure pressure change for 0.16% (N_2) and 38% (Kr) at relative pressure (P/P_0 = 0.3, N_2 = 30400 Pa, Kr = 80 Pa). As it is easier to measure higher-pressure changes, accuracy is obviously better. To summarize, the lower the vapour pressure at adsorption temperature, the greater the accuracy in measuring lower surface areas of the sample.

Table 2.1. Adsorbent properties.

Adsorptive	**Temperature** K	**Vapour pressure** Pa	**Cross sectional area** nm^2	**Range** m^2
N_2	77.4	101325	0.162	>1

Ar	77.4	26664	0.166	0.1～10
Kr	77.4	267	0.202	0.01～1
Xe	77.4	0.23	0.232	Ca. 1cm^2
CO_2	273.2	3490 k	0.195	Coal, active carbon

2.3 Scanning electron microscopy

Scanning electron microscopes (SEM) can image and analyse bulk specimens. Electrons are accelerated through a voltage difference between cathode and anode that may be as low as 0.1 keV or as high as 50 keV. The signals that derive from electron-sample interactions reveal information about the sample, including external morphology (texture), chemical composition, and the crystalline structure and orientation of materials making up the sample. In most applications, data are collected over a selected area of the surface of the sample, and a 2-dimensional image is generated that displays spatial variations in these properties. The SEM is routinely used to generate high-resolution images of shapes of objects and to show spatial variation in chemical composition. The SEM is also widely used to identify phases based on qualitative chemical analysis and/or crystalline structure. Precise measurement of very small features and objects down to 50 nm in size is also accomplished using the SEM [73,74]. Field emission scanning electron microscopy (FESEM) provides topographical and elemental information at magnifications of 10x to 300,000x, with virtually unlimited depth of field. Compared with a conventional SEM, FESEM produces clearer, less electrostatically distorted images, with spatial resolution down to 1.5 nanometers – three to six times better. Since aerogels are highly non-conductive materials, SEM imaging presents a special challenge. Therefore, sputter coating of such materials is essential prior to each analysis. Usually, aerogels are sputter coated with gold particles and then scanned at an accelerating voltage.

2.4 Differential scanning calorimetry and thermogravimetry

Differential scanning calorimetry (DSC) and thermogravimetry (TG) are two highly important analytical methods for determining the thermal characteristics of various materials. DSC (Figure 2.3a) is a thermal analysis technique that looks at how a material's heat capacity (Cp) is changed by temperature. The sample and an empty reference crucible are heated at a constant heat flow. A difference in the temperature of the two crucibles is caused by the thermal critical points of the sample and can be detected. This allows the detection of transitions such as melting, glass transitions, phase changes and curing. Because of this flexibility, since most materials exhibit some sort of transition, DSC is used in many industries, including pharmaceuticals, polymers, food, paper, printing, manufacturing, agriculture, semiconductors and electronics. The biggest advantage of DSC is the ease and speed with which it can be used to see transitions in materials. In TG (Figure 2.3b), the sample is heated under nitrogen or synthetic air with a constant heat rate, while the difference of the mass during this process is measured. A mass loss indicates that a degradation of the measured substance has taken place. The reaction with oxygen from the synthetic air, for example, could lead to an increase in mass.

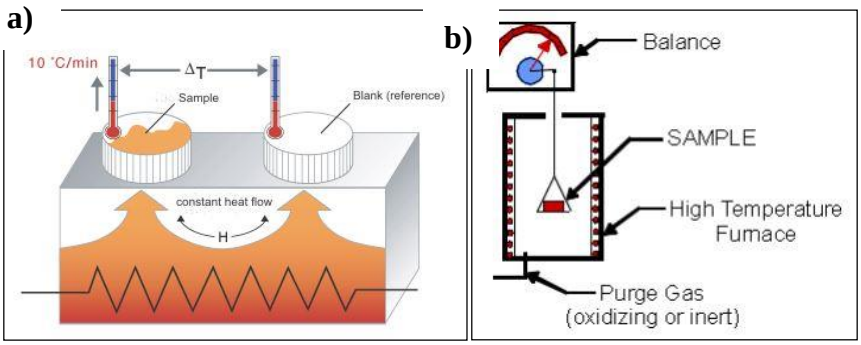

Figure 2.3. Schematic presentation of a) DSC [75] and b) TG [76].

TGA/DSC 1, Mettler Toledo was used for analysis of the aerogel samples. Calibration was performed by indium sample. A small amount of the sample (e.g. 10 mg) was weighed into an aluminium crucible and then heated to the desired temperature at a predetermined heating rate.

2.5 Thermal conductivity

Energy use in the EU is projected to decrease by 20% in 2020 and 50% in 2050 compared to energy use in 1990. A large amount of energy is used for heating buildings; therefore, the demand for new thermal insulation materials is increasing enormously [77]. The function of insulation materials is to minimize the transport of heat. Heat transport is a combination of three factors: conduction through solids, conduction through gas and radiation through pores. The largest component of total conductivity occurs through solid conduction. Therefore, it is preferable that insulation materials be highly porous, with only a small amount of solid structure [78,79]. Figure 2.4 is a schematic representation of conductivity in porous materials, in which the largest part is a result of conduction through gas.

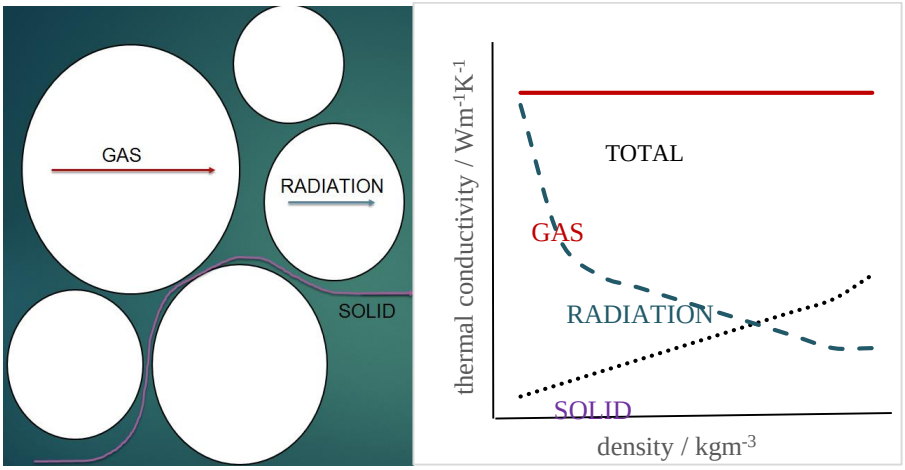

Figure 2.4. Thermal conductivity in porous materials as a result of several different mechanisms, including conduction through porous solids (purple arrow), conduction through gas contained in the pores (red arrow) and radiation (blue arrow).

The materials with the highest porosities (up to 99%) are aerogels prepared using the sol-gel process and dried under such conditions that the structure of the wet gel is preserved. Inorganic silica aerogels are most widely used for building applications. Because of the Knudsen effect, their thermal conductivity can be lower than that of still air [80,81]. Silica aerogels usually

possess some limitations caused by their brittleness. Other recent studies [82–85] are thus focusing on the mechanically more stable polysaccharide aerogels. To combine both the mechanical properties of polysaccharide aerogels and the low thermal conductivity of silica aerogels, composites of cellulose-silica with low conductivities of 27 $mWm^{-1}K^{-1}$ were reported [86].

There are many ways to measure the thermal conductivity of insulation materials [87]. One method is the DSC, which was first proposed by Hakvoort and van Reijen [88]. In this method, the melting behaviour of a pure metal (such as indium) on top of a cylindrical sample or disk is measured. During heating, the metal reaches its melting point, and the temperature remains constant while the metal melts. The temperature difference between the lower surface of the disk and the heat flowing into the disk is measured by the DSC, and the thermal conductivity is calculated from the temperature difference and the heat flow. The DSC method is a simple and useful method for measuring all sorts of materials, from polymers, ceramics and glasses [89], to powders [90]. This analysis was based on previously published studies on measuring the thermal conductivities of polymers with an uncertainty of 10% [91]. The assembly is shown in Figure 2.5. The sample is placed directly on the sensor. One should ensure that the sample does not melt in order to avoid destroying the sensor. Then the metal (e.g. indium) is placed on the top of the sample in a light aluminium crucible. On the reference side, an empty aluminium crucible is used.

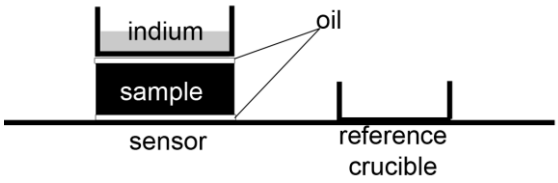

Figure 2.5. Schematic presentation of the sample arrangement on the DSC sensor.

After the setup, the heat flow is measured in the range where the selected metal melts. For indium, the heat flow is measured from 153°C to 162°C. The melting point of indium is 156.6°C.

The slope *S* (left side of the melting peak) is determined by plotting the DSC curve against the temperature [91]. This slope is essential for the determination of thermal conductivity according to Eq. 1:

$$S = \frac{\phi}{\Delta T} \quad (1)$$

Where Φ is the heat flow and ΔT is the difference between the temperature of the sample at time *t* and the melting point of the metal (T_{onset}). For determination of thermal conductivity, we then used Eq.2:

$$\lambda = \frac{\phi}{\Delta T}\frac{h}{A} = S\frac{h}{A} \quad (2)$$

Where *h* is the sample height, *A* is the cross-sectional area and λ is thermal conductivity in units ($WK^{-1}m^{-1}$).

2.6 Supercritical impregnation in drug delivery

Supercritical impregnation can be used in many different applications. One of the latest opportunities is its implementation in the pharmaceutical sciences. Because the vast majority of newly discovered drugs are poorly water soluble, incorporation into the matrix becomes a huge challenge. Supercritical impregnation is one option for incorporating such drugs into carriers. It has been proven [92] that supercritical impregnation is a more effective method for incorporation of drugs than, for instance, the traditional sol-gel method. However, supercritical impregnation requires detailed method design. The matrix and the desired drugs to be impregnated need to be carefully chosen. The solubility of a drug within the adsorption medium is one of the most relevant characteristics [93]. Final loading of a drug is affected by the solubility of the drug in SCF and by the carrier surface. It is advisable for the carrier to have as

high a surface area as possible, in order to provide more ‘space’ for the incorporated drugs, hence higher loadings [94]. Lately, aerogels have become highly investigated materials for supercritical drug impregnation.

Supercritical technology offers a more ecological alternative to conventional impregnation processes. Supercritical fluid properties--i.e. low viscosity, low surface tension, high density and gas-like diffusivity--allow faster and more homogeneous impregnation.

A very important parameter for supercritical impregnation (SCI) is the interaction between the SCF and the polymer matrix. Three possible effects need to be considered when attempting to understand these reactions [56]:

1. dissolution of SCF in the polymer matrix (polymer sorption);
2. swelling of the polymer matrix;
3. plasticisation (depression of polymer glass transition temperature - T_g).

Swelling and plasticisation are caused by the sorption of SCF. The sorbed gas acts as a ‘molecular lubricant’ making the polymer chains softer (the polymer transition from a glassy state to a rubbery state occurs) and able to move more freely. The impregnation compound should be soluble in SCF, and the diffusion coefficient between the compound and polymer molecules must be sufficiently favourable to charge the matrix with an adequate amount [95].

Supercritical impregnation of compounds into aerogels can be achieved by two different mechanisms [96]. The first one is the deposition approach for compounds that are highly soluble in SCF. This process starts with solubilisation of the compound in SCF. The polymer is then exposed to such a solution by consecutive depressurisation and removal of SCF. Thus, the SCF molecules quickly leave the polymer matrix, leaving the compound molecules inside. The second mechanism is the partitioning mechanism for compounds that are very poorly soluble in SCF. For successful impregnation, it is important that the compound have a high affinity for a certain polymer matrix, which would result in preferential partitioning of a compound in a

way that favours the polymer over the fluid phase. The partitioning mechanism has a major advantage over the deposition approach. The reason is due to the re-crystallisation process of the compound when using the deposition approach. Specific interactions between compound and matrix usually prevent such re-crystallisation.

There are two different ways to impregnate compounds into aerogels, depending on the contact between the SCF solution (SCF with compound) and the aerogel. The static method places the compound and an aerogel in a vessel that is heated to the desired temperature and charged with the fluid to the desired pressure. In the flowing mode in the dynamic method, the SCF solution is constantly passing over the aerogel matrix. The impregnation process is governed by the amount of the drug that can be carried by the SCF, as well as the diffusion coefficient of the compound [97].

2.7 Swelling and erosion

Swelling and erosion are important characteristics of polymeric systems. Clearly understanding the swelling kinetics and erosion behaviour of a polymer can reveal the drug release mechanism and kinetics. Swellable matrices are also termed gel-forming matrices, as their drug-delivery behaviour is characterized by the formation of an outer gel layer on the matrix surface. If the polymer gels slowly, the solvent can penetrate deep into the glassy matrix, thus dissolving the drug and disintegrating the matrix. This gel layer acts as a ‘protective’ layer for the matrix, and its stability is as essential as its rapid formation. Therefore, gel-layer thickness behaviour is crucial in describing the release kinetics of swellable matrices [98].

The swelling behaviour can be described by the front positions. Front indicates the position in the matrix where the physical conditions sharply change. The swelling front is where the rubbery region of a matrix is clearly separated from the glassy region. The erosion front separates the matrix from the solvent [98]. The gel-layer thickeness as a function of time is determined by the relative position of the swelling and erosion moving fronts (Figure 2.6).

It is reported that swelling and erosion of drug matrices in dissolution media have a significant effect on controlled drug release [99,100]. The swelling properties of polymers vary in different solutions. High swelling progress with a low erosion rate results in a thick swelling gel layer or a long diffusion distance for the drug. Moreover, the strength of the gel layer also affects the diffusion coefficient of a drug [101].

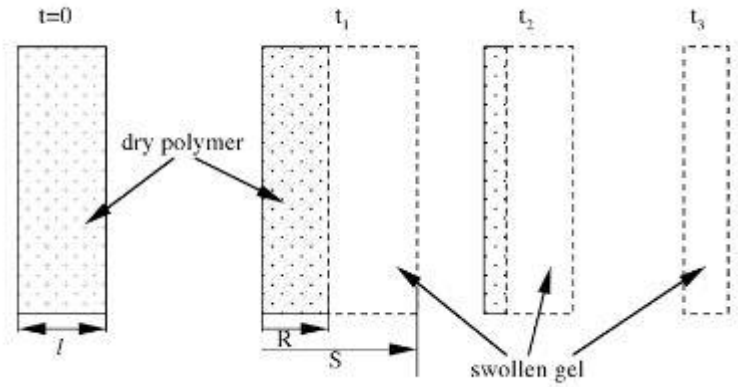

Figure 2.6. Swelling and erosion phenomena of a water-soluble polymer [102].

The most common technique for determining the swelling properties of polymers is the gravimetric technique (weight difference between dry and wet polymer) [99]. The dry matrix is accurately weighed (W_0) then placed in closed containers with the dissolution medium at 37 ± 0.5°C. After a predetermined time, the matrix is withdrawn from the medium and lightly blotted with tissue paper to remove excess dissolution medium. It is then re-weighed (W_1). The percentage increase in weight due to absorbed dissolution medium is estimated at each time point from the Eq 3:

$$swelling\ ratio\ (\%) = \frac{W_1 - W_0}{W_0} \cdot 100 \qquad (3)$$

Studies of erosion are followed by those of Roy and Rohera [103]. After the swelling studies, the wet samples are dried in an oven at 80°C for 24 h, then cooled and weighed until a constant weight is achieved (final dry weight, W_2). The matrix erosion at predetermined times is estimated from the Eq. 4:

$$matrix\ erosion = \frac{W_0 - W_2}{W_0} \quad (4)$$

2.8 *In vitro* dissolution test

Dissolution tests are usually performed *in vitro* or *in vivo*. *In vivo* tests are extremely costly, tedious and time consuming. In addition, healthy subjects are often exposed to risks from the drugs. In the early stages of drug formulation development, *in vitro* dissolution tests are thus a desirable alternate for *in vivo* tests as quality control tests.

The drug must first be dissolved to be absorbed by the gastrointestinal tract (GIT). Dissolution tests are designed to mimic the conditions of the GIT. The dissolution of drugs from orally administered solid dosage forms *in vivo* and *in vitro* is influenced by variation in the natural or simulated gastrointestinal fluid (and physical variables such as hydrodynamic flow and mechanical stress). Intestinal transit time, gastric emptying time and variable pH can also affect drug release.

Depending on the material, *in vitro* tests are performed by different apparatus according to USP (United States Pharmacopeia) standards. There are 7 different apparatus according to USP: basket, paddle, reciprocating cylinder, flow-through cell, paddle-over-disk, cylinder and reciprocating holder [104].

Dissolution tests of solid oral dosage forms are normally employed by USP I or II apparatus, also known as basket and paddle. Both are considered closed-system methods, since a fixed volume of dissolution medium is used. Both apparatus consist of a large vessel with 500 to 1000ml of fluid that is immersed in a thermostatic water bath. In the center of both apparatus, there is a rotating axis with a basket (USP I) or paddle (USP II) (Figure 2.7). These are the apparatus of first choice in dissolution testing of solid oral dosage forms. They are easy to operate, but the main disadvantage is the limited volume of dissolution media [104].

For extended release, at least three specification points should be fulfilled according to European Pharmacopeia. After 1-2 h, around 20-30% drug release should be achieved, to provide assurance against premature drug release. The second specification point should be around 50% drug release to define a dissolution pattern. At least 80% of a final drug release should be obtained for the last point.

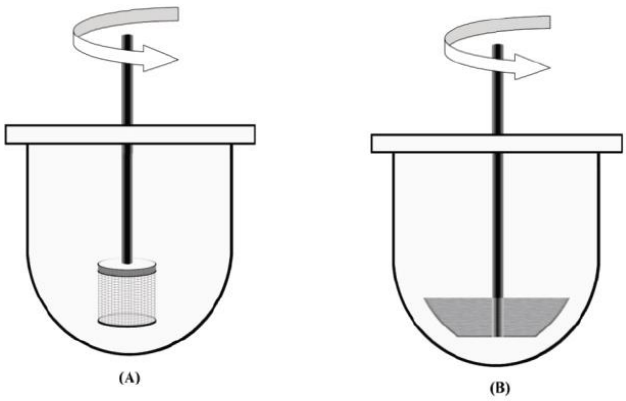

Figure 2.7. Schematic diagram of (a) USP I and (b) USP II [104].

The method for dissolution tests of oral dosage forms is prescribed by EU Pharmacopoeia. When using paddle or basket apparatus, the prescribed volume of the dissolution medium is placed in the vessel, and the apparatus is assembled. The dissolution medium is warmed to 37 ± 0.5°C. The tablet is then placed into the apparatus, and the rotation of the apparatus is started immediately at the prescribed rate. In the case of paddle apparatus and basket apparatus, the aliquots are withdrawn at the prescribed time, at the prescribed intervals or continuously. The volume of aliquots is prescribed. Sampling is performed in the positon midway between the surface of the dissolution medium and the top of the basket and not less than 10 mm from the vessel wall. Except where continuous measurement is used with the basket or paddle method or where a single portion of fluid is removed, it is necessary to add a volume of a dissolution medium equal to the volume of liquid removed. The removed liquid has to be filtered using an inert filter of appropriate pore size that does not cause significant adsorption of the active ingredient from the solution and does not contain substances extractable by the dissolution medium that would interfere with the prescribed analytical method. The analysis of the filtrate

is then performed by UV spectrophotometer or high-performance liquid chromatography (HPLC). The quantity of the active ingredient dissolved in a specified time is expressed as a percentage of the content. The cumulative release is calculated by Eq. (5).

$$cumulative\ release = \frac{C \cdot V}{m_t} \cdot 100\ \%\ , \qquad (5)$$

where C is the concentration of the drug in the release medium after the selected time intervals, V is the volume of the release medium, and m_t is the final amount of the drug within the release medium. At least three replicates should be performed for each formulation.

3 GELATION BY DIVALENT IONS

This chapter investigates the influence of various ions used as cross-linking agents for low-methoxyl pectin (lmP) and alginate (Al) on aerogel characteristics. Calcium, strontium and zinc were used as cross-linkers for lmP, Al and lmP:Al to produce microspheres by the diffusion method. Gels were dried in the presence of supercritical carbon dioxide, and surface area, adsorption capacity, pore size distribution, swelling and erosion of final aerogels were investigated.

TKALEC, G., KNEZ Ž., NOVAK Z., PH sensitive mesoporous materials for immediate or controlled release of NSAID, *Microporous and mesoporous materials*, 224 (2016), 190-200

3.1 Introduction

Both low-methoxyl pectin (lmP) and alginate (Al) and their gelation mechanisms were thoroughly described in the introduction to Chapter 1.5. Both are built of G-G blocks, G-M blocks and M-M blocks. These blocks can be found in different ratios and in different molecular weights, which gives alginate and pectin different physical and chemical characteristics. Although there are a number of different gelation methods for Al and lmP, cross-linking with calcium ions is one of the most widely used methods and can be used with both polysaccharides [105–110]. However, calcium ions can form cross-links by either the diffusion method or the internal setting method. The difference is in the salt being used for the gelation. Gelation with calcium chloride is faster; thus, this is used for the diffusion method. Phosphates or carbonates are then used for the internal setting method, where the gelation is induced by the addition of glucono – δ – lactone. By the diffusion method, the resulting gels are mostly in the form of (micro)spheres. In this method, Al or lmP are usually collected in a solution containing a high concentration of cations, which leads to gel formation. Very often, the polysaccharide solution is dropped into the salt solution in order to obtain small spheres, as shown in Figure 3.1.

The model that describes this gelation mechanism is called egg-box. Figure 3.2 shows the two-step reaction in which in the first step (Step I) calcium ions attach to functional groups on Al or lmP and those groups then loss their reactivity. Further in Step II, bounded calcium ions are still active and therefore they can react with other available functional groups, forming a junction zone between two chains. The constitutive uronic molecules in Al create zones in the gel that are interconnected and this causes the rigidity. But the rigidity is not only determined by the type of polysaccharide but also of the cation, used for the gelation. Namely, atomic number, ionic radius, ionic strength, association constant and chemical affinity toward Al or lmP all take part [111].

Diffusion of calcium ions through Al or lmP depends on the concentration of calcium ions in the reservoir [112]. Zhao *Et al.* [111] used population balance model to describe the sol-gel transition in Al which could be very useful for the examination of relative values of the reaction

rate constants and the gelation time. Other ions could be used for gelation of Al or lmP [113–115]. Kinetics and mechanism of the sol-gel process between Al and some heavy divalent metal ions (Cu, Ni and Co) was investigated by Khairou *Et al*. [116]. Zinc cross-linking was investigated in contrast to calcium. Results show that calcium ions can form more homogenous network than zinc cations (Figure 3.3) [117].

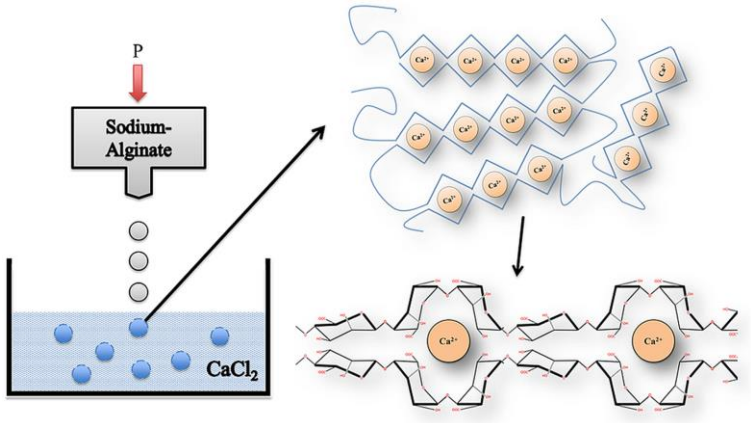

Figure 3.1. Gelation process of alginate. Alginate dropped from an air droplet generator into a $CaCl_2$ solution to form a non-homogenous microcapsule in an "egg" formation. Gels are formed by cross-linking of alginate-polymers with calcium ions between G-G and M-G-blocks. [118]

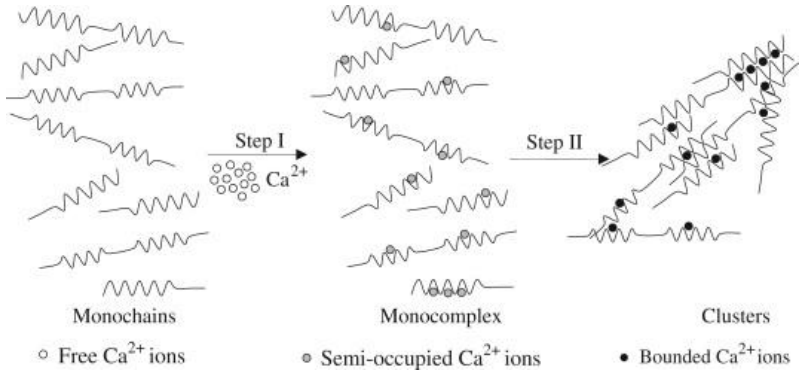

Figure 3.2. Schematic representation of the multiple-step binding of Ca^{2+} ions to alginate [111].

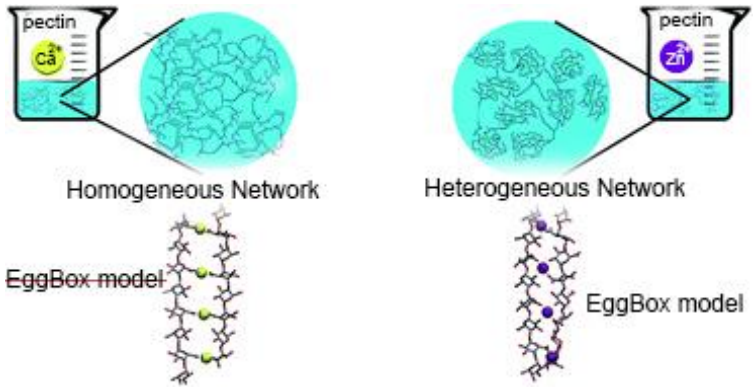

Figure 3.3. LmP cross-linking with calcium and zinc ions [117].

It is proposed that zinc ions interact with carboxylate and hydroxyl groups of galacturonic acid similar to its description in the egg-box model. On the other hand, calcium interacts only with carboxylate groups. It is so that the interactions between water molecules and zinc are stronger. Therefore, zinc binds less easily to pectin than calcium [117]. Alginate's affinity toward the different divalent ions has been shown to decrease in the following order: Pb > Cu > Cd > Ba > Sr > Ca > Co, Ni, Zn > Mn. Binding studies revealed that different block structures in the alginate bind the ions to a different extent. More specifically, Ca^{2+} was found to bind to G- and MG-blocks, Ba^{2+} to G- and M-blocks, and Sr^{2+} to G-blocks solely [119].

Given these findings, the attempt was made to prepare lmP, Al and lmP:Al aerogels by cross-linking with various divalent ions and to investigate their properties. The influence of calcium, strontium and zinc ions on specific surface area, adsorption capacity, pore size distribution, swelling and erosion of prepared aerogels was investigated.

3.2 Experimental

3.2.1 Materials

LmP (citrus, degree of esterification=23-28%, degree of amidation=22-25%) was provided by Herbstreith & Fox and Al was purchased from Sigma Aldrich. Three different salts were chosen for the cross-linking as the source of divalent ions: $Sr(CH_3COO)_2$ – Sigma Aldrich,

$Zn(CH_3COO)_2$ and $CaCl_2$ – Kemika. Prior supercritical drying with CO_2 (Messer), absolute ethanol (Sigma Aldrich) was used to obtain alcogels. The hydrochloric acid and NaCl were from Merck. KH_2PO_4 and NaOH were obtained from Sigma Aldrich.

Hydrochloric acid (HCl) medium (pH 1.2) was prepared by mixing 250 mL of 0.2 M NaCl and 425 mL of 0.2 M hydrochloric acid and diluting to 1000.0 mL with distilled water. A phosphate buffer solution (PBS) with a pH of 6.8 was prepared by mixing 250.0 mL of 0.2 M potassium dihydrogen phosphate and 112.0 mL of 0.2 M sodium hydroxide and diluted to 1000.0 mL with water.

3.2.2 Aerogel formation

The formation of Al and lmP aerogel started with the traditional sol-gel synthesis using the diffusion method (Figure 3.4). Al and lmP were weighed and then slowly transferred to water while stirring, in order to avoid the formation of clumps. Three different polysaccharide solutions were obtained: 2% wt lmP, 2% wt Al and 2% wt Al:lmP (1:1). Each of those solutions was dropped into its respective salt solution (2% wt $Zn(CH_3COO)_2$, $Sr(CH_3COO)_2$ and $CaCl_2$) by using a 5 mL syringe equipped with a 0.8 mm needle. The solutions formed spherical gels immediately upon contact with the salt solution, and these gels were then aged in the cross-linking solution for an additional 1 h in order to achieve the complete inner gelation of spherical gels. The solution was vacuum filtered, and the remaining spherical gels were washed and then stored in water.

Since hydrogels cannot be dried by supercritical CO_2, which was theoretically explained in Chapter 2.1, the dehydration step was performed. In order to avoid the collapse of the gel framework, dehydration took place in stages. Water in the hydrogels was slowly removed by absolute ethanol. First, the hydrogels were exposed and left for 1h in 10% wt ethanol solution. Then the gels were replaced every hour in an ethanol solution at increasing concentrations: 30, 50, 70, 90 and 100%. In this way, shrinkage of the gel was minimised.

The resulting alcogels (gels with alcohol in the pores) were transferred to a 500 mL autoclave, which was filled with absolute ethanol in order to avoid diffusion of the solvent from the alcogels during the heating period. Once the autoclave was sealed, the temperature was slowly raised up 40°C. Then the CO_2 was slowly released into the autoclave (3 bar min^{-1}) until it reached the set value of 120 bars. Samples were dried for 5 h and then the pressure was slowly released. Samples were left to cool down until room temperature and then stored in a desiccator.

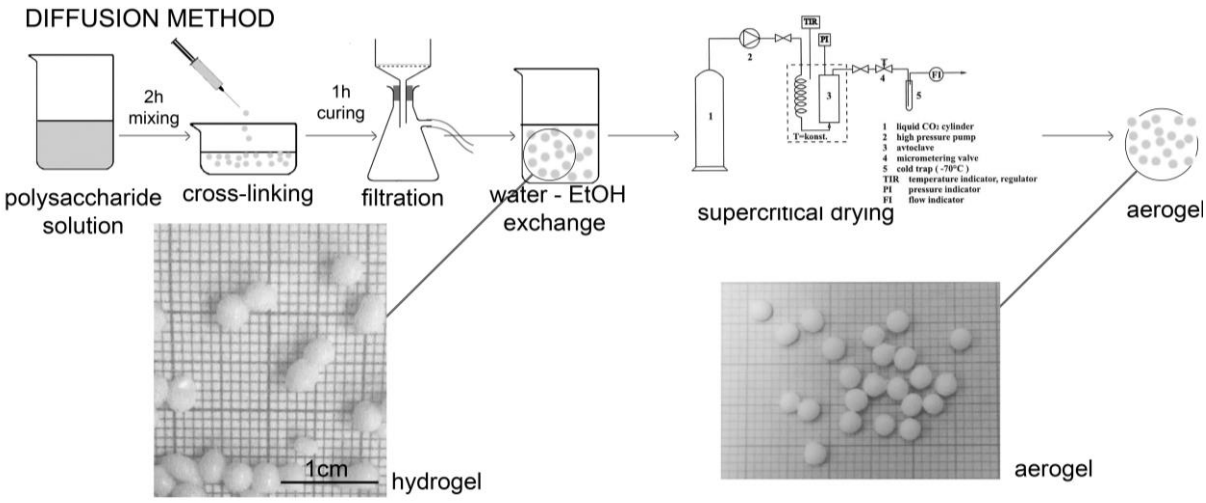

Figure 3.4. Diffusion method for producing aerogels.

3.2.3 Aerogel characterization

The shrinkage after supercritical drying was determined by sieve analysis. At least 100 spherical samples were used for the analysis, which was repeated three times.

Nitrogen adsorption analysis was used to determine the total surface area of the prepared aerogels (Micromeritics Asap 2020MP). The aerogel sample was weighed and then outgassed at 343 K until 10 μmHg was reached. Adsorption-desorption isotherms were registered at 77 K, and the surface area was evaluated by the BET method. The average area of nitrogen at 77 K was assumed to be 0.162 nm^2. Mean mesopore size was determined by the Barrett-Joyner-Halenda (BJH) method from the desorption branch of the isotherm.

Swelling studies were performed as described in Chapter 2.7. Briefly, aerogel samples were weighed and placed in 100 mL of HCl medium at a pH of 1.2 or PBS at a pH of 6.8. Samples were withdrawn after a predetermined time, blotted dry with tissue paper to remove excess solution and weighed. At least three measurements were performed for each sampling. Then the swelling ratio was calculated according to Eq.3.

Aerogel erosion was measured by recording mass lost during the experiment. After the swelling experiments, samples were dried in an oven at 70°C for 24 h until a constant mass was reached. Then the samples were weighed, and the erosion was estimated using Eq. 4.

3.3 Results and discussion

3.3.1 Aerogel formation

The binding of ions is highly selective, and the affinity strongly depends on the Al or lmP composition and sequence. For instance, Zn^{2+} binds to G-G and M-M blocks, Ca^{2+} to G-G and M-G blocks and Sr^{2+} binds only to G-G blocks (Figure 3.5). Therefore, the varying properties of the final materials are the result of the chosen ion.

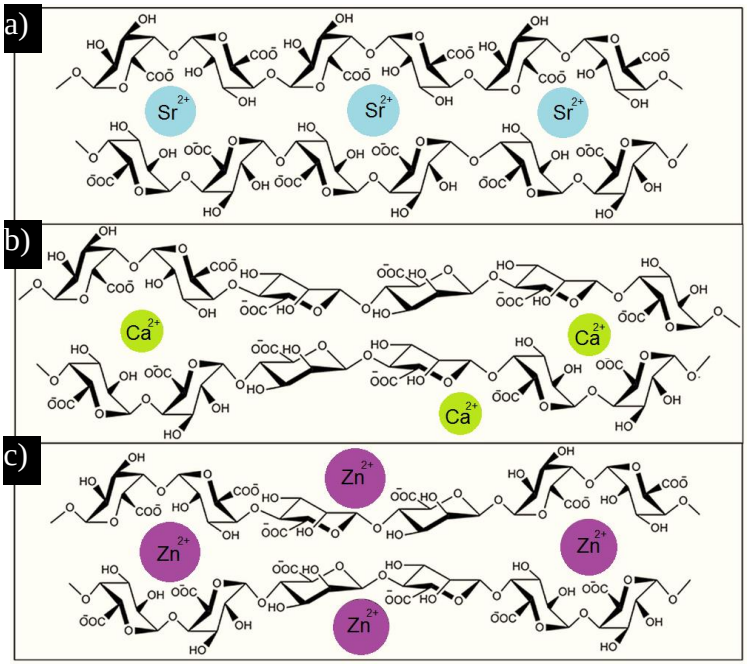

Figure 3.5. Binding of Sr^{2+}, Ca^{2+}, and Zn^{2+} to alginate. Cross linking between ions and G-G and M-M or G-M blocks of alginate occurs in specific conformations, (a) Sr^{2+} binds to G-G blocks solely, (b) Ca^{2+} binds to G-G and M-G blocks, and (c) Zn^{2+} binds to G-G and M-M blocks [118].

3.3.2 Aerogel characterization

Shrinkage of the aerogels was measured by sieve analysis. The diameter of the resulting hydrogels was measured at 2.1 ± 0.2 mm. After supercritical drying, some shrinkage was observed; therefore, the resulting spherical aerogels had a diameter of 1.8 ± 0.3mm (Figure 3.6).

Nitrogen adsorption was used to determine the type of isotherm in the prepared aerogels. Figure 3.7 shows the adsorption isotherm for the sample Al-Zn, obtained from Micromeritics ASAP 2020. All other prepared samples showed the same characteristic isotherm.

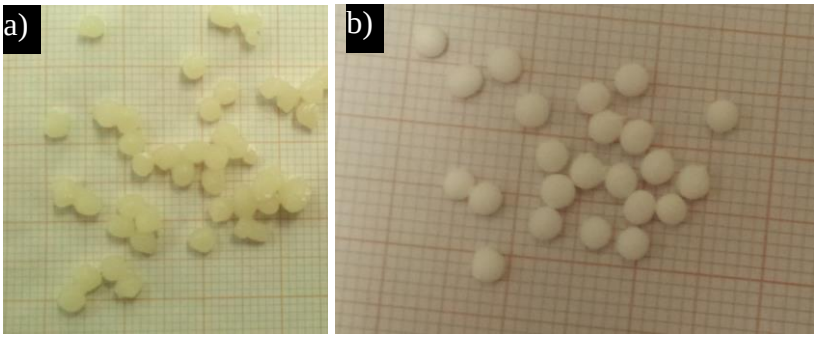

Figure 3.6. Al-Zn A) hydrogels and B) aerogels.

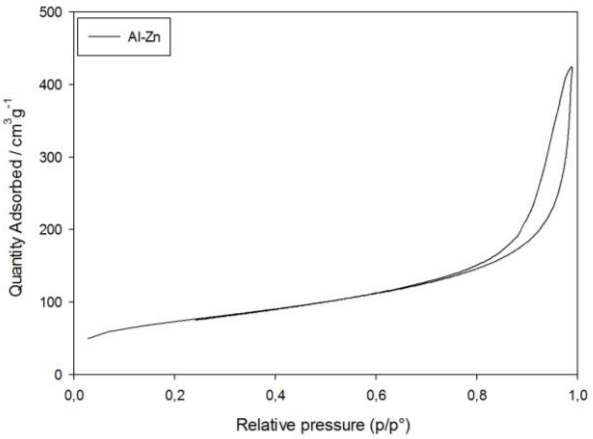

Figure 3.7. Adsorption isotherm for Al-Zn, classified as type IV isotherm.

Isotherms for all prepared aerogels (Al-Zn, Al-Sr, Al-Ca, lmP-Zn, lmP-Sr, lmP-Ca, Al:lmP-Zn, Al:lmP-Sr, Al:lmP-Ca) registered on a Micromeritics ASAP 2020 apparatus are classified as type IV, as specified in Figure 2.2.

Further classification of the type IV isotherm divides the hysteresis loops into four types. As shown in Figure 3.8, H1 and H4 represent two extreme cases, and H2 and H3 are the intermediate situations.

The adsorption and desorption branches of H1 are almost vertical and nearly parallel over an appreciable range of gas uptake. The adsorption and desorption branches of H4 are almost

horizontal and nearly parallel over a wide range of relative pressure. The shapes of hysteresis loops are associated with specific pore structures.

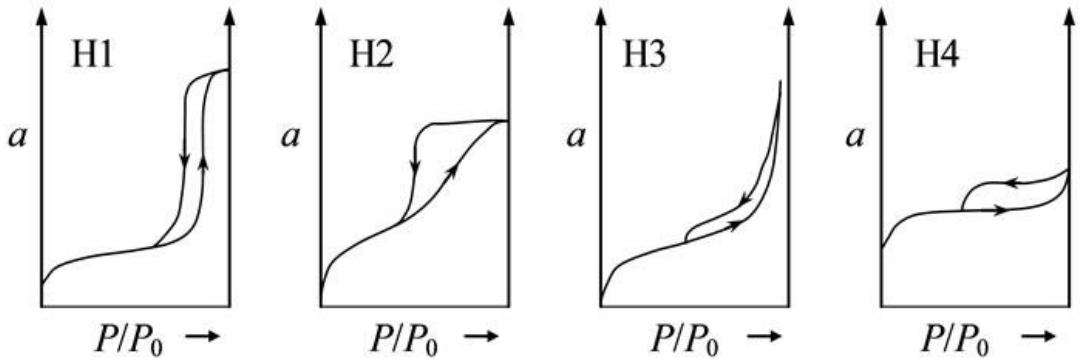

Figure 3.8. Categories of gas adsorption loops (IUPAC).

For example, porous materials that consist of well aligned spheres and briquettes can produce an H1 type loop line, and materials of this type tend to have relatively narrow pore size distributions. For the H2 type loops, the hysteresis loop is wide, and the desorption curve is more precipitous than the adsorption curve. This situation usually occurs when the distributions of pore size radii are wide. The presence of slit-shaped pores and/or panel-shaped particles generates the H3 and H4 curves. However, the exhibition of H4 loops indicates the existence of the micropore.

According to this classification, the isotherm of the sample Al-Zn (Figure 3.7) and all other aerogel samples belong to a type IV isotherm (Figure 2.2) with an H1 hysteresis loop (Figure 3.8). This clearly indicates that polysaccharide aerogels cross-linked with divalent ions are typical mesoporous materials. The detailed data are listed in Table 3.1.

The greatest surface areas were recorded by Ca cross-linked aerogels; however, these aerogels had the smallest mean pore sizes. In contrast, Zn cross-linked aerogels provided the smallest surface areas.

Table 3.1. Nitrogen adsorption measurements.

Sample [a]	**Surface area BET** m^2g^{-1}	**Mean pore size**[b] nm	**Pore volume**[b] cm^3g^{-1}
Al-Zn	261	12.65	0.64
Al-Sr	287	13.14	0.73
Al-Ca	437	11.07	0.94
lmP-Zn	272	16.67	1.44
lmP-Sr	292	16.78	1.56
lmP-Ca	407	13.07	1.09
Al:lmP-Zn	299	14.16	1.14
Al:lmP-Sr	332	11.32	1.03
Al:lmP-Ca	417	10.44	0.85

[a] Al: alginate, lmP: low-methoxyl pectin, Al:lmP: alginate-pectin, Zn: zinc, Sr: strontium, Ca: calcium

[b] Only pores up to 100 nm are taken into account by the BJH method

Among the ions used (Zn, Sr and Ca), Zn has the lowest affinity towards Al and lmP. The gelation is weaker and the cross-links are not so dense, resulting in a smaller surface area. Even though the affinity of Sr towards Al and lmP is higher compared to Ca, the resulting surface area of samples prepared by Sr ions is lower than for those prepared with Ca ions.

In order to investigate the behaviour of the prepared samples in simulated body fluids, swelling and erosion experiments were performed. By immersing an aerogel within body fluid, aqueous solutions enter the gel, transforming the aerogel into a hydrogel. The physical properties of the hydrated gel layer are therefore an important parameter in aerogels, especially when using aerogels for pharmaceutical application and thus performing drug dissolution tests [120]. The pH of the release media (HCl 1.2 and PBS 6.8) affects the cross links between Al or lmP chains and divalent ions. De-protonation of Al and lmP carboxyl groups occurs at higher pH [121]. In an acidic environment, Al and lmP are converted to their parent acids. Pectinic or alginic acid have lower swelling capacities than lmP or Al [120], so it is assumed that they resist the acidic environment of the stomach (pH 1.2) and degrade in the basic medium within the intestines (pH 6.8).

Therefore, minimal swelling was expected within the acidic environment in HCl media at pH 1.2. and the experimental results confirmed our assumptions. The swelling rates were 4.72% and 4.55% for Al-Zn and lmP-Zn, respectively. Higher swelling rates were obtained for Al-Sr (6.42%) and lmP-Sr (5.32%). There was almost no disintegration over the 7 h period. After immersing the samples in a higher pH of 6.8 (PBS), the samples started to swell rapidly. This behaviour is shown in Figure 3.9.

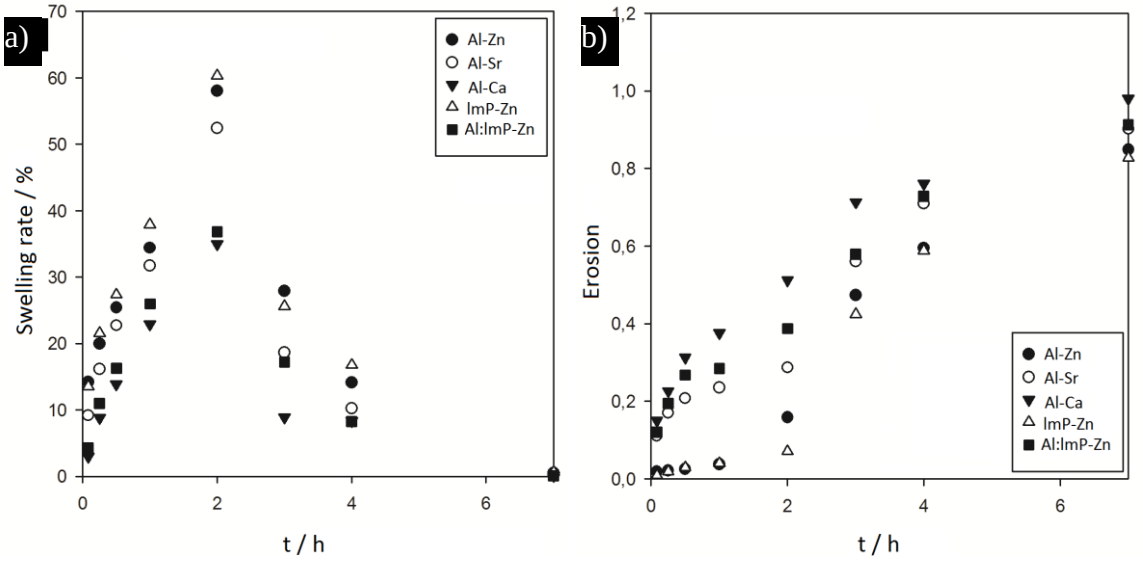

Figure 3.9. a) Swelling and b) Erosion of the aerogels, cross-linked with zinc, strontium and calcium in PBS (pH 6.8)

As shown in Figure 3.9a, the lmP-Zn samples can achieve the highest swelling rate, up to 60%. For all samples, the highest swelling rate is achieved after 2 h, after which, the swelling rate again decreases, showing in the sample's mass loss. Figure 3.9b shows the results of erosion tests. For all surface-eroding devices, the mass loss should be linear. Here, the polymer chain cleavage is much faster than the water intrusion into the material. Erosion therefore affects only the outermost layers. In contrast, if the water uptake is faster than the degradation, bulk erosion occurs [122,123]. The water uptake in Ca cross-linked aerogels is high. Therefore, bulk erosion occurs quickly after contact with the buffer solution. On the other hand, water uptake in Zn

cross-linked aerogels is slower and so is the erosion. Complete degradation of Al-Ca aerogel occurs after 7 h. The most stable aerogel after this time is lmP-Zn, with only 80% degradation.

4 ETHANOL INDUCED AEROGEL FORMATION

The fourth chapter of this thesis describes the development of a new method for the formation of polysaccharide aerogels. Ethanol was used for the formation of pectin, alginate, xanthan and guar aerogels. Formation of hydrogel and the dehydration step were avoided in this process. The polysaccharide aerogels obtained by this method possessed outstanding properties, including a porosity of up to 97% and a surface area up to 500 m^2g^{-1}. Pectin aerogels possessed lower thermal conductivity than that of still air. The production process for alginate aerogels was optimised in order to obtain materials with higher surface areas and lower thermal conductivity. Methanol was chosen as the best solvent for the formation of alginate aerogels.

TKALEC G., KNEZ Z., NOVAK Z., Formation of polysaccharide aerogels in ethanol, *RSC Advances*, 5 (2015), 77362-77371.

TKALEC G., KRANVOGL R., PERVA-UZUNALIĆ A., KNEZ Z., NOVAK Z., Optimisation of critical parameters during alginate aerogels' production, *Journal of Non-Crystalline Solids*, 443 (2016), 112 – 117.

HORVAT G., FAJFAR T., PERVA-UZUNALIĆ A., KNEZ Z., NOVAK Z., Thermal properties of polysaccharide aerogels, *Journal of Thermal Analysis and Calorimetry*, (2016), 1 – 8.

4.1 Introduction

The sol-gel process is essential for the production of all aerogels. Briefly, wet gels are produced by chemical or physical gelation, as previously described in Chapter 1.5. With physical gelation, the resulting gels are usually weaker, since the interactions between chains are weaker. Bonds between the chains are formed by ionic bonds, hydrogen bonds or hydrophobic bonds, as presented in Figure 4.1.

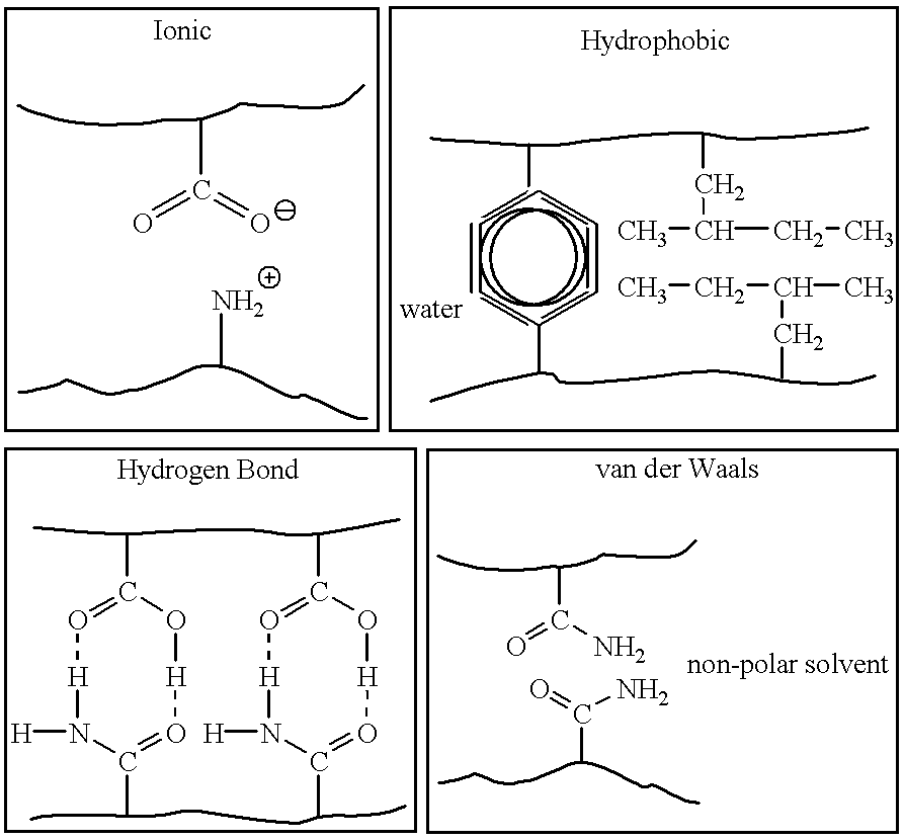

Figure 4.1. Types of interaction in the process of gelation [124].

Until now, LmP aerogels had been prepared mostly by cross-linking with calcium or other divalent ions [125,126] and hmP aerogels by thermal or acidic gelation [1,82,127,128]. Alginate aerogels have been highly researched materials in recent years [129–131]. The gelation of this naturally-occurring polysaccharide is obtained by divalent or multivalent

cations (except Mg^{2+}) [132]. Xanthan gum/Clay aerogels were prepared by Wang et al. [133]; however, pure xanthan or guar aerogels have never yet been prepared. Recently, the gelation of xanthan gum was performed in glycerol [134], but only wet gels were produced in this research. Guar freeze-dried aerogels were prepared by enzymatic oxidation and possessed some outstanding properties, such as high compressive modulus [135]. Table 4.1 briefly summarizes the already prepared polysaccharide monolithic aerogels, together with their specific surface areas.

Long production times for aerogel preparation, together with high organic solvent consumption has led us to investigate new possibilities for polysaccharide aerogel production. This high consumption of organic solvents (mostly alcohol) is the result of the interexchange between water and the organic solvent before supercritical drying. Therefore, a new method of producing polysaccharide aerogels should be developed and presented in order to decrease organic solvent consumption and reduce overall processing time to make those polysaccharide aerogels more desirable and industrially applicable.

The conventional route for polysaccharide aerogel preparation is presented in Figure 4.2, following the black arrows. The simplest way to decrease organic solvent consumption and total production time is then clearly seen from the same Figure 4.2, marked with a green arrow. It simply shows that, in order to decrease the consumption of organic solvents due to the dehydration step, wet gels should be prepared directly in alcohol. Hence, the production of hydrogel is avoided and the resulting alcogels are directly dried with supercritical carbon dioxide.

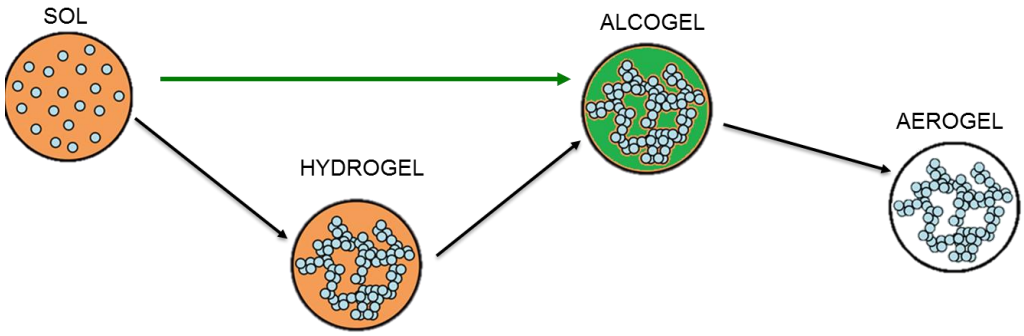

Figure 4.2. Hypothetic production of polysaccharide aerogels, avoiding high organic solvent consumptions and large processing times.

Table 4.1. Specific surface areas of monolithic polysaccharide aerogels.

Aerogel	**Crosslinking method**	**Polysaccharide concentration** %	**S_{BET}** m^2g_{-1}	**Reference**
hmP	Acid gelation	5	200	[128]
hmP	Thermal gelation	6	247	[127]
hmP	Acid gelation	2-6	230-270	[82]
lmP	Calcium ions	2 2	213 (apple) 248 (citrus)	[125]
Al	Calcium ions	2	150-300	[136]
Al	Acid gelation	2	391	[137]
Al	Cation ions	1	298-374	[137]
Al	Cation ions	1	187-356	[138]
Al	Cation ions	0.25-2.98	545-264	[84]
Starch	Thermal gelation	2	72 (potato) 90 (corn)	[136]
Cellulose	NaOH	1	200	[139]
Cellulose	NaOH	5-7	200-240	[140]
Cellulose	Ionic liquids	3 15	230 130	[83]
Cellulose	Catalyst	1	500-600	[141]
Chitin	Acid gelation	1	560	[142]

Since most of the naturally occurring polysaccharides are soluble only in water, the task of preparing alcogels directly was not easy. After making a literature review, we found that hydrophobic interactions in polysaccharides are increased with the addition of alcohol [143]. This was then the outline for further research. Hydrophobic interactions are among the

possibilities for the production of gels. Thus, we assumed that polysaccharides can form gels only by the addition of alcohol. The hypothetical model is presented in Figure 4.3.

Hence, we further investigated the applicability of the model by preparing polysaccharide aerogels in ethanol. The first part of the research was performed on pectin and subsequently on other polysaccharides, e.g., alginate, xanthan and guar.

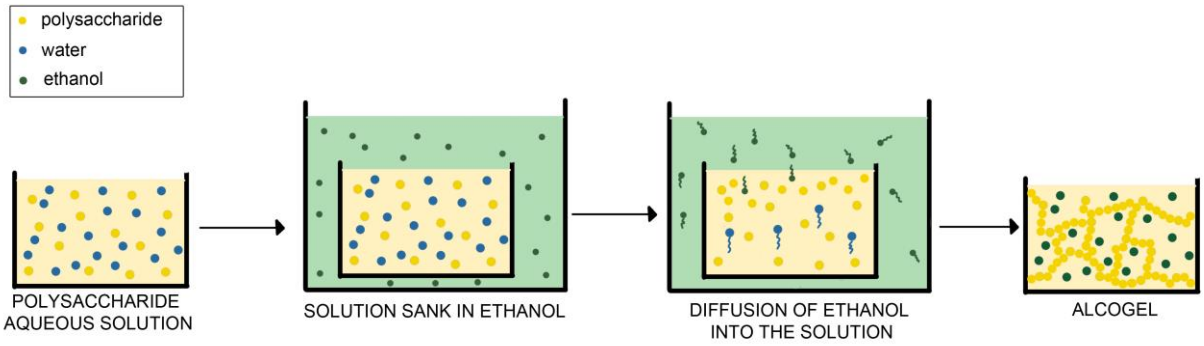

Figure 4.3. The ethanol induced gelation – a model.

High-methoxyl pectin aerogels

4.2 Experimental

4.2.1 Materials

High-methoxyl pectin (hmP) (Pectin Classic CU-L 069/13, degree of esterification: 78%) was kindly provided by Herbstreith&Fox. Absolute ethanol (Sigma Aldrich) was used to induce the gelation of polysaccharides. Wet gels were dried with supercritical CO_2 (Messer).

4.2.2 Aerogel formation

The initial part of the research involved investigating the proper concentration of polysaccharide solution in order to achieve the best properties in the final material. HmP was dissolved in water in order to form 1%, 2% and 4% solutions. To each solution, 10 v/v% ethanol was added. The solutions were then transferred to molds and immersed in absolute ethanol for an additional 1 h. The process is presented in Figure 4.4.

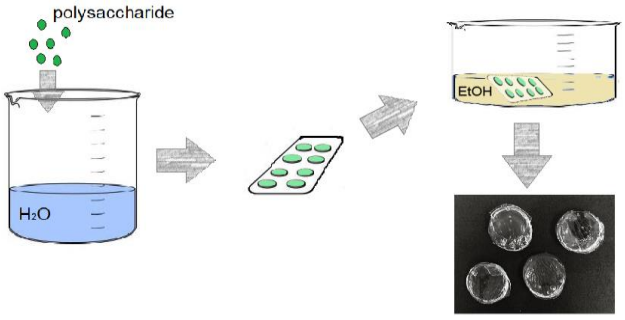

Figure 4.4. Production of polysaccharide alcogels by ethanol-induced gelation.

Supercritical drying was chosen to obtain dry materials with their structure unchanged. No solvent exchange was needed prior to the drying. The wet gels were placed in a 500 ml autoclave filled with 100% ethanol. The autoclave was heated to 40°C, and then the pressure was slowly increased to 150 bar. After 6 h of drying at the desired temperature and pressure, the autoclave was slowly depressurized and left to cool down.

4.2.3 Aerogel characterization

Nitrogen adsorption measurements for polysaccharide aerogel monoliths were performed by outgassing the samples; the adsorption-desorption isotherms were then obtained at 77 K. Surface area was determined by the BET method and mean pore size by the BJH method from the desorption side of the branch.

Scanning electron micrographs of the prepared aerogel samples were obtained using a Sirion 400NC field emission scanning electron microscope (FESEM). The samples were fractioned and then sputter-coated with gold particles and scanned at an accelerating voltage of 5-10 kV.

Aerogel shrinkage was determined by measuring the diameter and height of the alcogels and the resulting aerogels with a digital caliper.

Porosity was determined as the ratio between bulk and true density by Eq. 6:

$$\varepsilon(\%) = (1 - \frac{\rho_B}{\rho_T}) \cdot 100 \quad (6)$$

where ρ_B is the bulk density of the aerogel, and ρ_T is the true density of the aerogel.

True densities (ρ_T) of the aerogels were measured by gas pycnometer (Micromeritics AccuPyc II 1340). Bulk densities were then determined as the ratio of mass to volume. The mass of the aerogel was determined by five-digit analytical balance, and the volume was determined by measuring the diameter and height of an aerogel of cylindrical shape.

4.3 Results and duscussion

4.3.1 Aerogel formation

This chapter describes a new method for the formation of polysaccharide gels. The first part of the research is devoted to the formation of hmP gels. It is proposed that junction zones are strengthened by hydrophobic interactions between methyl ester groups. These are needed to overcome the entropic barrier to gelation [143].

An immediate increase in viscosity was observed after the addition of 10% wt ethanol to the hmP solution. Therefore, the hmP solutions were mixed and after the homogenization transferred to molds, which were then immersed into absolute ethanol. The time of gelation was

strongly influenced by the size of the monolith. Tablet shaped wet gels (15 mm in diameter) became set in 1 h.

Gelation is governed by the diffusion of ethanol into the polysaccharide aqueous solution (Figure 4.5). Selected polysaccharides are soluble in water but poorly soluble in ethanol. As the solvent exchange occurs, hydrophobic interactions are strengthened. The affinity of polysaccharide is greater between the polysaccharide molecules than between polysaccharide and ethanol. Therefore, polysaccharide molecules bind together, leaving ethanol in the pores. Ethanol can then be easily removed by supercritical drying without collapsing the inner structure of the gel.

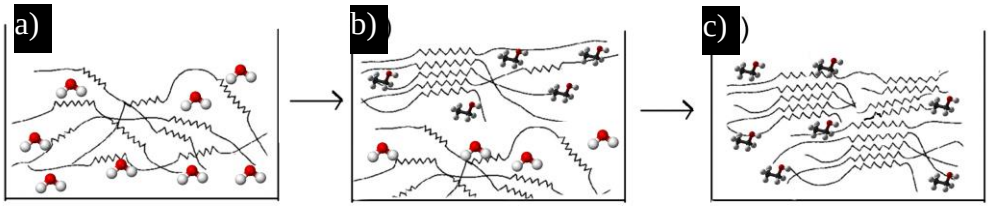

Figure 4.5. Gelation, governed by the diffusion of ethanol into the aqueous solution.

Three different concentrations of hmP were used to prepare aerogels in order to investigate the impact of concentration on the morphological characteristics of the dry material. Figure 4.6 shows hmP alcogel on the left, and the obtained aerogels on the right. It is apparent that the concentration of hmP has a significant impact on shrinkage of the gel during supercritical drying. All three aerogels were dried together under the same conditions in the specially designed autoclave. Therefore, all other impacts except the concentrations were limited

From Figure 4.7, it can be concluded that the lower the pectin concentration, the higher the shrinkage. Moreover, a clear trend can be observed. By increasing the concentration by 1%, shrinkage decreases by 6.66%. A possible option to avoid shrinkage among 1% and 2% hmP gels would be longer aging in absolute ethanol, hence providing denser cross links and a more stable inner structure for those gels.

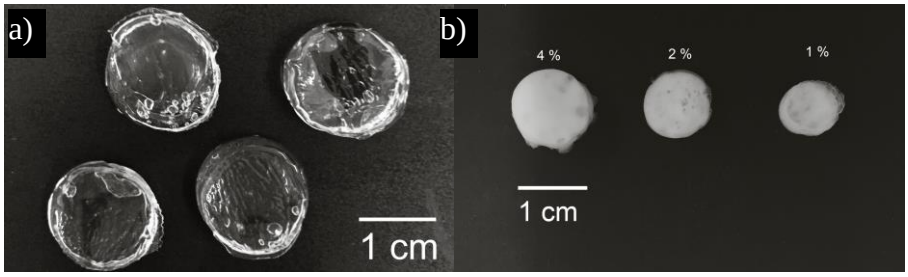

Figure 4.6. hmP A) alcogels and B) aerogels.

Additionally, Figure 4.7 shows the difference between the drying of aerogels at two different pressures, 150 bars and 200 bars. It is observable that higher pressures do not necessarily mean less shrinkage (see 4% hmP aerogel). In 1% and 2% hmP aerogels, the shrinkage is not significantly lower and surely does not cover the cost of higher pressures.

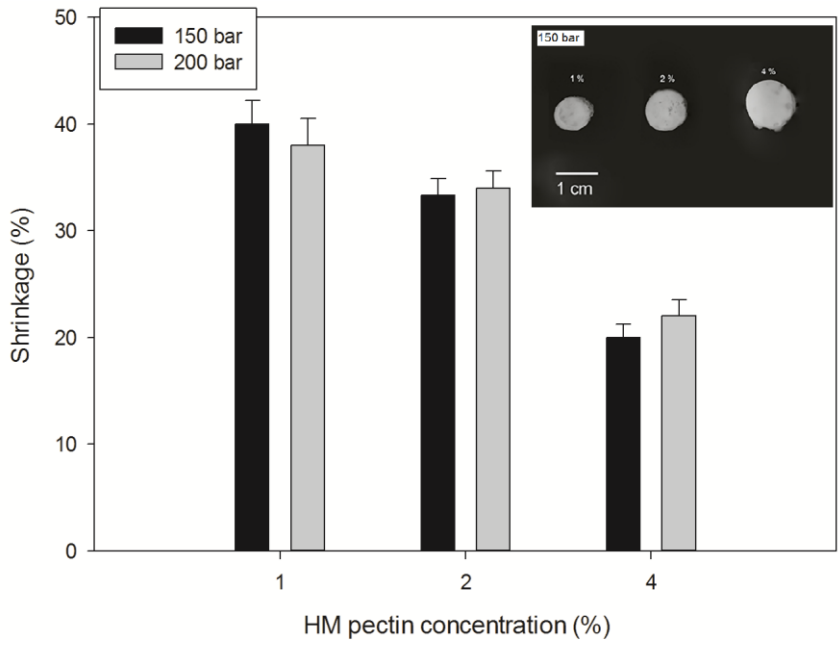

Figure 4.7. Shrinkage of obtained monolithic aerogels after supercritical drying under 150 bar and 40 °C and 200 bar and 40 °C.

4.3.2 Aerogel characterization

Nitrogen adsorption was employed for determining the surface area, pore size distribution and pore volume of the prepared 1, 2 and 4% hmP aerogels. Surface area is determined when relative pressures P/P_0 are lower than 0.05, and nitrogen is adsorbed in the form of single molecules. With an increase in relative pressure, multi-layered adsorption and subsequent capillary condensation occur in some small micropores which are larger than the pore of monomolecular adsorption, accompanied by increases in the amount of adsorption. When the relative pressure achieves a particular high value, capillary condensation approaches the largest pore size, and the processes of adsorption and condensation are terminated. With a decrease in relative pressure, the absorbed nitrogen begins to desorb, and the adsorption layers weaken. When the relative pressure decreases to a certain point, capillary evaporation occurs, and the condensed nitrogen starts to desorb, providing the adsorption isotherms and pore size distribution. Adsorption isotherms were obtained by the BJH method and were of class IV (Figure 4.8a), which is typical for mesoporous materials according to IUPAC classification (Figure 2.2). The hysteresis loop occurs when the adsorption and desorption branches of the adsorption isotherms do not coincide. The shapes of the hysteresis loops provide information about pore structure. Therefore, the pore structures of various materials can be indirectly analysed by investigating the hysteresis loops. When the shapes of the capillary pores are similar, the relative pressure of evaporation and condensation are equal, and the adsorption and desorption branches of the adsorption isotherm coincide, so there is no hysteresis.

Results for pore size distribution obtained with nitrogen adsorption-desorption and the BJH method are presented in Figure 4.8b. Micropores (< 2nm) were not considered in the evaluation. The largest surface area was achieved by 4% hmP aerogel, 384 m^2g^{-1} and the least by 2% hmP aerogel (Table 4.2). However, these low variations could be attributed to experimental error. The surface area of 2% hmP aerogel was 8% lower than for 4% hmP aerogel. Even more, pore size was comparable among all three samples. Pore size decreases along with increased concentrations of pectin. The volume was slightly higher in the case of 4% hmP aerogel, which certainly has an impact on the greater porosity of those samples.

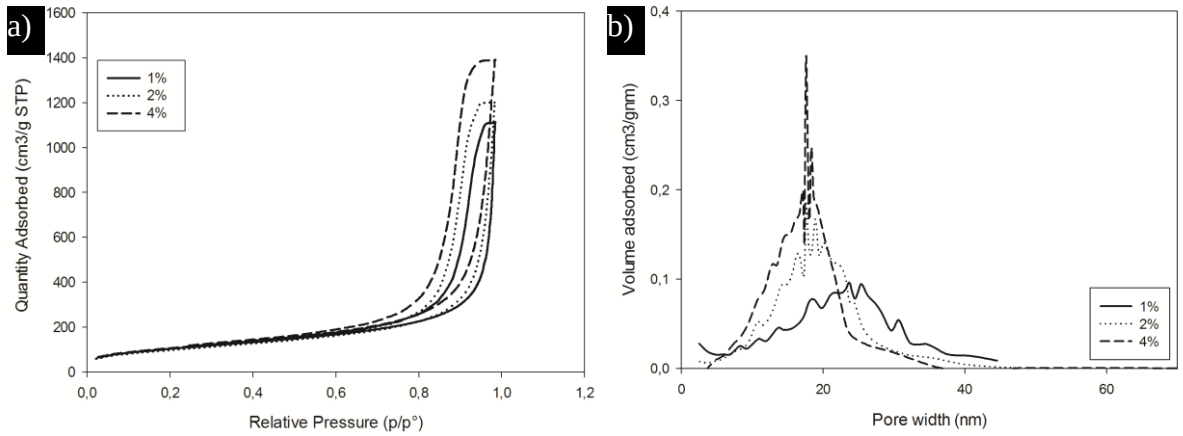

Figure 4.8. Nitrogen adsorption analysis. a) Adsorption-desorption isotherms and b) pore size distribution for different hmP concentrations.

Table 4.2. Physicochemical characterization of hmP aerogels, prepared at 40 °C and 150 bar.

Sample	ε / %	S_{BET} / m^2g^{-1}	Pore size / nm	Pore volume / cm^3g^{-1}
1 % hmP	70.8 ± 0.8	374	17.08	1.73
2 % hmP	75.3 ± 0.9	354	16.67	1.86
4 % hmP	95.7 ± 0.6	386	15.64	2.15

These surface areas are the highest yet reported in the literature concerning hmP aerogel monoliths. Until now, to our knowledge, monolithic hmP aerogels have only been prepared by White et al [128], Rudaz et al [82] and González-García et al [127], who obtained the largest surface area of S_{BET} = 200 m^2g^{-1}, S_{BET} = 270 m^2g^{-1} and S_{BET} = 284 m^2g^{-1}.

Rudaz et al. [82] prepared high methoxyl pectin aerogels by dissolving pectin in HCl aqueous solution and then leaving it to gel for 24 to 48 h. The sample was then coagulated with 50% ethanol and dried with supercritical CO_2. González-García et al [127] and White et al [128] both used thermal gelation with the addition of ethanol.

The porosities for 4% hmP aerogels were high, around 96%. HmP aerogels prepared from lower concentrated solutions showed less porosity, which is probably caused by the greater shrinkage of those gels. The SEM picture (

Figure 4.9) shows the highly compact structure of hmP aerogel.

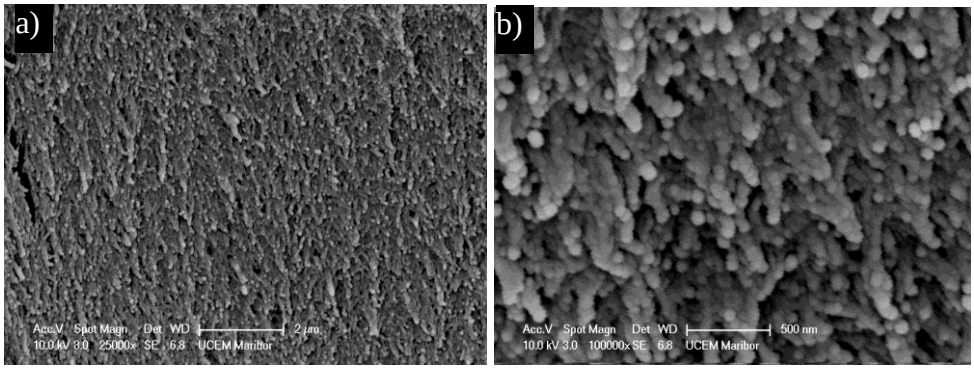

Figure 4.9. SEM micrographs of 4% hmP aerogel at 25,000 times magnification (a) and 100,000 times magnification (b).

Pectin, alginate, guar and xanthan aerogels

Based on the research on hmP aerogels, later research was performed using other polysaccharides, such as low-methoxyl pectin (lmP), alginate (Al), guar (Gu) and xanthan (Xa).

4.4 Experimental

4.4.1 Materials

LmP (citrus, degree of esterification=23-28%, degree of amidation=22-25%) was kindly provided by Herbstreith&Fox. Al, Gu and Xa were purchased from Sigma Aldrich.

4.4.2 Aerogel formation

Polysaccharide aqueous solutions (4 wt%) were prepared. Ethanol was added (10 wt%) to the homogenised solution, after which the solution was transferred to molds. These were immersed in 100% ethanol, whereupon the surface layer gelled immediately. Tablet shaped gels were left in ethanol for an additional 1 h until complete gelation and then dried above supercritical conditions of CO_2.

4.4.3 Aerogel characterization

All prepared polysaccharide aerogels were characterized as previously described in Chapter 4.2.3. Additionally, the thermal and rheological properties of aerogels were determined as described below.

Thermogravimetric analysis (TG) of the materials was carried out with a TGA/DSC1 Mettler Toledo instrument. About 10 mg of the sample was placed in the crucible and heated at a rate of 10°C min^{-1} to 600°C. As described in the literature [144], heating rates between 5 and 20°C min^{-1} do not markedly influence the final signal. 10°C min^{-1} is suggested as the most suitable compromise between the time and resolution of the analysis. The initial decomposition temperature (*IDT), $T_{20\%}$, $T_{50\%}$* of mass loss, the temperature of the maximum mass loss (T_{max}) and the residue after 600°C were determined.

Thermal transitions were studied using a differential scanning calorimeter (DSC) with a 10°C min^{-1} heating-rate. DSC analysis was performed for studying the phase transitions of melting, glass transitions and exothermic decomposition. The analysis was performed on a TGA/DSC1 Mettler Toledo instrument. The temperature range during analysis was set at between 30°C and 600°C.

To determine the thermal conductivity of prepared aerogels, a 40 µL light aluminium crucible without a lid was used. Thermal conductivity was determined as described in Chapter 2 and in

Figure 2.5. Pure indium (80 mg) was measured into the crucible. The bottom of the crucible was completely covered when the indium melted.

Aerogels were prepared in the form of discs with a height of 0.5 to 1.5 mm. The circular end surfaces were carefully polished with fine emery paper so that the height and diameter could be accurately determined. The diameter of the sample was the same as that of the bottom of the crucible (6 mm). Silicone oil was placed on the sensor and on the bottom of the lid, which was then placed onto the sample. Excess oil was removed before placing the sample on the sensor. The oil was used only to provide complete contact between the surfaces. The aerogel sample was then placed directly on the sensor. The crucible with indium was placed precisely and directly on top of the sample. The silicone oil at the bottom of the crucible essentially fixed the crucible at the top of the sample and allowed it to be precisely oriented. An empty crucible was used as a reference site.

The measurements were performed on an HPDSC1 Mettler Toledo. Heat flow was measured by heating from 153 to 162°C at 0.5°C min^{-1}. The purge gas was nitrogen, with a gas flow of 50 ml min^{-1}. The slope S was determined from the thermogram, and thermal conductivity was calculated by Eq. 2. The experimental results are expressed as the mean ± standard deviation (SD) of three parallel experiments (n=3).

Rheological measurements were performed at Anton Paar Ljubljana on a MCR302 Rheometer. 1-2 mm thick wet gels were measured by the amplitude sweep (AS) method. The temperature for all measurements was 25°C.

4.5 Results and discussion

4.5.1 Aerogel formation

It was reported in the literature [145] that xanthan gum cannot form a gel individually but only together with locust bean gum. By employing the new method, we were able to produce stable xanthan gels without the addition of any other polysaccharide.

The gel formed by the diffusion of ethanol into the polysaccharide solution. The surface layer gelled immediately. Inner layers of the polysaccharide solution, however, gelled as ethanol diffused into the solution, strengthening the hydrophobic interactions and inducing gelation. Therefore, the gelation time is dependent mainly on the diffusion path. In other words, if the height of the mold is low, the gelation time is much lower compared to higher molds where the diffusion time is much longer. Rheology measurements were performed on the alcogels (Figure 4.10). The greatest difference between the storage and the loss modulus was observed in the lmP alcogel. Here the loss modulus (G'') was around 30% of the elastic modulus (G'), which indicates full elasticity of the system. Other polysaccharide gels provided similar results (G'>G''), although the difference between the figures was lower.

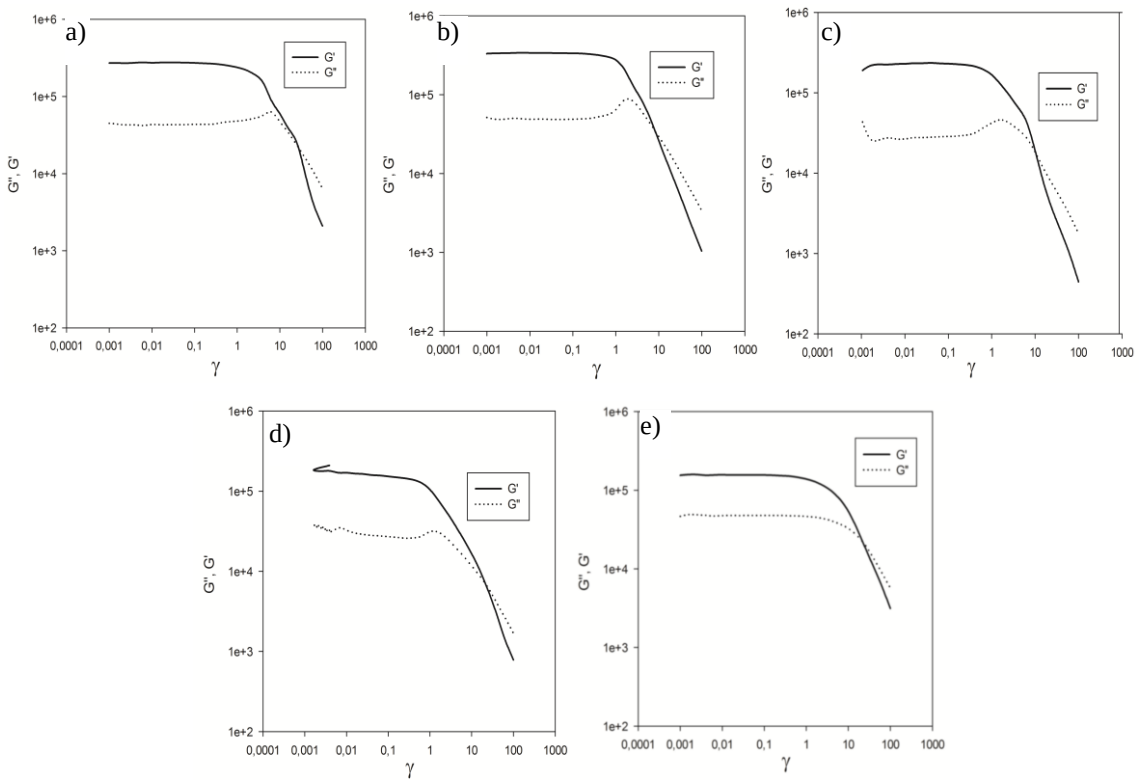

Figure 4.10. Strain sweep experiments of polysaccharide alcogels at constant frequencies. a) hmP, b) lmP, c) Xa, d) Al and e) Gu.

When strain is increased, the elastic structure breaks down. Consequently, the elastic modulus decreases. At the point where the G'' becomes greater than G' it is a crossover strain, and here the elastic structure is broken. The loss modulus was similar for all the samples; the greater difference was observed in the elastic modulus. The elastic modulus decreased in order, starting with lmP, hmP, Xa, and ending with Al and Gu. The same behaviour was subsequently observed in aerogels when measuring the surface area and porosity, as well as the thermal conductivity. Therefore, it is clear that all these variables are connected and depend mostly on the type of polysaccharide.

4.5.2 Aerogel characterization

The obtained aerogels (Figure 4.11) were characterized by nitrogen adsorption and SEM. Thermal properties together with thermal conductivity were analysed by TG/DSC. One of the main properties of aerogels is their low density. Bulk density was determined by pycnometer. True densities were determined as the ratio mass/volume. Then the porosity of aerogels was determined as the ratio between bulk and true density. Table 6 collates the results of aerogel characterization.

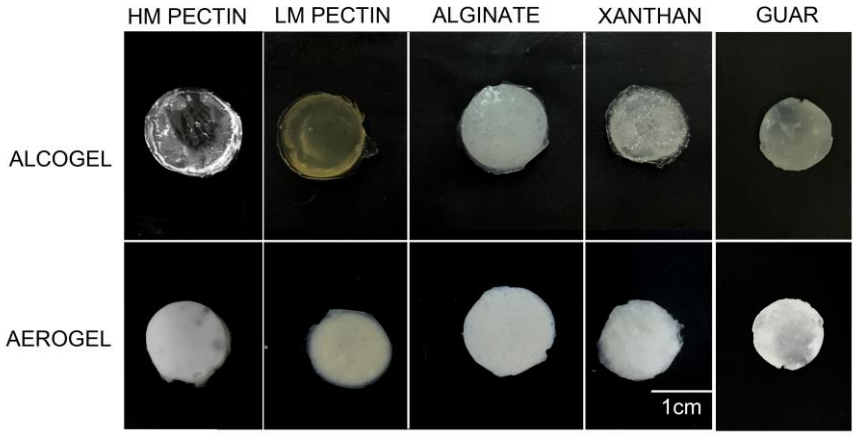

Figure 4.11. Ethanol induced gelation of some polysaccharides: from alcogels to aerogels

It has been observed that lmP aerogels possess the lowest bulk density and the highest porosity. Moreover, this also results in an extremely large surface area, which is the largest yet reported in the literature, according to Table 4.1. the greater surface areas were obtained by preparing small spherical aerogels [110]. The surface area of hmP and Xa aerogels was also high, more than 300 m^2g^{-1}. This is also the largest reported surface area for both hmP and Xa monolithic aerogels. It must be admitted that pure Gu or Xa aerogels have never been prepared. This gelation method thus seems highly promising for these types of polysaccharides. However, Al aerogels with better results have already been prepared. Thus, this method for producing Al monolithic aerogels should be further improved and optimized.

Adsorption isotherms (Figure 4.12) exhibit behaviours similar to those for different concentrations of hmP. All isotherms belong to Class IV, and aerogels are therefore classified as mesoporous materials. HmP aerogels seem to have the highest capacity to adsorb gas. This is probably due to the high pore volume and high surface area. As expected, Gu and Al aerogels have low adsorption capacity. The difference between aerogels is indeed the result of polysaccharide structure. It is assumed that hydrophobic interactions are increased in the case of lmP, hmP and Xa. The polysaccharide chains get closer, and the final gel is more porous and consequently has a larger surface area, hence higher adsorption capacity.

Table 4.3. Characterization of polysaccharide aerogels.

Sample	ρ_B [c]	ρ_T [c]	ε [c]	S_{BET}	**Pore volume**	**Pore size**
	gcm^{-3}	gcm^{-3}	%	m^2g^{-1}	cm^3g^{-1}	nm
hmP	0.0861 ± 0.0022	2.5805 ± 0.0551	96.6 ± 0.01	384	1.84	19
lmP	0.0771 ± 0.0008	2.5700 ± 0.0523	97.0 ± 0.03	510	1.87	17
Xa	0.0961 ± 0.0021	1.8742 ± 0.0150	94.9 ± 0.01	363	1.50	20
Al	0.1569 ± 0.0061	3.1804 ± 0.0325	95.0 ± 0.16	147	0.34	14
Gu	0.2942 ± 0.0065	2.2451 ± 0.0233	86.9 ± 0.16	111	0.38	15

[c] the results are given as the mean value ± standard deviation of five replicates.

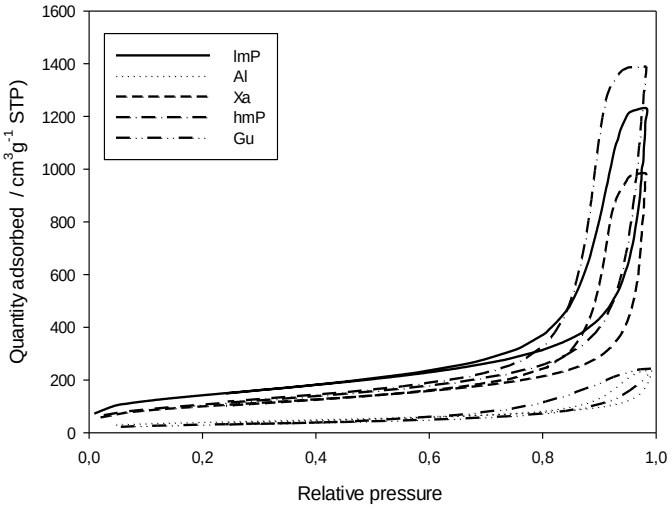

Figure 4.12. Adsorption-desorption isotherms of polysaccharide aerogels.

Scanning electron measurements were performed to characterize the novel materials and mainly to visually investigate their structure. The gaps in Figure 4.13 are the result of low hydrophobic interactions. Unfortunately, we could not observe meso- or microporosity at those magnitudes. As is evident from Table 4.3 the average pore size in prepared aerogels is less than 20 nm. This could not be seen in the SEM figures, owing to the lower magnitudes. In contrast, nitrogen adsorption analysis did not generally allow us to measure macropores larger than 100 μm. Therefore, the results from nitrogen adsorption and SEM could not be compared but instead are discussed separately. However, together with gas adsorption analysis, we can conclude that in hmP, lmP and Xa aerogels, hydrophobic interactions cause denser cross-linking, resulting in increased micropore and mesopore volume. This phenomenon is thus responsible for those materials being mechanically stable, in contrast to the brittle alginate and guar aerogels.

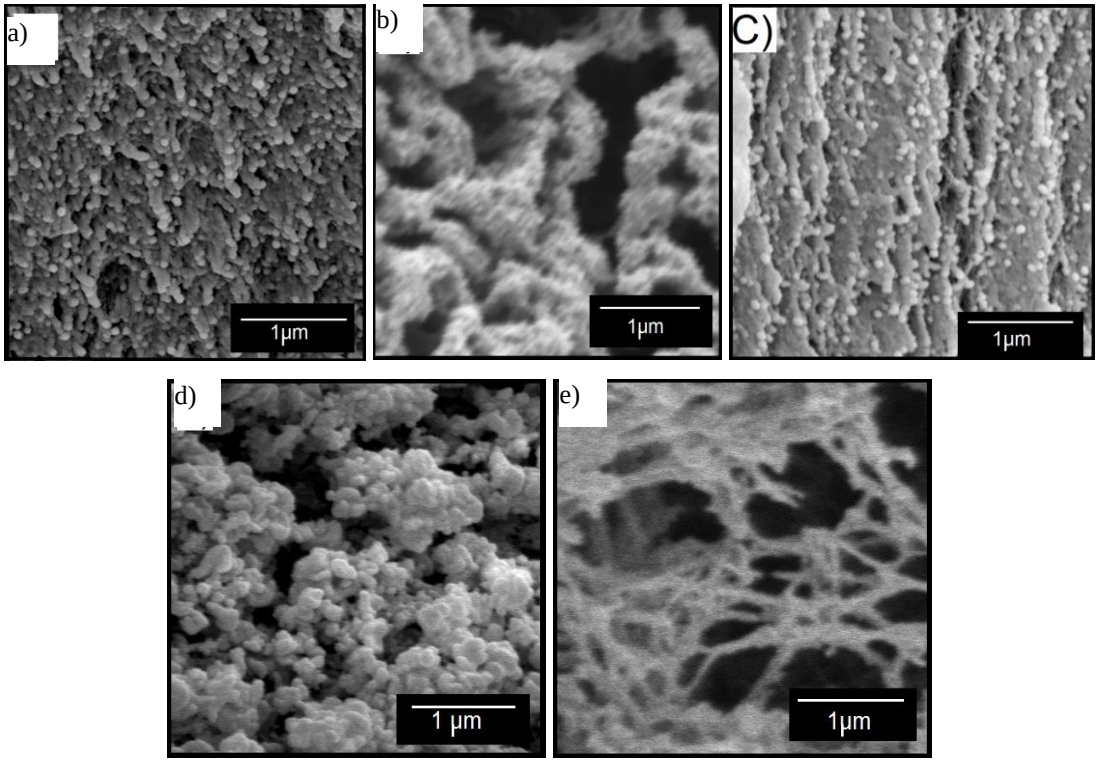

Figure 4.13. SEM figures of a) hmP, b) lmP, c) Xa, d) Al and e) Gu.

The thermal behaviour of all the samples was investigated by means of thermogravimetry (TG) and differential scanning calorimetry (DSC). TG curves obtained at the heating rate of 10°Cmin^{-1} in inert conditions are presented in Figure 4.14. The main parameters evaluated on the basis of these curves are presented in . Parameters obtained from TG curves include the initial decomposition temperature (*IDT*), temperature of 20% mass loss ($T_{20\%}$), temperature of 50% mass loss ($T_{50\%}$), residue after 600°C and the temperature of the maximum mass loss (T_{max}), which was determined from the first derived mass loss.

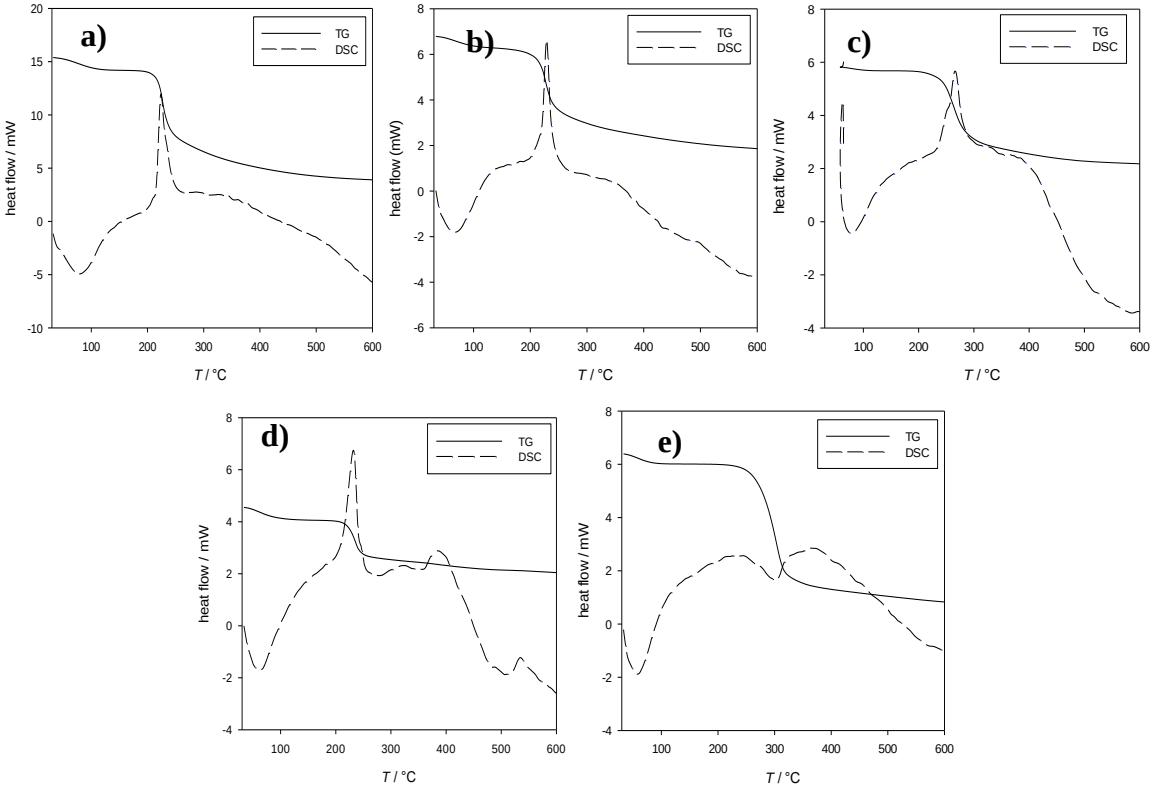

Figure 4.14. TG/DSC of a) hmP, b) lmP, c) Xa, d) Al and e) Gu aerogels.

The TG curves in Figure 4.14 show that lmP, hmP, Xa and Gu aerogels decompose in one step. Initially at around 70°C, the loss of remaining ethanol is present in all samples. Then the degradation occurs in one step for each polysaccharide individually. Al aerogel decomposes like pure alginic acid [144]. This makes sense, since aerogels are prepared by gelation of polysaccharide in ethanol, which is then extracted from the wet gel by supercritical drying, leaving a pure polysaccharide matrix. Heating of alginate aerogels initially shows a dehydration process, which is followed by decomposition in two overlapping stages.

Samples were analysed by DSC (Figure 4.14) at 10°C min^{-1} heating rate. All samples have a porous structure and are highly hydrophilic in nature, so that they easily adsorb moisture from the air. Despite the supercritical drying, some moisture is still present in the samples. Thus, the first endothermic peak with a maximum at about 100°C observed in all samples could be attributed to water evaporation. Both lmP and hmP show an exothermic peak at around 230°C,

where the degradation of pectin occurs. Xa remains stable for slightly longer and degrades at 270°C. Al exothermic peaks at 230°C and 390°C are present in the degradation of this biopolymer. Guar seems to behave completely differently; its endothermic peak indicates the point of degradation to be 300°C.

Table 4.4. Parameters obtained from TG curves

Sample*	***IDT***	$T_{20\%}$	$T_{50\%}$	**Residue at 600°C**	T_{max}
	°C	°C	°C	%	°C
lmP	199 ± 3	216 ± 2	225 ± 2	27.1 ± 1.5	228 ± 2
hmP	205 ± 5	216 ± 3	221 ± 2	25.0 ± 0.8	223 ± 2
Xa	228 ± 3	251 ± 2	268 ± 1	33.3 ± 2.1	269 ± 3
Gu	251 ± 2	280 ± 2	298 ± 1	13.8 ± 0.8	303 ± 5
Al	199 ± 3	222 ± 1	245 ± 2	40.0 ± 2.2	225 ± 2

* The results are given as the mean value ± standard deviation of three replicates.

Aerogels were analyzed to determine thermal conductivity using DSC. Figure 4.15 shows the difference in the melting curve of pure indium (Figure 4.15a), and Figure 4.15b presents the method for determining the thermal conductivity of aerogels. From the slope presented in Figure 4.15b, we determined the thermal conductivity as presented in Table 4.5. Among the samples, the best conductivity was observed for both pectin aerogels, whose conductivity figures were lower than that of free air (Figure 4.16). Low-density porous materials can have superinsulation properties as a result of the air confined in their pores, when the pore size is below the free mean path of air molecules. The thickness of pore walls is increased, and so is the solid phase conduction. This results in decreasing the gas phase conduction, a phenomenon widely known as the Knudsen effect.

It is likely that both hmP and lmP form a more compact gel with highly interacted chains. After gelation, the polysaccharide chains are closer together, avoiding the formation of voids or larger macropores. The result is higher mesopore volume, which favors the Knudsen effect. Knudsen diffusion occurs when the mean pore diameter of the porous medium is smaller than the mean free path of the gas particles. However, the average pore size of prepared polysaccharide

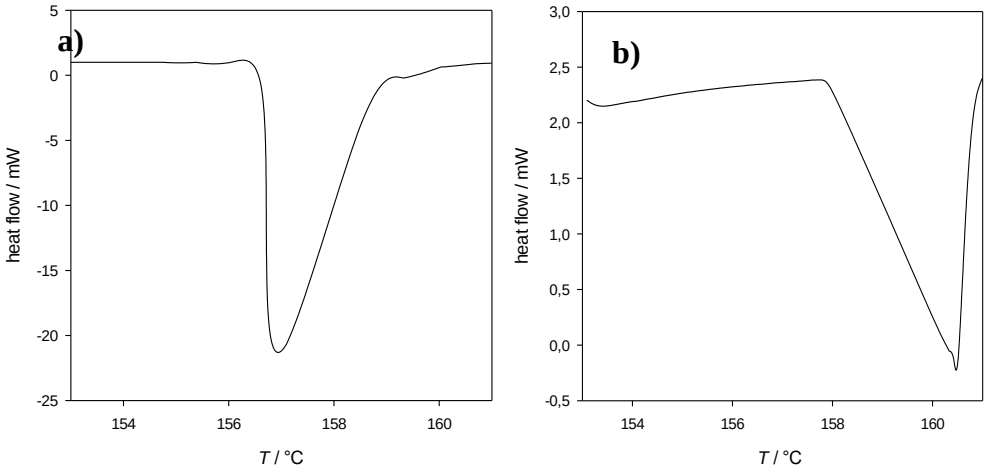

Figure 4.15. Thermal conductivity of aerogels by DSC. The black curve shows the DSC curve of a) indium reference and b) lmP aerogel as a function of temperature. The red line is the slope from which the conductivity is calculated.

aerogels is somewhere between 10 and 20 nm. This is the typical mesoporous range. In order to lower the thermal conductivity to achieve the conductivity of silica aerogel, the average pore size should be lowered to the microporous range (2 nm). Xa structure is different from that of pectin and hence results in lower hydrophobic interactions in ethanol. Al and Gu form clumps after contact with ethanol because of weak hydrophobic interactions; hence, those aerogels possess lower mesopore volume (Table 4.3) compared to the others. Thus, the conduction through solids is higher and so is the total conductivity. Lower thermal conductivity was observed for silica aerogels [80,81], but because of their fragility, real life applications are limited. Some recent studies have proposed the production of silica-polysaccharide [86] composites to merge the lower thermal conductivity of silica with the mechanical stability of polysaccharide aerogels. Polysaccharide aerogels have so far mainly been used for pharmaceutical or biomedical applications [62,146]. The results on thermal conductivity show another possibility for using those materials, especially pectin, as super-insulators.

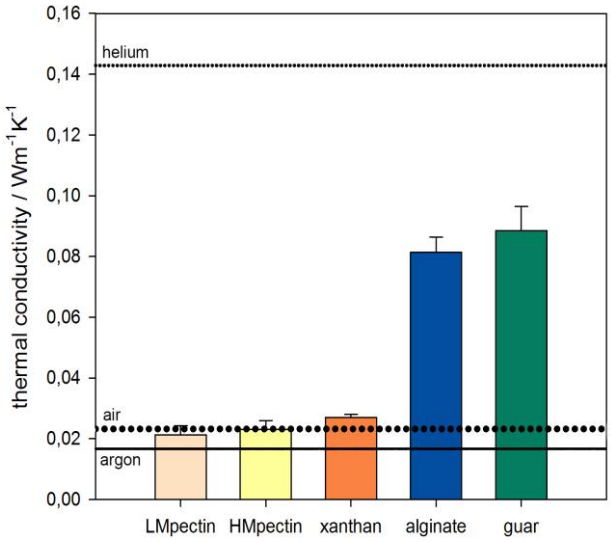

Figure 4.16. Comparison of thermal conductivities of polysaccharide aerogels, determined by the DSC method at the melting point of indium (156.6 °C) with air, argon and helium (at 25 °C).

Table 4.5. Determination of the thermal conductivity of aerogels

Sample	**Slope***	**Diameter***	**Height***	T_{onset}* [d]	$T_{melting}$* [e]	**Therm.cond***
	mWK^{-1}	mm	mm	°C	°C	$Wm^{-1}K^{-1}$
lmP	0.9973 ± 0.0023	6.0 ± 0.2	0.61 ± 0.01	157.86 ± 0.23	160.50 ± 0.32	0.0213 ± 0.011
hmP	0.8683 ± 0.0030	6.2 ± 0.1	0.82 ± 0.03	158.33 ± 0.24	160.63 ± 0.15	0.0230 ± 0.015
Xa	0.8323± 0.0021	5.6 ± 0.1	0.81 ± 0.02	158.13 ± 0.28	160.63 ± 0.21	0.0270 ± 0.008
Gu	1.9819 ± 0.0124	5.6 ± 0.2	1.11 ± 0.05	157.43 ± 0.18	159.98 ± 0.13	0.0885 ± 0.023
Al	1.7919 ± 0.0089	5.8 ± 0.2	1.23 ± 0.02	157.45 ± 0.14	160.10 ± 0.26	0.0814 ± 0.026

* The results are given as the mean value ± standard deviation of three replicates.

[d] T_{onset} = the point of intersection of a baseline before the thermal effect with a tangent.

[e] $T_{melting}$ = peak temperature

Optimisation of alginate aerogels production

As discussed previously, the method of ethanol-induced gelation was not optimal for preparing Al aerogels. This process should therefore be optimised.

Since alginic acid comes in different viscosities, its impact was investigated. Three alginic acids of different viscosities were used to prepare a 4% solution.

The gelation time of tablet shaped gels was investigated. Normally, 1 h of gelation in ethanol is enough to produce stable alcogels. However, a longer gelation time (24 h) was used in order to investigate the impact on the final aerogel characteristics.

Additionally, four alcohols were used for the gelation of Al. In the previous research, ethanol was used to induce the gelation of all polysaccharides. Initially ethanol was used to induce the gelation of all polysaccharides. In order to optimise the Al aerogels' characteristics, the impact of methanol, propanol and n-butanol was also investigated.

4.6 Experimental

4.6.1 Materials

Alginic acid sodium salts were purchased from Sigma & Aldrich. Three different types were used: Al_1 - Alginic acid sodium salt (Viscosity 15 – 20 cP); Al_2 - Alginic acid sodium salt from brown algae (Viscosity 100-300 cP); Al_3 - Alginic acid sodium salt from brown algae (Viscosity > 2000 cP). CO_2 (Messer) was used for supercritical drying. N-butanol, propanol and methanol were purchased at Merck, absolute ethanol was from Sigma & Aldrich.

4.6.2 Aerogel formation

The viscosity of alginate, gelation time and the type of alcohol were set as the limiting parameters in optimising the alginate gel setting and hence its final properties.

Viscosity of alginate

Three different alginic acid sodium salts were used in this research. First, the alginate was mixed with water to form a 4% aqueous solution. Then the solution was transferred to a mold and immersed in absolute ethanol. The gelation was performed for 24 h. The gels were subsequently transferred to an autoclave and dried with supercritical carbon dioxide at 40°C and 120 bar.

Gelation time

A 4% aqueous solution of alginate was prepared and transferred to a mold. The solution was left in absolute ethanol for 24 h to form a gel. Next day, another 4% aqueous solution of alginate was prepared, and the gelation time in absolute ethanol was 1 h. Then all wet gels were dried with supercritical carbon dioxide at 40°C and 120 bar.

Table 4.6. Process parameters used in the research.

Sample	**Gelation time**	**Viscosity (cP)**	**Alcohol**
Al_1E-24	24h	Low (15-20)	Ethanol
Al_2E-24	24h	Middle (100-200)	Ethanol
Al_2E-1	1h	Middle (100-200)	Ethanol
Al_3E-24	24h	High (>2000)	Ethanol
Al_3B-24	24h	High (>2000)	1-Butanol
Al_3M-24	24h	High (>2000)	Methanol
Al_3P-24	24h	High (>2000)	Propanol

Alcohol

It has been published that ethanol induces the gelation of alginate; however, the material's characteristics were not really promising. The effect of different primary alcohols on the gelation of alginate was therefore investigated. An alginate solution was prepared as already described. Instead of ethanol, the mold was then immersed either in methanol, propanol or n-butanol. Subsequent supercritical drying was the same as for ethanol-induced gelation. Table 4.6 summarizes the samples prepared in this research.

4.6.3 Aerogel characterization

All prepared polysaccharide aerogels were characterized as previously described in Chapter 4.2.3 and Chapter 4.4.3. Additionally, gas chromatography headspace (GC-HS) analysis was performed as described below.

Polysaccharide aerogels are highly sophisticated materials that have recently been investigated for their pharmaceutical applications [62,146,147]. Consequently, their preparation method has to be strict, following the Pharmacopoeia prescriptions. It is well known that organic solvents are constantly present in pharmaceutical production processes. However, for toxicological reasons, the amount of organic solvents needs to be minimized or kept below a certain level as prescribed by the Pharmacopoeia. The organic solvents used in this research were primary alcohols: methanol, ethanol, propanol and butanol. All of these, except methanol, are classified as Class 3 by USP [148]. The permitted daily exposure for those solvents is 50 mg or less. In contrast, methanol belongs to Class 2, and its daily exposure is limited to 20 mg [148].

The organic solvents usually cannot be completely eliminated from the product by the drying process, and some residuals may remain in the final product. Therefore, we performed Headspace GC analysis in order to quantify the amount of methanol remaining in the dry aerogels. The analysis was performed on an HS-20 + GC-2010Plus Shimadzu apparatus. Samples were accurately weighed and placed into the analyser. A ZB-5 30.0m X 0.25µm column was used for the analysis, and the oven temperature was 90°C.

4.7 Results and discussion

4.7.1 Aerogel characterization

The largest surface area among alginate aerogels was observed following gelation in methanol (Al_3M-24). The surface area of the alginate aerogels then decreased enormously, along with the increasing chain length of the alcohol. Gelation in methanol was the most promising, since during the gelation step, no visual shrinkage could be observed and the gel was set quickly. Gelation in propanol did occur, but after a couple of hours left in propanol, the gel started to shrink drastically. The resulting surface area was therefore much smaller than that from methanol gelation. Complete gelation of Al in butanol did not occur. The resulting alginate solution was highly viscous after 24 h, but the formation of the gel network was not achieved.

Table 4.7. Characterization of aerogels by nitrogen adsorption.

Sample[#]	S_{BET}	**Pore volume**	**Pore size**
	m^2g^{-1}	cm^3g^{-1}	nm
Al_2E-1	135.7 ± 5.8	0.4911 ± 0.0071	16.79 ± 0.39
Al_2E-24	168.7 ± 4.1	0.6613± 0.0062	17.34 ± 0.21
Al_1E-24	126.9 ± 4.3	0.4357 ± 0.0123	15.48 ± 0.25
Al_3E-24	173.3 ± 7.4	0.6413 ± 0.0136	16.01 ± 0.32
Al_3M-24	367.8 ± 8.8	2.1014 ± 0.0098	20.12 ± 0.13
Al_3P-24	20.5 ± 1.2	0.0511 ± 0.0032	12.81 ± 0.45
Al_3B-24	1.6 ± 0.3	0.0005 ± 0.0002	57.23 ± 0.87

[#] See table 4.6 for sample names

A clear pattern emerges from Figure 4.17: by increasing the chain length of the primary alcohol, the gelation becomes weaker and weaker until it finally reaches the bottom, and Al no longer forms a gel. From Figure 4.17, it can be concluded that only methanol or ethanol yield adequate results. Gelation in propanol or in higher alcohols is no longer meaningful.

The gelation time had a slight influence on the aerogel characteristics. Thus, after 1 h of gelation, the surface area of the aerogels was only 30 m^2g^{-1} lower than those after 24 h gelation. The visual appearance of the aerogels exhibited much more difference, as is evident in Figure

4.18. The surface of aerogels obtained after 1 h of gelation was coarser. In contrast, 24 h of gelation was enough to produce nicely shaped aerogels with a fine polished structure. Figure 4.19 shows the isotherms obtained after nitrogen adsorption/desorption analysis. It is evident that in almost all samples (excluding the aerogel prepared in butanol), the isotherm has a hysteresis loop. This classifies those isotherms as type IV (Figure 2.2), and they have H1 type hysteresis (Figure 3.8). This type of curve describes the adsorption of a swellable hydrophilic solid until its maximum site hydration is reached. Materials of this type tend to have relatively narrow distributions of pore size.

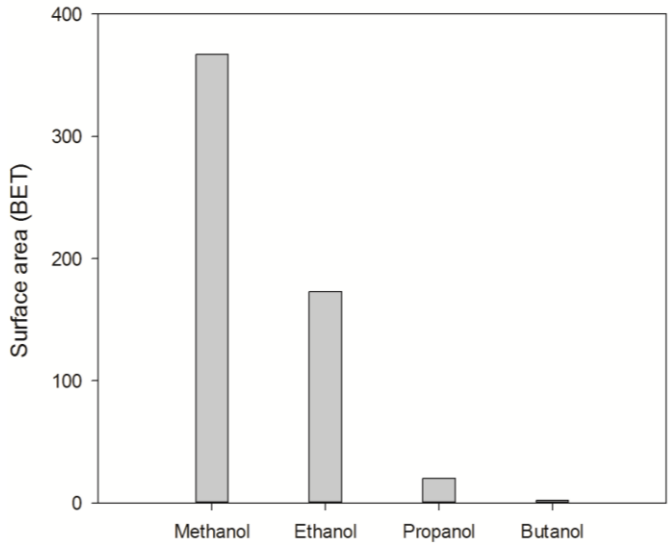

Figure 4.17. Average surface area (m^2g^{-1}) of alginate aerogels, formed in methanol, ethanol, propanol and butanol

By increasing the viscosity of Al, the aerogel possesses a larger surface area, along with greater adsorption capacity (Figure 4.19a). Slightly higher adsorption capacity was observed in aerogels whose gelation time was longer: 24 h compared to only 1 h (Figure 4.19b). Figure 4.19c shows isotherms obtained by measuring the adsorption of nitrogen by aerogels prepared in various alcohols. It is clear that methanol-induced gelation yielded the best results: around 1400 cm^3g^{-1} STP.

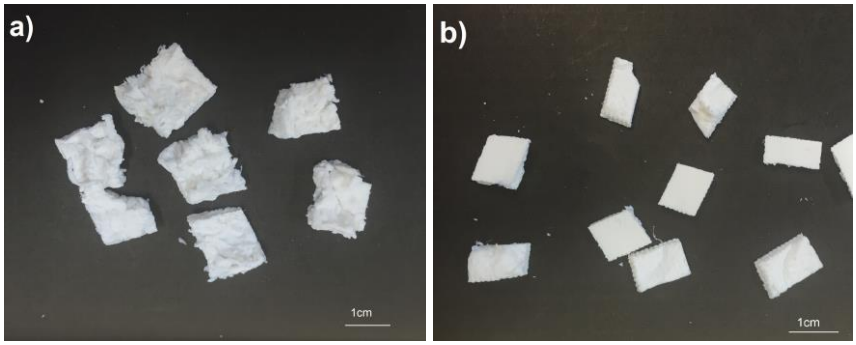

Figure 4.18. Alginate aerogels after a) 1h gelation time and b) 24 h gelation time.

As can be observed in Table 4.7, propanol and methanol were among the worst alcohols to be used for the gelation of Al. Aerogels prepared in propanol were still able to adsorb a small amount of the gas: around 35 cm^3/g STP. On the other hand, as mentioned earlier, complete gelation in butanol did not occur. As is clearly visible from Table 4.7 and Figure 4.19c, the materials obtained could hardly be called aerogels. The surface area is very low, while the adsorption capacity is near zero.

SEM images were recorded for three samples, Al_1E-24, Al_3E-24 and Al_3M-24. The Al_1E-24 sample has a denser structure with larger voids in the polysaccharide matrix (Figure 4.20A). This is most probably due to the lower viscosity of Al, compared to the more viscous Al used for Al_3E-24 and Al_3M-24. Smaller mesopores (2 – 50 nm) and micropores (<2 nm) could not be observed at those magnifications, but were detectable by nitrogen adsorption analysis. A similar structure could be observed for gelation in ethanol (Figure 4.20b) and in methanol (Figure 4.20c).

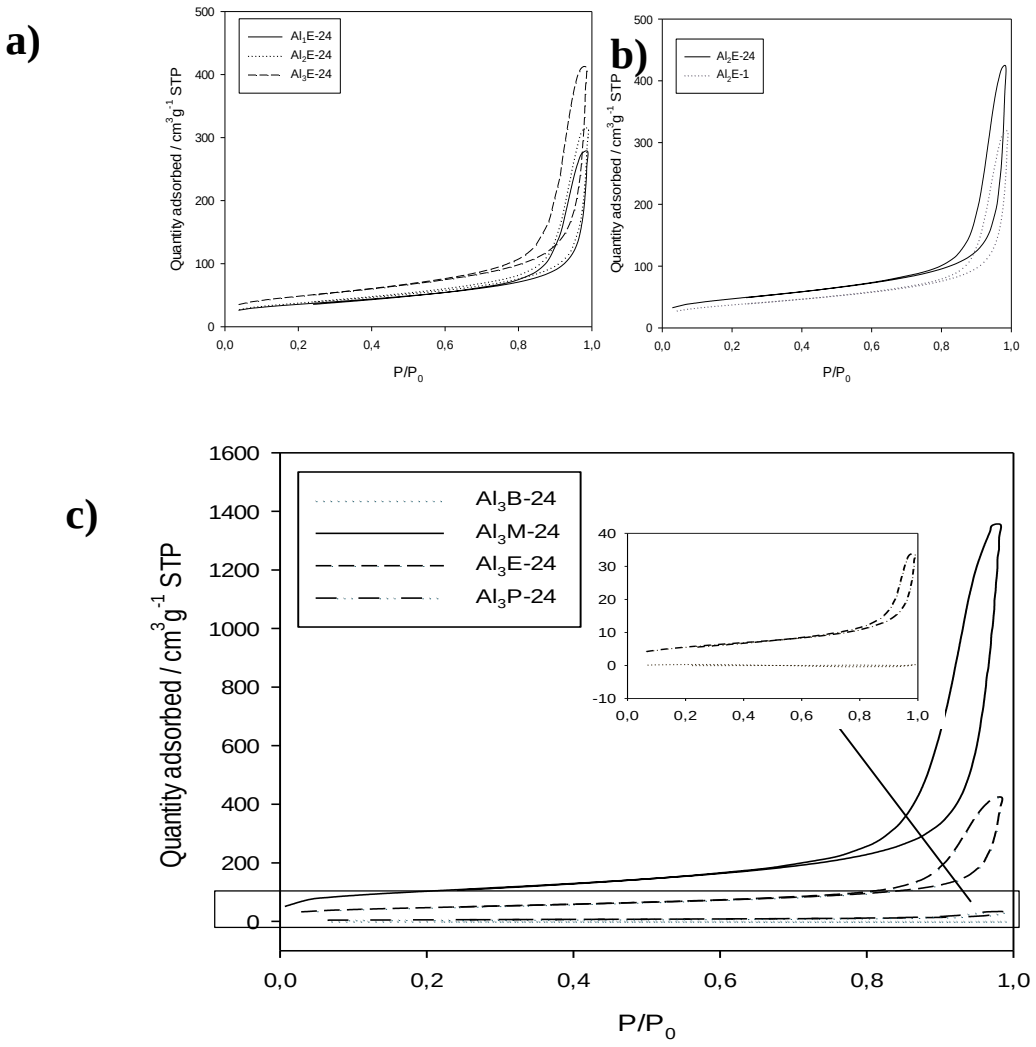

Figure 4.19. Adsorption isotherms of aerogels, prepared by different a) alginate viscosity b) gelation time and c) alcohol.

In order to determine the residues of methanol in the aerogel, headspace GC analysis was performed. First, the calibration curve was obtained in order to quantify the methanol content in the samples. Samples were then analysed three times and the mean value calculated. The amount of the samples was around 65 mg. The determined methanol quantity in the samples was 5764 ± 375 ppm, which corresponds to approximately 58 $mgkg^{-1}$ of aerogel. These aerogels could be used for pharmaceutical applications, since the weight of one tablet is around 20 mg,

and the corresponding trace of methanol is then much less than 20 mg. A longer supercritical drying time would be needed in order to obtain a 'solvent free' product.

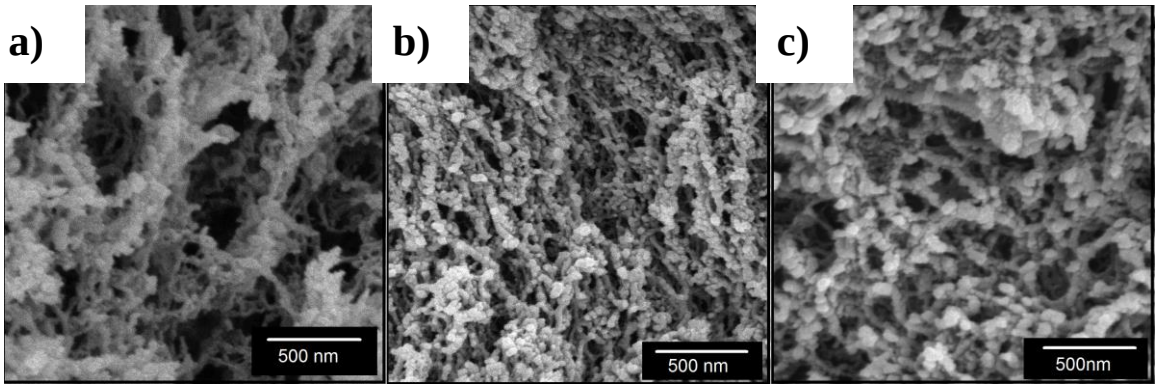

Figure 4.20. SEM images of a) Al_1E-24, b) Al_3E-24 and c) Al_3M-24

The thermal behaviour of two samples (Al_3E-24 and Al_3M-24) was investigated by means of TG and DSC. The TG curves obtained at a heating rate of 10 $Kmin^{-1}$ in inert conditions are presented in Figure 4.21a.

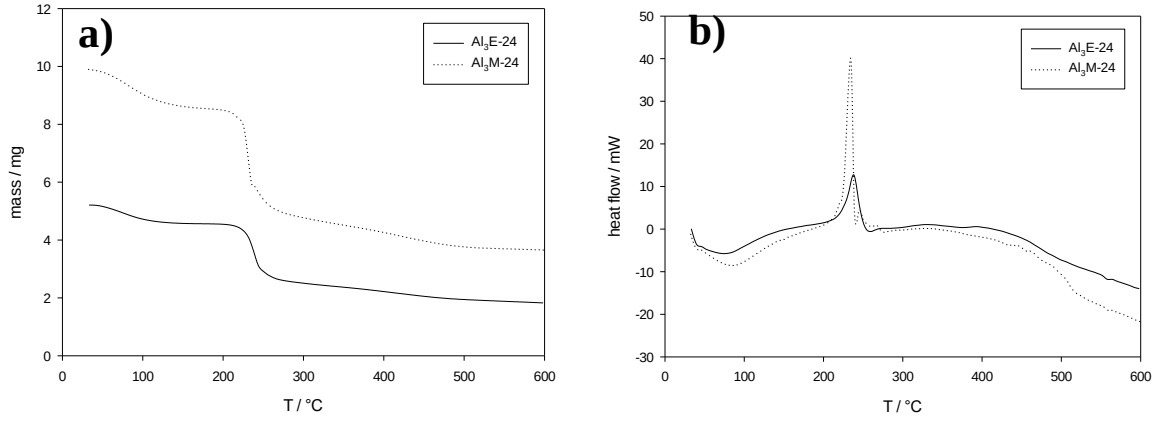

Figure 4.21. a) TG and b) DSC analysis of alginate aerogels, prepared in ethanol and methanol.

TG analysis shows the decomposition of both Al aerogels in two stages. Polysaccharides are highly hydrophilic materials that adsorb water or moisture from the air. Initial mass loss is thus due to dehydration, which is also observed on the DSC (Figure 4.21a) as an endothermic peak

around 100°C. Both aerogels decompose at around 230°C. The alginic acid sodium salt decomposes to Na_2CO_3 [144]. This residue then decomposes around 400°C. Higher enthalpy (Figure 4.21b) is needed for the decomposition of Al aerogel prepared in methanol (A_3M-24). This could indicate the higher stability of aerogels produced in methanol.

Two samples were chosen to measure their thermal conductivity: Al_3E-24 and Al_3M-24. The samples were chosen based on the nitrogen adsorption measurements. Thus, Al_3E-24 possessed the largest surface area for ethanol-based gelation, and Al_3M-24 possessed largest surface area among the samples. Conductivity was measured by the DSC method as described in Chapter 2.5. Among Al samples, the lowest thermal conductivity was observed in the Al_3M-24 sample. Thermal conductivities were 0.042 and 0.085 $Wm^{-1}K^{-1}$ for A_3M-24 and Al_3E-24, respectively. These thermal conductivities were rather high, probably because of the presence of macropores. Lower thermal conductivity of 'bio-aerogels' was obtained for pectin and alginate [84]; however there are not many published results on the thermal conductivity of bio-aerogels. The conductivity of Al aerogels could be lowered, e.g., by making Al-silica composites, as has already been shown in the case of cellulose-silica composites [86]

5 AEROGELS IN PHARMACEUTICAL AND MEDICAL APPLICATIONS

The first four chapters of this thesis have described the development of the new method for preparation of polysaccharide aerogels and their characterization. Given their outstanding properties, these materials are promising for use in pharmacy or medicine. First, spherical aerogels were used as carriers for diclofenac sodium, and the impact of the cross-linking ion on drug release was investigated. Later, aerogels prepared by the new method developed by our group were used as carriers for the low water-soluble drug, nifedipine, and the drug release was monitored. It was established that the release from aerogels is much faster compared to the crystalline drug, which opens up a new potential for using these materials to increase the bioavailability of drugs. Finally, new polysaccharide aerogel coatings were developed on medical-grade stainless steel. Two drugs, diclofenac sodium and indomethacin, were incorporated into these coatings, and their release profiles were investigated *in vitro*. Additionally, results from electrochemical and cell analysis have shown that these materials have great potential for use as bone implants in the future.

TKALEC, Gabrijela, KNEZ, Željko, NOVAK, Zoran. PH sensitive mesoporous materials for immediate release of NSAID. Microporous and mesoporous materials, 2016, vol. 224, 190-200

TKALEC, Gabrijela, KNEZ, Željko, NOVAK, Zoran. Fast production of high-methoxyl pectin aerogels for enhancing the bioavailability of low-soluble drugs. *The Journal of supercritical fluids*, 2015, vol. 106, 16-22,

HORVAT, Gabrijela, XHANARI, Klodian, FINŠGAR, Matjaž, GRADIŠNIK, Lidija, MAVER, Uroš, KNEZ, Željko, NOVAK, Zoran. Novel ethanol-induced pectin-xanthan aerogel coatings for orthopaedic applications, *Carbohydrate polymers*, 2017, vol.166, 365-376

HORVAT, Gabrijela, PANTIČ, Milica, KNEZ, Željko, NOVAK, Zoran.Encapsulation and drug release of poorly water soluble nifedipine from bio-carriers, *Journal of Non-Crystalline Solids*, 2018, vol.481, 486-493

5.1 Introduction

During recent decades, the pharmaceutical industry has grown at a tremendous rate. Along with discoveries of new drugs, comes the need for novel delivery materials and methods, hence great opportunities for materials scientists. New materials are thus being introduced not only to new formulations, but also to existing ones, in order to improve bioavailability, ease administration and decrease side effects. The pharmaceutical industry is constantly being challenged by factors including expiration of patents, price pressure and global competition. Development costs are continually increasing and therefore slowing new product approval. Many pharmaceutical companies are nowadays seeking to develop new drug delivery formulations. Indeed, such new excipients enable the development of new dosage forms, while improving efficiency and may reduce the cost of drugs. Moreover, drug carriers can add functionality to pharmaceutical products. By introducing new dosage forms, they also facilitate the extension of patent life. Because of the wide variety and range of physicochemical properties and the possibility of performing a large number of specific modifications, polysaccharides are ideal starting materials. Nowadays, many polysaccharides are used, modified and transformed to serve the ever-evolving pharmaceutical needs, as excipients, surfactants, adhesives, carriers, protectors or active substances themselves [149]. Plants and their products have always been a source of various drugs and excipients used in pharmaceutical formulations.

Pectin forms a natural part of the human diet. Pectin is able to pass the small intestine more or less intact and is thereafter acted upon by microbial growth in the large intestine. Pectin is also known for its ability to reduce blood cholesterol levels. In the large intestine and colon, microorganisms degrade pectin and liberate short-chain fatty acids, which is known as the probiotic effect [6]. Pectin is used as a demulcent, as an active agent in preventing constipation and diarrhea and in medical adhesives, such as colostomy devices. In cosmetics, it is used as a stabilizer. Pectin is also known to reduce the rate of digestion by immobilizing food components in the intestine, which results in lower levels of food absorption. This is therefore a very useful approach in the treatment of overeating. A highly promising application of pectin is its use in

controlled release formulations [150]. Pectin has been used in tablet formulations as a binding agent and also in controlled-release matrix tablet formulations. Pectin has a promising pharmaceutical usage and is considered for colon-specific drug delivery systems. Pectin will retard drug release in the upper gastrointestinal tract, owing to its insolubility and because it is not degraded by gastric or intestinal enzymes. Further along the gastrointestinal tract, pectin will be degraded by colonic pectinolytic enzymes. This approach could be potentially used to treat diseases such as ulcerative colitis, Crohn's disease, colon carcinomas etc. [151,152].

Guar gum is used as a disintegrating and binding agent in the pharmaceutical industry. It has been found to be superior to some common disintegrants such as corn starch, cellulose, aligns etc. Guar gum has been shown to retard drug release better than other excipients such as acacia and sodium carboxymethylcellulose. Guar has also been studied for the development of controlled release dosage forms and has been shown to increase the dissolution rate of poorly water soluble drugs. It is also its ability to form a gel that promotes its usage in controlled release formulations. The gel layer formed by guar is not as thick as that of other water-soluble polysaccharides such as pectin or alginate. However, in combination with other polymers, it could provide tablets with suitable characteristics and appropriate drug release profiles for poorly soluble drugs [153].

Alginate is used to lower cholesterol levels and to reduce the amount of heavy chemicals including strontium, barium, tin, cadmium, manganese, zinc and mercury that are taken up by the body. Alginate is also used for the prevention and treatment of high blood pressure. Sodium alginate may help improve weight loss when combined with a reduced-calorie diet. Alginate is known to act as a physical barrier in order to reduce reflux episodes. There are a number of available alginate-based pharmaceutical products used for the symptomatic treatment of heartburn and oesophagitis. Several studies have revealed that sodium alginate is able to move to the oesophagus ahead of the gastric contents and hence might be helpful in decreasing the number of acid esophageal episodes. Alginate is also considered as a promising candidate in obesity and type 2 diabetes treatment, as it can attenuate the postprandial glycemic response by

modulation of gastric emptying or inhibition of glucose transporters and the glucose intestinal absorption rate [154].

Xanthan gum is frequently added to semiliquid cosmetics and lotions. Adding xanthan gum to cosmetic agents allows for a smoother, more even application. Xanthan gum can also be found in medications and pills, and has been used alone as a synthetic saliva for people who suffer from dry mouth. Several studies [155,156] have found that xanthan gum can lower blood sugar when consumed in large doses. It is believed that it turns fluids in your stomach and small intestine into a viscous, gel-like substance. This slows digestion and affects how quickly sugar enters your bloodstream, decreasing blood sugar spikes after eating. Xanthan gum may also lower cholesterol and is known to increase fullness by delaying stomach emptying and slowing digestion, thus helping in weight loss.

The benefits of natural polysaccharides are also appreciated by scientists and consumers for their biodegradability. For safe and reliable application of active ingredients, the dosing matrix is very important. Indeed, the active ingredient is only a small element in the final drug. The formulation of an active ingredient into the drug matrix (the drug delivery system) is what influences the final drug release. The drug delivery system has the main role in controlling the pharmacokinetic effect of an active ingredient, since it influences the pharmacokinetic profile of the substance, the release rate, site and duration of its action and also its side effects. The optimal delivery system provides the substance in the right location for the correct amount of time. Drug concentration should be above the minimum effective concentration and below the minimum toxic concentration, in other words, within the therapeutic window (Figure 5.1).

Controlled drug delivery has recently become a more and more valued method in medicine for the treatment of various diseases, from diabetes to cancer. Actually, this kind of therapy provides lower drug dosages, a prolonged therapeutic medicinal effect and, last but not least, the patient compliance and convenience. The active ingredient in traditional systems is immediately released after dosing. For prolonged release, it is thus necessary to use a higher concentration of the ingredient or more frequent dosages. In both cases, it would be easy to

exceed the toxic level (Figure 5.1). Therefore, there is increasing interest in controlled drug delivery systems.

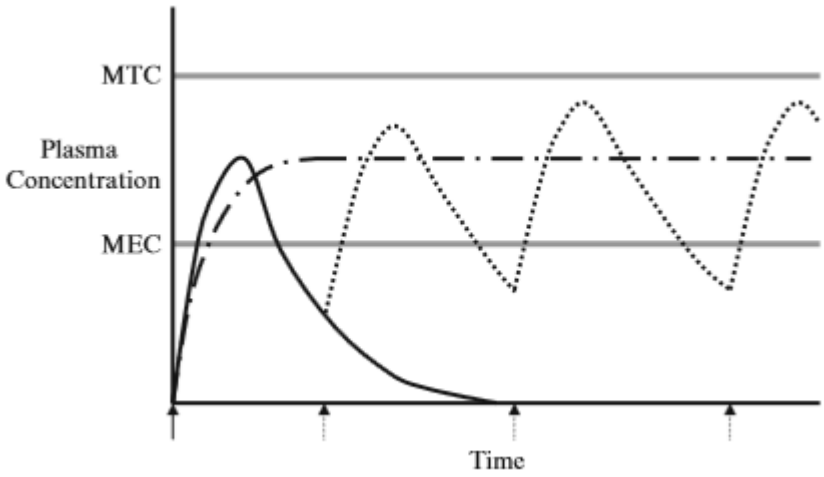

Figure 5.1. Therapeutic window bounded below by the minimum effective concentration (MEC) and above by the minimum toxic concentration (MTC). Solid curve presents rapidly absorbed and rapidly eliminated drugs, given as a single dose, which leads to rapid rise and fall in drug concentration. Multiple dosing at regular interval (solid and dotted arrow) leads to oscillating drug concentration. Dot-dash curve presents zero order release that leads to a constant concentration in plasma [157].

Drugs can be delivered into the body via different routes (Figure 5.1). Drugs can be administered directly into the body, though injection or infusion. This form of drug administration is termed parenteral drug delivery. Depending on the site of administration into the body, one can differentiate between intravenous, intramuscular, subcutaneous, intradermal and intraperitoneal administration. Usually, aqueous solutions are used for intravenous delivery. Drugs can also be administered on the skin to enter the body. Mostly, semisolid dosage forms are used for this, including creams, ointments, gels and pastes. However, liquid dosage forms, such as emulsions, or solid dosage forms, such as transdermal controlled drug delivery systems (patches), can also be used. The most important route for drug administration into the body is through the mucosal membranes. Mucosal membranes are much less of a barrier to uptake than the skin, and some mucosal membranes (such as those in the small intestine) are

indeed specialised sites for absorption. There are many mucosal membranes that can be used for drug administration. Of the greatest importance are the mucosal membranes of the gastrointestinal tract, allowing oral drug delivery. The suitability and convenience of this route of delivery make oral dosage forms the most common of all drug delivery systems.

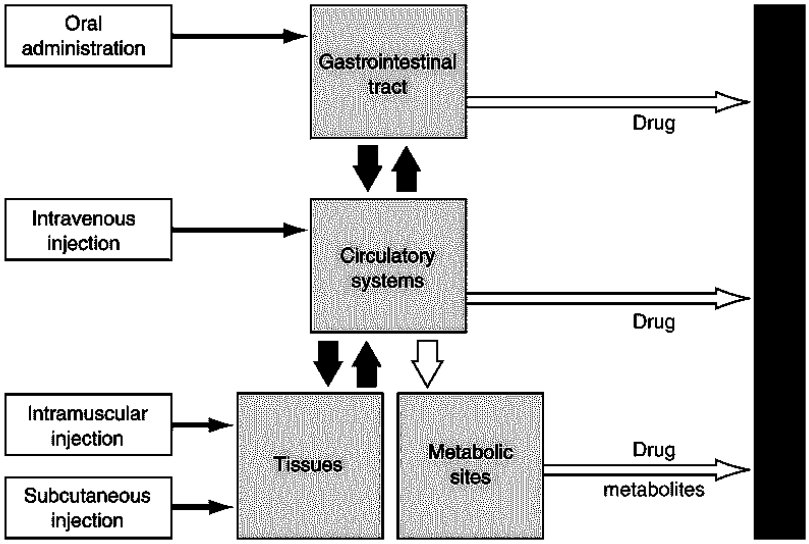

Figure 5.2. Routes of drug administration and its later absorption, metabolism and excretion [158].

Some factors should be considered before development of an oral drug delivery system; the transit time in the gastrointestinal tract may vary considerably between patients and within the same patient. The pH conditions in the gastrointestinal tract also vary considerably, from a low pH in the stomach (1.5–2 in the fasting state, to around 5 in the fed state), to a higher pH in the small and large intestine. The pH in the small intestine varies from 4 to 7, with an average value of approximately 6.5. This may affect stability and will influence the degree of ionisation of ionisable drugs, which in turn will influence their absorption (unionised forms of drugs are usually taken up better than ionised forms of the same drug) and solubility (unionised forms are usually less soluble than ionised forms of the same drug).

The main disadvantage in developing an oral drug delivery system lies in the very low bioavailability of some drugs. Indeed, bioavailability depends on a range of factors: water solubility, permeability, dissolution rate and metabolism. More than 40% of newly synthesized active ingredients are low-soluble or insoluble in water. Since solubility is one of the key parameters in delivering drugs, increasing solubility is a priority in developing a new drug. Low solubility and low dissolution rate in the gastrointestinal tract are the reasons for low bioavailability. Thus, increasing the solubility or increasing the dissolution rate of the active ingredient could increase bioavailability. The most effective and common way to increase the bioavailability of a drug is to encapsulate it within a carrier, which has the ability to increase its dissolution rate. Additionally, encapsulation is a highly used technique in pharmaceutical/ biomedical applications for controlled/sustained drug delivery. Potential applications of this drug delivery system include replacement of therapeutic agents (not taken orally today, as with insulin), gene therapy and in use of vaccines for treating AIDS, tumors, cancer and diabetes [159]. The efficacy of many drugs in conventional dosage forms, including film-coated tablets and hard or soft gelatin capsules, is often restricted by their limitations in delivery to the targeted body site, as the drugs may be degraded by the acidic gastric fluid and this induces stomach irritation. Therefore, seeking biotechnologies to offer the desired excipients for achieving targeted drug delivery is particularly important. More than 90% of nutrients, including proteins, minerals, carbohydrates, fats, vitamins and water are absorbed in the small intestine [160].

The small intestine has a larger surface area and a longer transit time than the stomach. Thus, for steady adsorption, an oral formulation must target the small intestine as much as possible. The desired oral dosage forms should protect the drug under unstable biological environments, including drug degradation by the gastro-intestinal tract (GI) and first-pass liver effects after oral administration before reaching the targeted sites and should maximize drug uptake and absorption in the cellular intestinal regions.

Taking into account all of the above-mentioned needs and desires in developing the ‘ideal drug carrier’, bio-based aerogels emerge as a great choice. Biodegradable polymers, such as polysaccharides, are essential for controlling drug delivery, mainly to avoid accumulation of

polymers in the body during treatment [161]. For biomedical applications, degradation in a human time scale is important. For example, the most desirable drug carrier would be one that degrades completely after the drug release, leaving no residuals in the body. Polysaccharide aerogels are biodegradable and biocompatible; given their high surface area and open pore structure, they are able to retain a large drug amount. High surface area also promotes drug dissolution, hence improving the bioavailability of a drug. Nevertheless, pH sensitive polysaccharides are able to deliver the drug through the stomach to the active site: the intestines.

Release of diclofenac sodium from spherical aerogels

Diclofenac sodium (2-(2,6-**dichlo**ranilino) **phen**ylacetic **ac**id) (DCF) (Figure 5.3) is a non-steroidal anti-inflammatory drug (NSAID). It is used for rheumatic and certain non-rheumatic conditions and can be delivered orally, rectally or intramuscularly. It is widely used to treat rheumatoid arthritis, osteoarthritis and ankylosing spondylitis [162]. Because of its short elimination half-life (1.1 – 1.8 hours), the drug's accumulation is limited. It has a rapid onset and long duration of action and rarely produces serious side effects. Considering all these aspects, DCF is one of the NSAIDs of first choice when treating acute, chronically painful and inflammatory conditions [163].

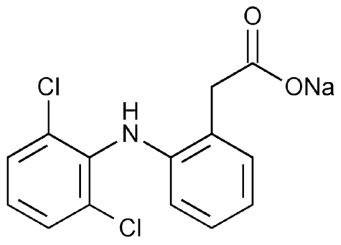

Figure 5.3. Diclofenac sodium.

DCF was developed in 1973 by the Ciba-Geigy company, today known as Novartis. The substance is used as sodium or potassium salt. DCF is an anti-inflammatory drug that inhibits the cyclooxygenase enzyme, hence the synthesis of prostaglandins, which belong to the tissue hormones. DCF undergoes first-pass metabolism, and it is eliminated by the hepatic metabolism and urinary and biliary excretion of glucuronide and sulphate conjugates of the metabolites. Only around 60% of the drug reaches systemic circulation unchanged after oral administration

[163]. Daily dosage should not exceed 150 mg. DCF is usually given three times daily, and this could be a disadvantage compared to less frequent administration with other NSAIDs. Repeated oral administration in long term therapy may cause digestive disorders [164] and gastrointestinal damage such as bleeding, ulceration and perforation [165]. In addition, with its very short half-life, controlled release of DCF sodium is of great interest. DCF is practically insoluble in acidic solution (pK_a 4.0), but it does dissolve in intestinal fluid [166].

5.2 Experimental

5.2.1 Materials

The low-methoxyl pectin was a kind gift from Herbstreith & Fox, Germany; alginic acid sodium salt and $Sr(CH_3COO)_2$ were obtained from Sigma & Aldrich and $CaCl_2$ and $Zn(CH_3COO)_2$ from Kemika. The active pharmaceutical ingredient used as a model drug was diclofenac sodium (DCF), kindly provided by Krka d.d., Slovenia. Capsules (size 00) were purchased from Farmalabor. Absolute ethanol (Sigma & Aldrich) was used for solvent exchange prior to supercritical drying with CO_2 (Messer). For drug loading and entrapment efficiency tests and for *in vitro* dissolution tests, the following chemicals were used without further purification: KH_2PO_4, NaOH, HCl and NaCl.

5.2.2 Encapsulation of diclofenac sodium into aerogels

The solubility of DCF in water is high, 5 g / 100 g H_2O. Therefore, to prepare the drug-loaded aerogels, the drug was added to the sol in the first step of the sol-gel process. Briefly, 1% polysaccharide solutions (pectin, alginate and pectin:alginate) were prepared, to which DCF was added. The solution was further mixed for 1 h and then cross-linked in 2% $CaCl_2$, $ZnCH_3COOH$ and $SrCH_3COOH$. A syringe with a needle was used to transfer the polysaccharide solution into the cross-linking solution in order to form fine spherical gels (Figure 5.4). The resulting spheres were cured for 1 h in a cross-linking solution and then vacuum-filtered. Water in a hydrogel is not miscible with supercritical CO_2; thus, the solvent

exchange step is needed prior to supercritical drying. The hydrogels were dehydrated in ethanol baths with increasing ethanol content: 10, 30, 50, 70, 90 and 100%. The resulting spherical alcogels were placed in an autoclave and dried under supercritical conditions of CO_2 at 100 bar and 40°C. All solutions used in the process of obtaining aerogels were saturated with the model drug to prevent diffusion from the gel.

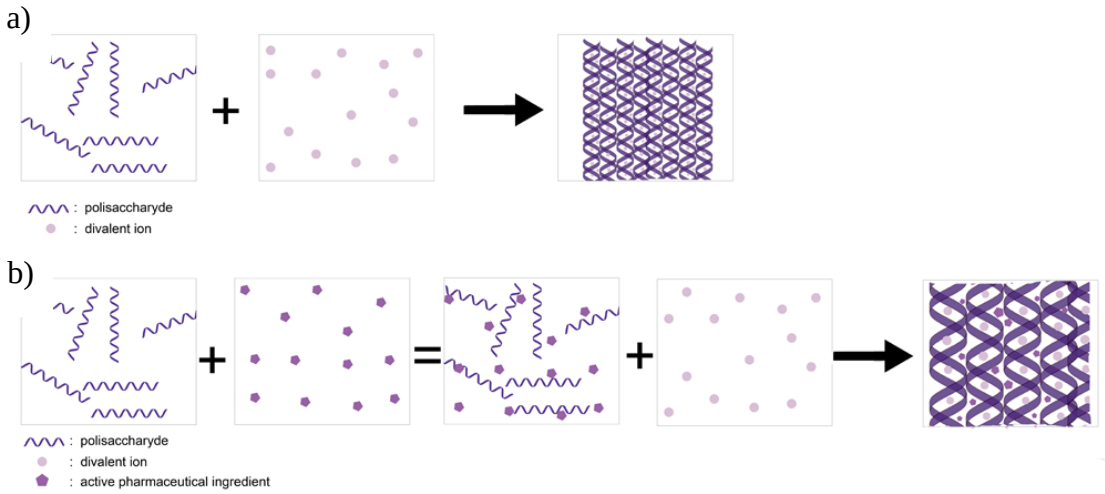

Figure 5.4. a) Cross-linking of polysaccharide with divalent ions and b) drug-loading in the first step of the sol-gel process.

5.2.3 Final drug formulation

After the dissolution tests on DCF-loaded aerogel microbeads, low methoxyl pectin - zinc (lmP-Zn) was chosen as the best candidate to control the release of the model drug. Henceforth, the lmP-Zn microbeads, loaded with DCF, were encapsulated within the gelatine capsule. 0.125g of aerogel microbeads were encapsulated in order to fulfil the criterion of the daily DCF dosage (100mg). The amount of aerogel needed in one capsule was calculated from the drug loading data using Eq. 7.

$$M = \frac{100\ mg}{DL}, \quad (7)$$

where M is the amount of aerogel for one capsule and DL is drug loading.

5.2.4 FT-IR

In order to investigate the possible chemical reactions between the drug and the carrier (polysaccharide, cross-linker), we recorded FTIR spectra of aerogel beads without the substance and of drug-loaded aerogels. The ATR method was used for aerogel samples. All samples were scanned over 400 – 4000 cm^{-1} wavelengths.

5.2.5 Drug loading and entrapment efficiency

To investigate the content of the drug in the carrier, drug loading experiments were performed in PBS. Drug-loaded aerogels were immersed in 100 ml of PBS and sonicated for 10 min. The solution was subsequently stirred for 6 h at 250 rpm and 37±1°C until complete degradation of the samples. The solution was then filtered through a TEFLON 0.45µ filter. The drug loading was determined spectrophotometrically by measuring the absorbance and then transforming it into the concentration using a calibration curve. Drug loading (DL) was calculated by Eq. 8:

$$DL = \frac{m_d}{m_s} \cdot 100\%, \quad (8)$$

where m_d is the mass of the drug (mg) obtained by UV analysis, and m_s is the initial mass of the weighed aerogel sample. Each test was performed in triplicate.

Entrapment efficiency was calculated as the ratio between the actual DCF content and the theoretical data. The total mass of aerogel obtained from a batch was considered as the practical yield of the process. Entrapment efficiency was calculated by Eq. 9:

$$EE = \frac{experimental\ drug\ loading}{nominal\ drug\ loading} \cdot 100\% \quad (9)$$

5.2.6 *In vitro* dissolution test

An *in vitro* dissolution test of DCF from lmP, Al and Al:lmP aerogels was performed according to the standardized procedure (EU pharmacopoeia, FIP guidelines). All tests were performed on the USP Apparatus 2 (paddle method). The apparatus consists of a cylindrical basket placed in a thermostatic bath. First, 900 mL of PBS was introduced into a cylindrical basket and left overnight to set at 37 ± 0.5°C. The aerogel was weighed and placed into a container to avoid floatation. The container was then placed at the bottom of the cylindrical vessel with the solution, and rotation speed was set at 50 rpm. Sampling was performed at selected time intervals, using a 2 mL syringe. The sample was passed through a 0.45 μm membrane filter, and 2 mL of fresh solution was added to the dissolution solution to maintain constant volume. All samples were analysed (Model Varian, Cry 50 Probe spectrophotometer) at a wavelength of 276nm for DCF. The concentration of DCF in the sample was estimated by the calibration curve of DCF in HCl and PBS. The calibration curve was obtained by preparing a stock solution (100 mgL^{-1}) of DCF in either HCl or PBS. The stock solution was then diluted to predetermined concentrations by fresh HCl or PBS and analysed spectrophotometrically; results (absorbance) were plotted against concentration (Figure 5.5).

The cumulative release was calculated by Eq. (5). The dissolution test for the final carrier (lmP-Zn in the gelatine capsule) was performed by a procedure similar to that for aerogels. First, a dissolution test of DCF from lmP-Zn aerogels was performed in distilled water, HCl media and in PBS. An additional experiment included changing the pH of the medium, meaning the samples were first placed into a HCl medium for 1 h, after which the dissolution medium was changed for PBS, where sampling was performed for an additional 23 h.

The capsules were then analysed in HCl and PBS media. Two commercial drugs of DCF controlled release tablets/capsules were analysed for comparison. First, was a coated tablet (100 mg DCF)-A1, and second was a sustained release capsule (100 mg DCF) – A2.

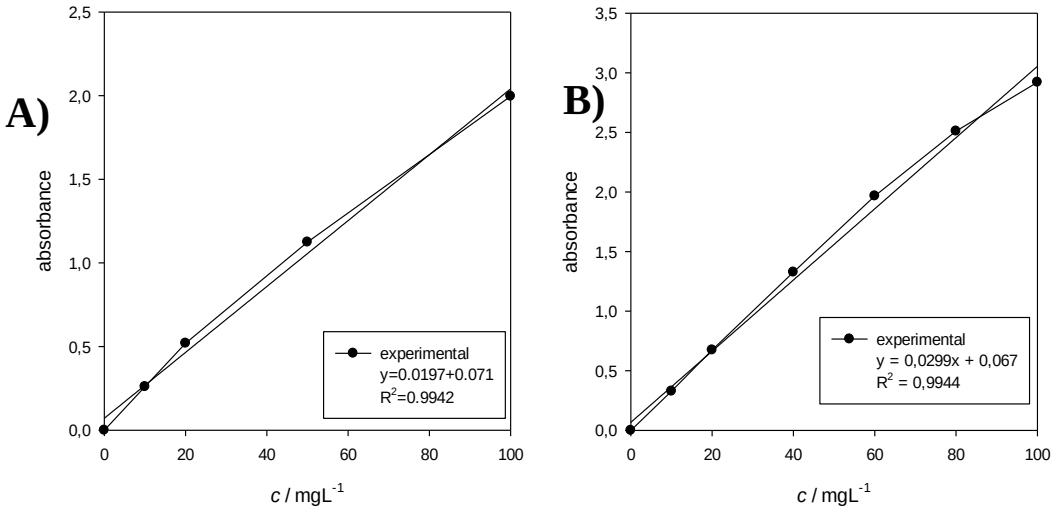

Figure 5.5. Calibration curve for DCF in A) HCl media and B) PBS.

5.2.7 Statistics

To investigate the impact of polysaccharide, ions and the combination of both on final dissolution testing, statistical analysis using analysis of variance (ANOVA) was performed. The independent variables were the type of polysaccharide (X_1) and the type of cross-linker (X_2) (Table 5.1). The time at which 50% of a DCF was released [$t_{50\%}$ (hour)) in PBS (pH 6.8)] (Y_1) was the dependent variable. The regression coefficients of all factors were calculated by two-way ANOVA (Table 5.2). Three null hypotheses were set at the beginning of the analysis: (1) Ion will have no significant effect on the dissolution rate. (2) Polysaccharide will have no significant effect on the dissolution rate. (3) Ion and polysaccharide interaction will have no significant effect on the dissolution rate. The program used for the calculations was IBM SPSS Statistics, version 22.

In order to compare dissolution profiles of DCF from the drug delivery carrier and from two commercial products, the similarity factor (f_2) was calculated from Eq. 10 [167]:

$$f_2 = 50\log\left\{\left[1 + \frac{1}{n}\sum_{t=1}^{n} W_t(R_t - T_t)^2\right]^{-0.5} \cdot 100\right\}, \qquad (10)$$

where W_t is the weighting factor at time t, R_t is the percentage dissolved from the commercial drug at time t, and T_t is the percentage dissolved from the capsule based on aerogels at time t.

Table 5.1. Factorial design parameters and experimental conditions.

The independent variables			
Polysaccharide (X_1)	Al (1)	lmP (2)	Al:lmP (3)
Ion (X_2)	Zn^{2+} (1)	Sr^{2+} (2)	Ca^{2+} (3)

Factorial design			
Sample	***X₁***	***X₂***	***Y₁*** [e]
Al-Zn	1	1	1.360 ± 0.036
Al-Sr	1	2	0.186 ± 0.008
Al-Ca	1	3	0.147 ± 0.010
lmP-Zn	2	1	1.977 ± 0.099
lmP-Sr	2	2	0.719 ± 0.007
lmP-Ca	2	3	0.410 ± 0.024
Al:lmP-Zn	3	1	0.519 ± 0.011
Al:lmP-Sr	3	2	0.421 ± 0.075
Al:lmP-Ca	3	3	0.965 ± 0.033

The independent variables are polysaccharide type (X_1) and ion type (X_2). The time at which 50% of all drug was released (Y_1) is the dependent variable.
[e] Mean ± SD., n = 3.

Table 5.2. Factorial ANOVA analysis.

Source	**Sum of squares**	**Degree of freedom**	**Mean square**	**F ratio** [f]
Ion	3.961	2	1.981	74.139
Polysaccharide	1.159	2	0.580	21.692
Polysaccharide*ion	3.528	4	0.882	33.013
Experimental error	0.481	18	0.027	

The effect of independent variables (type of polysaccharide and type of an ion) on the time by which 50% of a drug was released. [f] $P < 0.05$.

5.3 Results and discussion

5.3.1 Drug loaded aerogel formation

The ratio polysaccharide:API should be carefully determined, as this influences entrapment efficiency. Moreover, if the polysaccharide:API ratio exceeds the range, the bursting effect may occur [168]. First, a polysaccharide solution with DCF was prepared by mixing 2.0 g of polysaccharide and 2.0 g of DCF. After transferring the homogenized solution into a cross-linking solution, using a syringe pump with a needle, a bursting effect occurred. There was no production of fine spheres, but instead of rice-shaped gels (Figure 5.6a). When the ratio was set to 2:1 polysaccharide:DCF, fine spherical particles were formed after immersion in the cross-linking solution (Figure 5.6b).

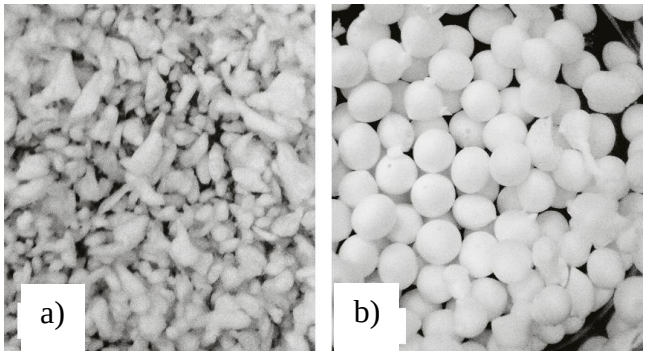

Figure 5.6. Comparison between produced gels at different lmP:DCF ratio. a) 1:1 and b) 2:1

Shrinkage was observed during two solvent exchanges (water -ethanol and ethanol -SC CO_2). Shrinkage of gels after the first solvent exchange was 15%, and after the second solvent exchange, 35%. The resulting diameters of the spherical hydrogels were 3.2 ± 0.2 mm for alcogels 2.8 ± 0.3 mm and for aerogels 1.8± 0.3 mm (Figure 5.7).

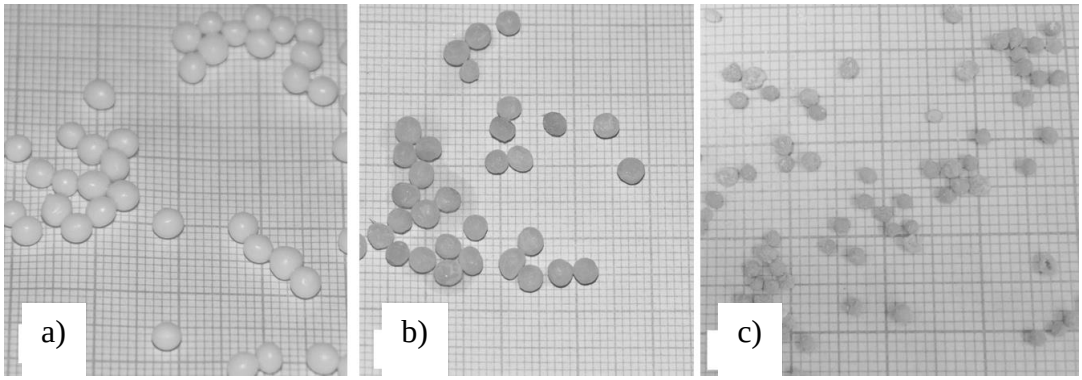

Figure 5.7. Shrinkage observation from a) hydrogel to b) alcogel and c) aerogel.

5.3.2 FT-IR

In order to investigate the possible interactions between ions and polysaccharide with DCF, two individual FTIR spectra were recorded and compared in Figure 5.8. As can be seen, there is no significant shifting of peaks, meaning that DCF is stable during the sol-gel process. Also, the absence of a drug-matrix interaction is proven. Therefore, aerogels are proven to act only as hosts for the active substances without changing their chemical or biological nature. In Figure 5.8a, the additional peaks that indicate the presence of DCF are highlighted.

5.3.3 Drug loading and entrapment efficiency

The drug loading results are collated in Table 5.3. From the collated data, the highest loading (Eq.8) was achieved by Al-Zn and lmP-Zn aerogels, at around 80%. Higher drug loading is highly desirable during the preparation of pharmaceutical dosage forms. When comparing two carriers of the same active substance but with different loadings, a smaller amount of the carrier with a higher drug loading was needed and vice versa. In conclusion, this led to less frequent and smaller dosages and to greater patient convenience and compliance. In addition, higher loading is also desirable from the economic and commercial point of view.

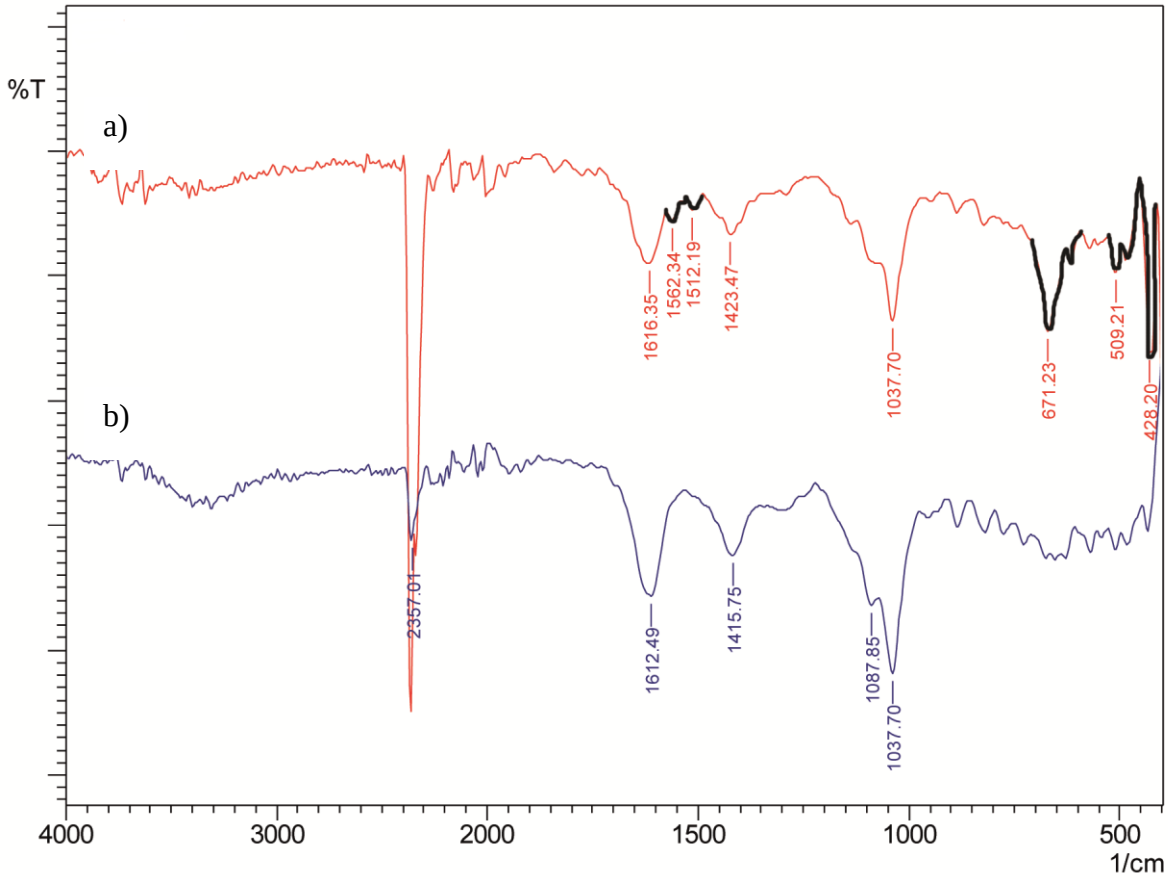

Figure 5.8. FTIR spectra comparing a) aerogel, loaded with DCF and b) pure aerogel.

Entrapment efficiency (Eq.9) was calculated in order to compare drug loading to the aerogel characteristics. Entrapment efficiency (Table 5.3) was much higher in the case of zinc cross-linked aerogels and lower in the case of calcium cross-linked aerogels. Impregnation of a drug took place during the first step of the sol-gel process. Thus, during washing and solvent exchange, there was the possibility of drug loss due to diffusion. Calcium cross-linked aerogels provide the highest dissolution rate, owing to their high surface areas [169]; hence, drug loss during washing and solvent exchange could also be higher [170]. Thus, the drug loading and entrapment efficiency was lower for larger surface areas. The results for drug loading and entrapment efficiency could differ when using other methods of drug impregnation, e.g. impregnation by solvent exchange or supercritical impregnation.

Table 5.3. Drug loading and entrapment efficiency of DCF, loaded in alginate, pectin and alginate-pectin aerogel.

Sample	Drug loading (%)	Entrapment efficiency (%)
Al-Zn	79.6	80.7
Al-Sr	49.8	51.8
Al-Ca	40.5	42.3
lmP-Zn	79.0	68.1
lmP-Sr	58.7	40.5
lmP-Ca	44.2	36.5
Al:lmP-Zn	56.9	70.6
Al:lmP-Sr	39.4	50.1
Al:lmP-Ca	35.9	45.0

5.3.4 *In vitro* dissolution test

DCF is slightly soluble in water and in a phosphate buffer but practically insoluble in HCl. According to BCS, DCF is classified as a Class II drug, i.e. a drug with high permeability and low solubility. For such drugs, solubility in aqueous media is insufficient for dissolution of the whole dose within the gastrointestinal tract. Therefore, their dissolution is the limiting step for absorption. Indeed, the choice of dissolution medium for *in vitro* dissolution tests is thus of great importance [171]. *In vitro* dissolution tests are very useful tests for predicting *in-vivo* behaviour of an API. Even more, they are used for characterising the biopharmaceutical quality of a product. *In vitro* dissolution data is also important when making changes in the manufacturing process or changing the dosing matrix [172].

Given the good solubility and high permeability of DCF in the alkaline medium at a pH of 6.8, the release behaviour depends mostly on the nature of the carrier. To prolong the release and adsorption of the drug, polysaccharide aerogels were prepared by ionotropic gelation, using three different metal ions as cross-linking agents. After contact between the carrier and the buffer solution, the solution diffuses into the nano-pores. The surface of the carrier begins to swell, thus allowing more of the solution to diffuse into the drug carrier. Moreover, the carrier starts to erode when in contact with the buffer solution, owing to the gradual exchange of

divalent ions between guluronic blocks with monovalent ions. Given the DCF salt molecule size, aerogel characteristics allow the drug to diffuse from the bulk material to its surface and to be further released into the solution.

Figure 5.9 shows the immediate release of DCF from calcium cross-linked aerogels. It can be observed that the release rate was the highest in the case of the alginate aerogels. From these results, we can conclude that calcium cross-linked aerogels will be better carriers for immediate release, and other cross-linkers should be used in order to prolong the release of water-soluble drugs.

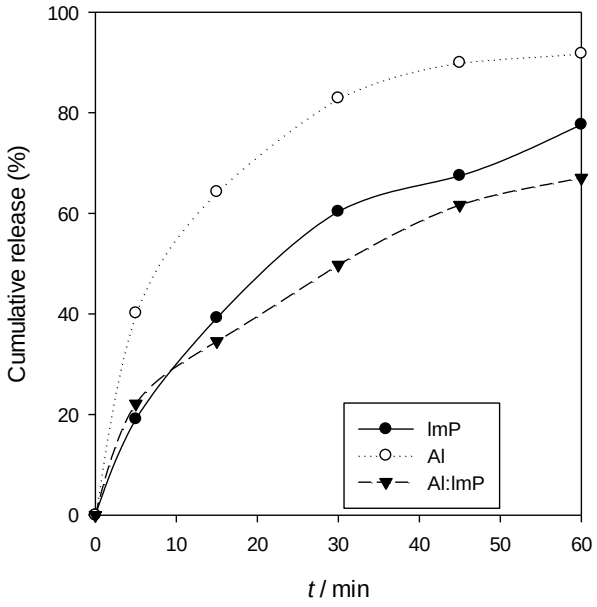

Figure 5.9. Immediate release from calcium cross-linked aerogels.

The release of DCF from Al and lmP aerogels using different ions as cross-linkers is compared in Figure 5.10A and B. Zinc cross-linked pectin and alginate aerogels are denser [113]; thus, slower release is expected, compared to that for strontium or calcium ions. Because of the varying degree of cross-linking and thus of the swelling of the aerogel matrix, penetration of a solution into the aerogel differs. Calcium ions form loose linkages with carboxyl groups in the chains of Al and lmP. Owing to mutual interaction, Zn^{2+} forms more extensive cross-linkage.

Zn^{2+} ions preferentially cross-link Al and lmP. The lower coordination number of Zn^{2+} would significantly retard hydration of both polymers as opposed to calcium. Zinc, calcium and strontium bind at different sites of Al and lmP. Zinc ions are less selective and hence produce more extensive cross-linkage [173].The use of strontium may increase the stability and strength of lmP and Al microbeads [119], which results in a delayed release of the drug. From a combination of both polysaccharides, composite aerogels were obtained, and cumulative release of DCF is shown in Figure 5.10C. Release figures are however similar to those from single Al or lmP aerogels.

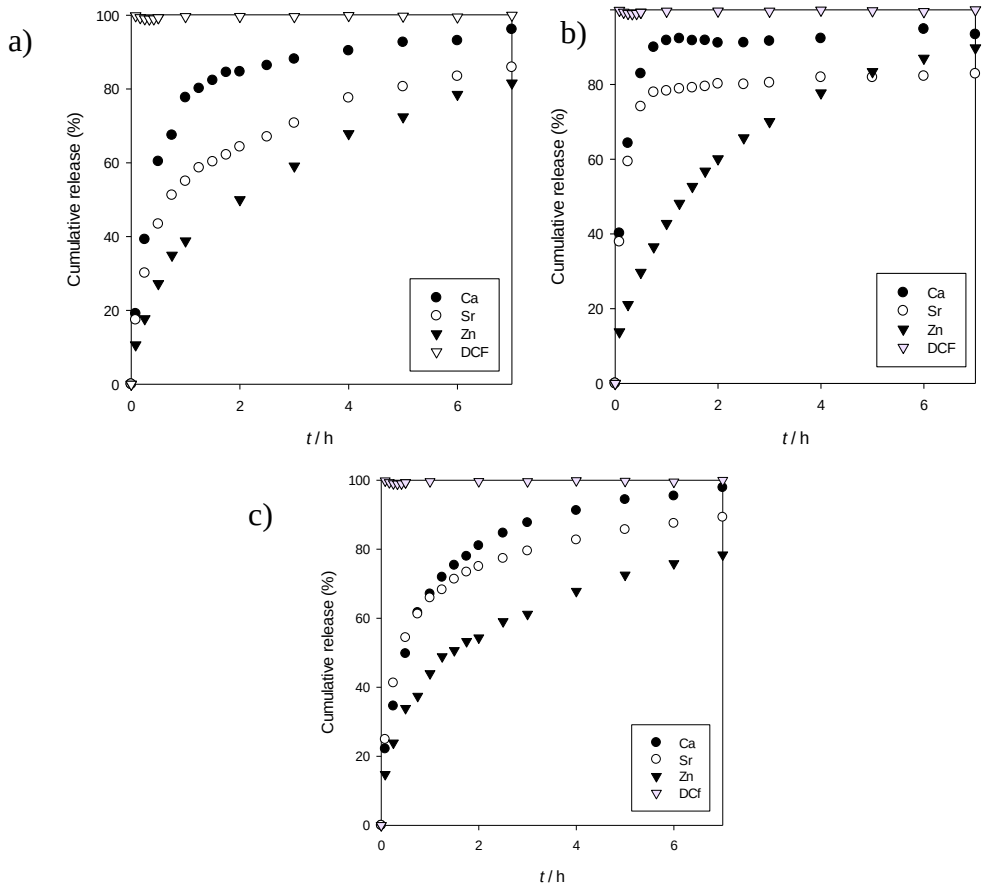

Figure 5.10. Cumulative drug release from a) lmP, b) Al and c) Al:lmP, cross-linked with three different ions.

The selection of ions has a greater impact on drug release than the selection of polysaccharides. Although there is also a significant difference between all three polysaccharides, comparing ion selection, the F ratio increases more than three times (Table 5.2). Thus, it is important to choose the right combination of ions and polysaccharides to obtain the best drug release results.

Table 5.4 compares release rates by using different cross-linking ions. It is evident that cross-linking with calcium ions is not suitable for controlled release, since more than 60% of the drug is released in the initial hour. Cross-linking with zinc decreased the release rate by almost a half and thus is considered the suitable choice for producing controlled-release formulations. Among the polysaccharides, the lowest release rate was achieved by lmP aerogels; thus, those carriers (lmP-Zn) were chosen for further analysis.

In vitro dissolution tests of lmP-Zn loaded with DCF were then performed in four different dissolution media (Figure 5.11): distilled water, HCl medium, PBS and HCl-PBS (1 h – 6 h).

Table 5.4. DCF release from Al, lmP and Al:lmP aerogels after 1h and 7h using three different ions as cross-linkers.

Sample	**1h**	**7h**
Al-Zn	42.8%	89.8%
Al-Sr	78.3%	82.9%
Al-Ca	91.8%	93.4%
lmP-Zn	38.8%	81.6%
lmP-Sr	55.7%	85.9%
lmP-Ca	77.6%	96.1%
Al:lmP-Zn	44.0%	78.4%
Al:lmP-Sr	65.9%	89.3%
Al:lmP-Ca	67.0%	97.8%

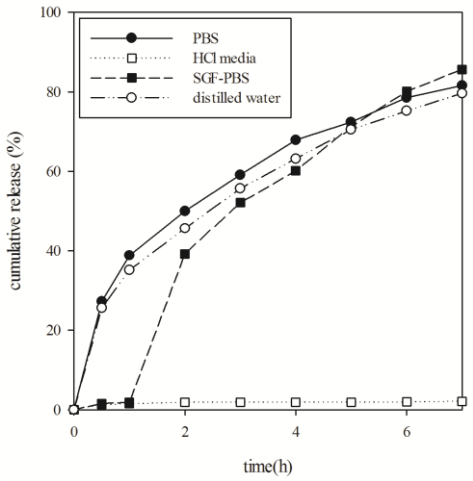

Figure 5.11. *In vitro* dissolution profiles of DCF from lmP-Zn aerogels in distilled water (-o-), HCl medium (-□-), PBS (-●-) and S-PBS (-■-).

A non-significant difference can be observed between the results obtained in PBS and distilled water. Limited drug release was observed in the HCl medium, which is mostly due to the nature of the carrier, lmP aerogel, which is resistant in acidic pH. After transferring the sample from HCl media to PBS, the release of the drug starts to increase rapidly.

LmP-Zn aerogels were then encapsulated within the capsule (Figure 5.12) to obtain the final drug formulation for later dissolution testing.

Figure 5.12. DCF loaded pectin aerogels placed in a capsule.

The *in vitro* dissolution test of the final drug formulation (a capsule) was investigated within the HCl medium (Figure 5.13a) and PBS (Figure 5.13b). Two commercial products were analysed for comparison.

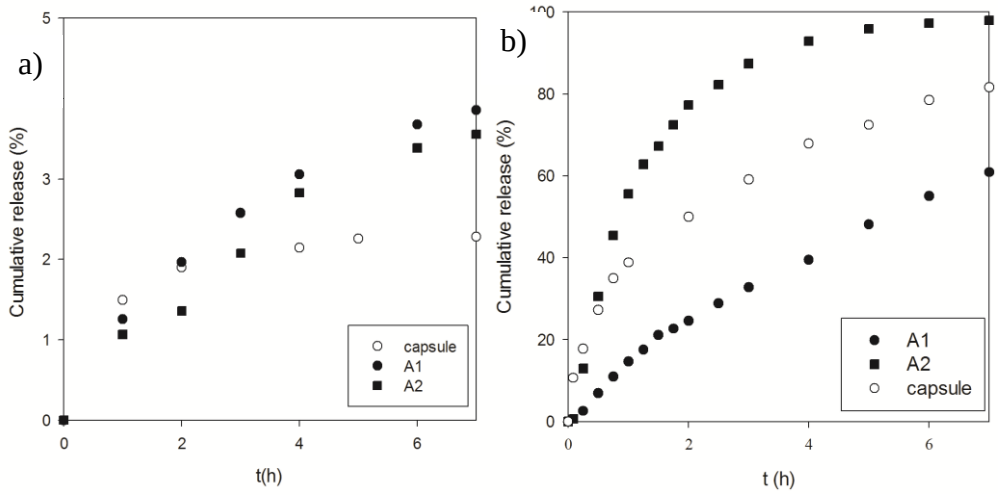

Figure 5.13. *In vitro* dissolution profiles of DCF from a capsule with comparison to commercially available formulations A1 and A2 in a) HCl media and b) PBS.

Comparing Figure 5.11 and Figure 5.13, it can be observed that the empty gelatine capsule has almost no impact on dissolution behaviour. There is an insignificant difference between the release profiles from lmP aerogel spheres with or without capsules in PBS. Gelatine capsules disintegrate immediately when immersed in either the acidic pH of HCl media or the neutral pH of PBS. Therefore, it was proven that capsules could be used for easier handling of lmP aerogels without any impact on dissolution behaviour.

DCF is absorbed rapidly after its oral administration. As there is an increased interest in its absorption in the intestines, the carrier should be designed to resist the acidic pH of the stomach and to disintegrate and release the drug within the lower gastrointestinal tract. Absorption of the drug in the stomach should be prevented, so as to reduce the risk of stomach irritation and ingestion. Moreover, the larger surface area of the intestines is designed for absorption to achieve better bioavailability of the drug. The release of DCF from the final drug formulation (a capsule) is restricted in the HCl medium (Figure 5.13a). Less than 5% of DCF is released in 7h. In PBS, all release profiles were different. The slowest release was provided by A1, which was in the form of a coated tablet. However, comparing both capsule-based formulations (final drug formulation and A2), release time from the final drug formulation was slower.

During the dissolution test, it was observed that the final drug formulation disintegrated within 7h in PBS. In contrast, neither A1 nor A2 decomposed completely. After 72 h, the residue was still in the basket (Figure 5.14).

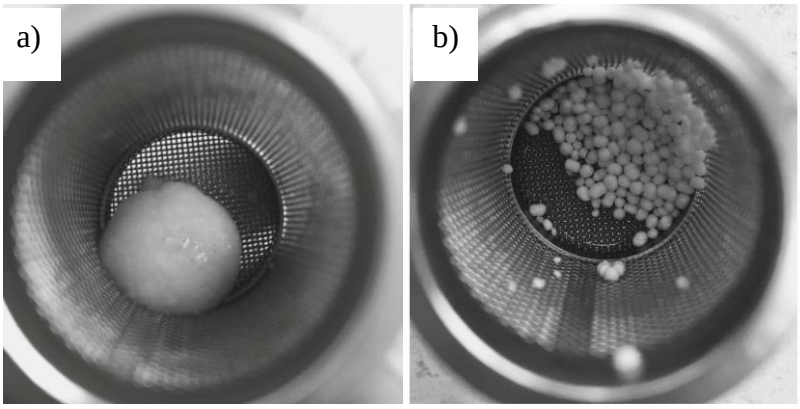

Figure 5.14. a) A1 and b) A2 formulations after 48 h within PBS.

By comparing the release profiles of DCF from our final drug formulation (capsule) with two commercial products A1 and A2, a similarity factor of f2 was calculated. The value of the similarity factor f2 was found to be 24 and 38 when using a capsule based on aerogel as a test product and A1 and A2 as a reference product, respectively. If the two release profiles are identical, f2 = 100. If a difference of 10% at all measured time points is observed, this results in an f2 value of 50. According to the FDA, if the f2 value falls between 50 and 100, this indicates similarity between two dissolution profiles. No similarity was found between the two commercial products.

The rapidity of solvent intrusion into a porous material rises along with greater surface area of the material. The solvent then dissolves the substance impregnated in the matrix, and the substance (i.e. API) diffuses out of the matrix. The rate of diffusion and thus dissolution increases with larger surface areas. Therefore, zinc-cross-linked aerogels could be the most promising materials for controlling the release of highly-water-soluble drugs, and calcium-cross-linked aerogels for improving the dissolution of poorly soluble drugs.

The *in vitro* dissolution test of DCF showed very high solubility within PBS. Thus, a proper carrier should be obtained in order to prolong the release of this drug. The prepared mesoporous aerogels have been shown to be suitable for prolonging the release of DCF. Aerogels are stable in dry air conditions and for the final drug product, are thus way more suitable than hydrogels. These matrices are also biodegradable and biocompatible and thus suitable for use within pharmaceutical applications. All prepared materials were mesoporous with high surface areas. Calcium cross-linked aerogels provided the largest surface area and zinc cross-linked ones the least. However, drug loading was highest in the case of zinc cross-linked aerogels. All the samples were stable in the HCl medium over a period of 7 h and started to swell when in contact with PBS. Undoubtedly, all samples show pH-dependent swelling. Comparing all the experimental work from *in vitro* dissolution studies, and drug loading to swelling and erosion, lmP aerogels, cross-linked with zinc, can be considered the most promising carriers for the controlled release of DCF. Calcium cross-linking is useful only in cases where immediate drug release is desired. The final drug formulation containing lmP-Zn aerogel within the gelatine capsule was compared with two commercial drugs of DCF. No similarity was found among the three controlled release products. 80% of the drug was released from the aerogel-based carrier in 7 h. In this period, the whole carrier was degraded. In contrast, the remains of the carrier of both commercial drugs were still present after 72 h in PBS.

Release of nifedipine from monolithic aerogels

Nifedipine (Figure 5.15) is a dihydropyridine calcium channel-blocking agent. Nifedipine inhibits the transmembrane influx of extracellular calcium ions into myocardial and vascular smooth muscle cells, causing dilatation of the main coronary and systemic arteries and decreasing myocardial contractility. This agent also inhibits the drug efflux pump P-glycoprotein, which is overexpressed in some multi-drug resistant tumors and may improve the efficacy of some antineoplastic agents. Nifedipine is considered the first-choice drug in the treatment of systemic and pulmonary arterial hypertension. Its characteristics indicate its use in the treatment of heart failure. It improves renal and cerebral circulation and does not produce orthostatic hypotension and in addition has diuretic, natriuretic and uricosuric effects, with very few side effects [174].

The term calcium channel-blocking agent or calcium antagonist was introduced in 1971 to describe a group of cardioactive drugs, such as nifedipine, which inhibit the influx of calcium ions into the cell through potential-dependent channels and whose action could be opposed by increasing the calcium ion concentration [174].

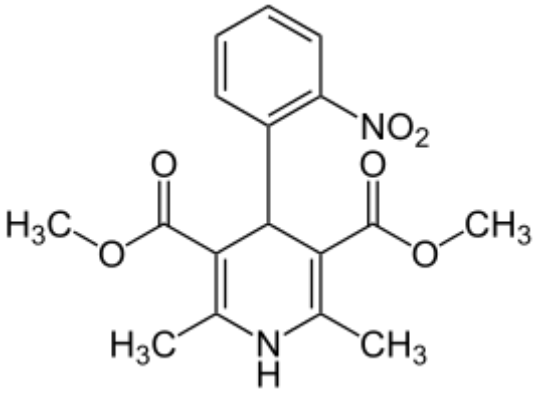

Figure 5.15. Nifedipine.

Nifedipine has greater activity on the potential-dependent channel, compared with other drugs. It has a specific binding site on the external side of the cell membrane, therefore allowing

interactions with selective calcium cannels. Hence, a lower nifedipine dosage is needed compared to other drugs, such as verapamil and diltiazem [174]. Nifedipine is most effective after oral or sublingual administration. Intravenous administration is not common, given nifedipine's photosensitivity and low solubility. After oral administration, 65% is absorbed in the digestive tract and appears in the blood after about 20 min. Its peak concentration is reached after 2 h. Most of the drug (about 90%) is bound to protein, cleared in the liver and excreted in urine. Its half-life is about 4 h.

5.4 Experimental

5.4.1 Materials

Low-methoxyl pectin (degree of esterification=23-28%, degree of amidation=22-25%) was kindly provided by Herbstreith & Fox. Xanthan, guar and alginate were purchased at Sigma Aldrich. Absolute ethanol with a purity higher than 99.8% was obtained from Sigma Aldrich. Carbon dioxide (CO_2) used for supercritical drying with a purity of 99.5% was supplied by Messer. Nifedipine was obtained from Chemos. Hydrochloric acid (HCl, 37%) was purchased from Merck. Sodium chloride (NaCl) with a purity of 99.6% was supplied by Fisher Chemicals. Potassium dihydrogen phosphate (KH_2PO_4) with a purity higher than 98% and sodium hydroxide (NaOH), also with a purity higher than 98%, were obtained from Sigma Aldrich.

5.4.2 Encapsulation of nifedipine into aerogels

Nifedipine is a poorly water soluble drug and belongs to BCS class II. It is soluble in ethanol; thus, the most convenient and effective way for its encapsulation would be diffusion through ethanol. Polysaccharide aqueous solutions were prepared as described in Chapter 4.4. After the solutions were transferred to a tablet-shaped mold, the mold was immersed in nifedipine-saturated absolute ethanol. While the solution gelled in ethanol, nifedipine also diffused inside the setting gel. After complete gelation, the resulting wet gels were encapsulated with nifedipine.

The supercritical drying was performed under the same conditions as for blank aerogels. An autoclave was filled with nifedipine-saturated ethanol prior to the drying, in order to avoid excess diffusion of nifedipine from the aerogels during the heating process. Some of the nifedipine was removed from the aerogels by supercritical CO_2 during drying. Lastly, the final drug loadings in the aerogels were determined.

Since nifedipine is also soluble in supercritical CO_2 [175], the second impregnation process was applied by using supercritical technology [176]. First, tablet shaped aerogel carriers were prepared as described in Chapter 5 – Ethanol-induced gelation. Then these prepared aerogels were placed into a 500 ml autoclave. Nifedipine powder was placed at the bottom of this autoclave in an amount such that the proportion of nifedipine to aerogel was 0.1:1 (w:w).

5.4.3 FT-IR

Fourier transform infrared spectroscopy (Scimadzu, IRAffinity-1) was employed in the characterization of nifedipine and pectin aerogels. All the samples were analyzed using the ATR-IR method. The pectin aerogel samples were cut into halves and placed on the ATR detector, while nifedipine was placed as a powder.

5.4.4 Drug loading and entrapment efficiency

To determine the drug loading in the carrier, experiments were carried out as already described [125]. Briefly, the drug-loaded aerogel samples were weighed and then placed in 1000 mL of PBS. Then the solution was sonicated for 10 min and stirred for 6 h at 37 ±0.5˚C until complete decomposition. Then 2 mL of the solution was withdrawn and filtered through a Teflon 0.45μm filter. The absorbance was measured spectrophotometrically (Varian, Cary 50 Probe UV spectrophotometer), and the concentration was then calculated using the calibration curves (Figure 5.16). All measurements were performed in triplicate.

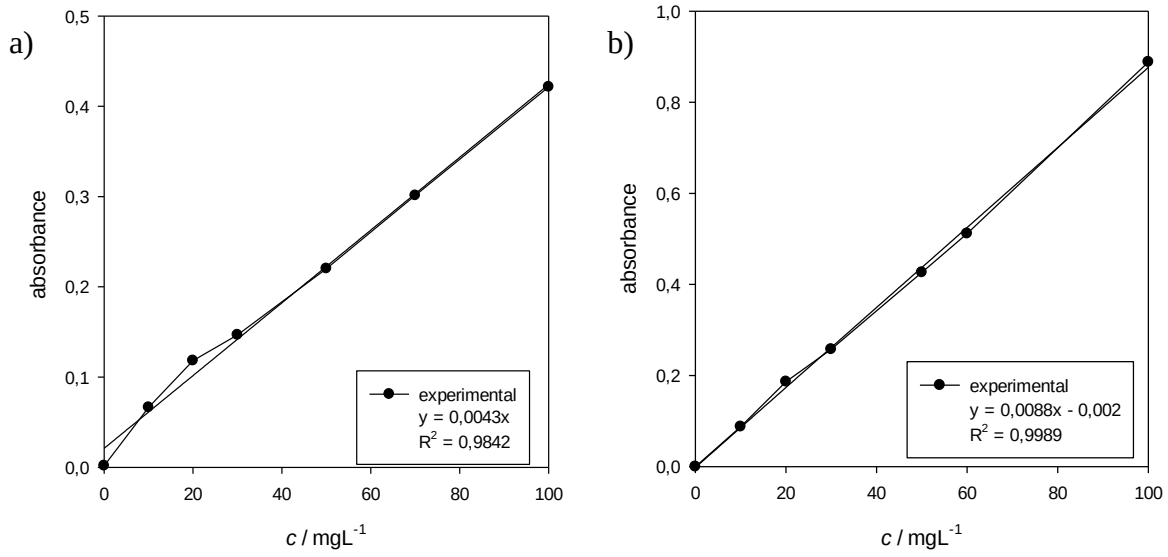

Figure 5.16. Calibration curve for nifedipine in a) HCl media and b) PBS.

5.4.5 *In vitro* dissolution test

Drug dissolution tests for nifedipine-loaded aerogels were performed in two different dissolution media. First, dissolution was performed in an acidic environment with HCl media (pH 1.2). A second dissolution medium was PBS with a pH of 6.8. Changing the dissolution medium to simulate the gastrointestinal tract was the additional method. First, a tablet shaped aerogel was poured into the HCl medium, and after 1 h the dissolution medium was replaced by a phosphate buffer solution. The analysis was performed for an additional 11 h. Drug dissolution studies were performed in triplicate at 37 ± 0.5˚C, employing the USP II apparatus (Farmatester 3). The speed of rotation was set to 50 rpm, and the volume of the dissolution medium was 900 mL. Aliquots (2 mL) were withdrawn at predetermined times and analysed spectrophotometrically at 238 nm. After each sampling, 2 mL of fresh dissolution medium was added to maintain a constant volume in the basket. All dissolution tests were performed in triplicate. The results are shown as the mean value ± standard deviation.

5.5 Results and discussion

5.5.1 Aerogel synthesis and characterisation

Four types of polysaccharide aerogels were obtained during the research work and are shown in Figure 1.

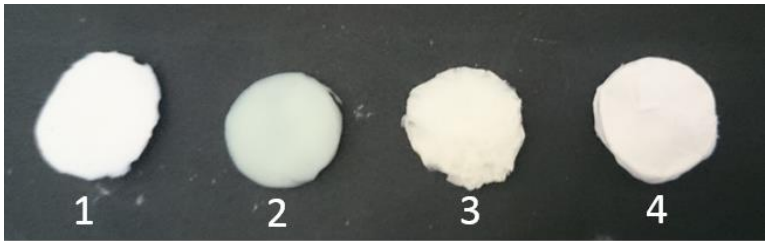

Figure 5.17. 1) guar, 2) pectin, 3) xanthan and 4) alginate aerogels.

Since the characterization of these aerogels had already been conducted and published in a recent paper, the aim of this research was to additionally investigate the properties critical for their drug dissolution performance. Swelling of polymeric matrices is one of the most significant properties for drug release. Swelling experiments were performed in HCl medium and in PBS.

First, the swelling of all prepared aerogels was investigated in the low pH of the HCl medium. Because of their structure, these polysaccharides are resistant to low pH and therefore do not degrade. However, the swelling ratio is high, owing to the high water absorbance capacity of aerogels. As is evident in Figure 5.18, initial HCl medium absorbance is followed by a constant swelling rate in the case of alginate and pectin up to 3 h. Xanthan and guar have an even higher absorbance capacity; therefore, the swelling ratio increases constantly, even after 3 h.

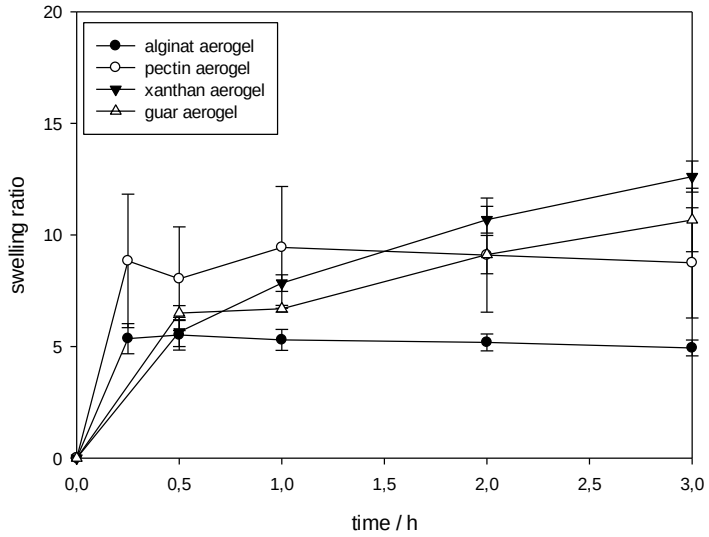

Figure 5.18. Swelling of aerogels in HCl medium

In contact with PBS, pectin swelled immediately to its maximum at 15 min, after which the swollen aerogel began to degrade slowly (Figure 5.19a). Complete degradation occurred only after 3 h. Similar behavior was observed in alginate. Nevertheless, alginate swelled to its maximum at 1 h, and after three hours there was still some residue in the solution (Figure 5.19b). Similar behavior is indeed the result of the very similar molecular structure in these two polysaccharides. Both are linear, as opposed to xanthan and guar molecules, which are both short branched. Thus the swelling rate of xanthan aerogel or guar aerogel is much higher compared to alginate aerogel or pectin aerogel. In the first three hours, both xanthan aerogel and guar aerogel start to swell, but both already show higher swelling capacity than the alginate and pectin aerogels (Figure 5.19c and d). The swelling ratio of xanthan aerogel is around 15 and of guar aerogel nearly 8, whereas highest swelling rate achieved by pectin aerogel after 15 min is around 7, and for alginate aerogel, less than 5. After 2 days, xanthan aerogel reached its maximum in swelling (Figure 5.20a). In that time, xanthan's aerogel weight increased 60 times from its initial weight, after which the xanthan aerogel began to slowly degrade. After 10 days, only minor residue was left in the PBS.

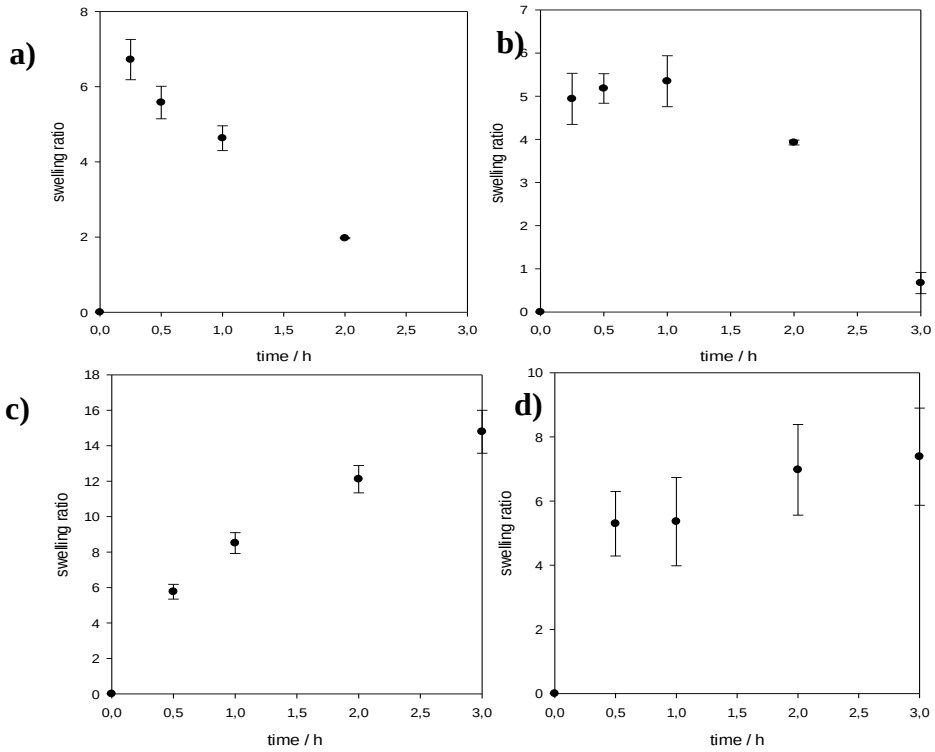

Figure 5.19. a) Pectin and b) alginate c) xanthan and d) guar aerogel swelling in PBS for 3 h.

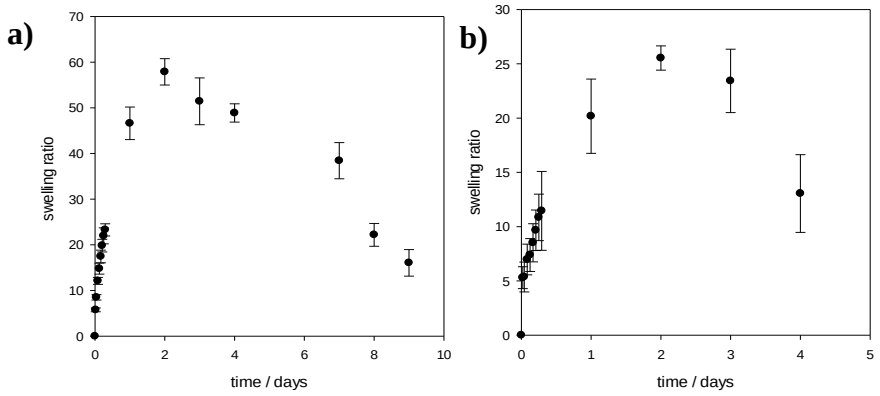

Figure 5.20. a) Xanthan and b) guar aerogel swelling in PBS after longer time period

5.5.2 FT-IR

While pure polysaccharide aerogels were white, nifedipine encapsulated aerogels were yellow. Nevertheless, to confirm the presence of nifedipine in the aerogel, FTIR analysis was performed.

Figure 5.21 shows FTIR spectra for the pure pectin aerogel, pectin aerogel loaded with nifedipine and pure nifedipine. For the pectin aerogels, three regions are visible. The region from 3500 to 1800 cm^{-1} has peaks at 3400 cm^{-1} corresponding to stretching of OH groups and at 2900 cm^{-1} corresponding to C-H stretching of CH_2 groups. The region from 1800 cm^{-1} to 1500cm^{-1} has peaks corresponding to COO- and $COOCH_3$. The last region, below 1500cm^{-1}, corresponds to coupled C-C, C-O-C and C-OH vibration modes. In the case of nifedipine, three regions are also visible. In the first region, two peaks are visible, at 3310 cm^{-1} corresponding to amine and hydroxyl groups and N-H stretching vibration, and a peak at 2950 cm^{-1} corresponding to OH stretching. In the second region, a characteristic peak at 1690 cm^{-1} corresponds to C=O stretching of the secondary amide but also C-O stretching of the ester group. Peaks at 1450 cm^{-1} and 1350 cm^{-1} correspond to NH stretching of the amide and ether bonds. The last region, below 1100 cm^{-1}, corresponds to CH-OH and C-O-C stretching.

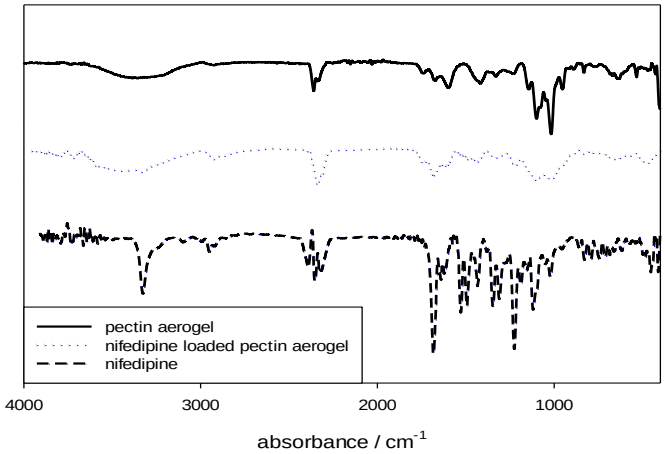

Figure 5.21. FTIR spectra of pectin aerogel, nifedipine loaded pectin aerogel and nifedipine.

As presented, almost all the peaks from pectin and nifedipine overlap. However, there is a noticeable difference between pure pectin aerogel and pectin aerogel loaded with nifedipine in the second region, in the peak corresponding to C=O stretching. Namely, in the case of loaded pectin aerogel, the intensity of this peak increases, indicating the presence of C=O groups from nifedipine.

5.5.3 Drug loading and *in vitro* release

Drug loading is an important parameter in pharmaceutical applications. The quantity of drug loading into aerogels may be limited, particularly in the case of hydrophobic drugs, such as nifedipine. Increasing the drug loading has several benefits. Since a high-loading carrier can deliver more drug into the body, it is more efficient at delivering the drug. The total amount of a carrier that is needed to deliver a given amount of a drug can thus be significantly reduced with a higher drug loading. Secondly, a higher drug loading carrier contains less non-drug components, and therefore lowers the potential adverse effect, not to mention reducing the manufacturing cost of the carriers [177]. Drug loadings to polysaccharide aerogels were thus determined as described in the experimental part. The highest drug loading was observed in the pectin aerogels, at 37.4%. A slightly lower loading, 34.9%, was exhibited by the xanthan aerogels. Lower loadings were then observed in alginate and guar aerogels, 21.7 and 25.7%, respectively. The latter could be explained by the aerogel's structural properties, which were published in a recent paper [178]. Due to the gelation of polysaccharides in ethanol, their structural properties are different. Larger surface areas and pore volumes were reported for pectin and xanthan aerogels [178], therefore resulting in higher drug loadings. Finally, alginate and guar aerogels have comparable pore volumes and surface areas [178], hence their similar final drug loading.

The prepared aerogels were first immersed in simulated gastric fluid at a pH of 1.2. The nifedipine release was monitored to check whether the prepared aerogels protected the drug from being released in the harsh conditions of the upper gastrointestinal tract.

Figure 5.22 shows nifedipine release from alginate and pectin aerogels. First, nifedipine release in the HCl medium was investigated (Figure 5.22a). It is evident from the figure that some release occurs in this low pH medium. Compared to crystalline nifedipine, the release rate is much higher in the first few hours, but after 6 h, the dissolution of crystalline nifedipine is comparable with the release from both carriers. Assuming that the drug stays in the stomach between 1 and 2 h, around 20% of the nifedipine is released from alginate aerogels and around 30% from pectin aerogels in that time.

Drug release experiments conducted in PBS showed faster drug release from both aerogels, compared to dissolution of a crystalline drug (Figure 5.22b). The total drug was released from both carriers after 5 h, showing the similarity of the two carriers. In the first hour in PBS, the release of nifedipine from alginate aerogel is 50-times higher than the dissolution of pure nifedipine. To mimic the gastrointestinal tract, additional study, changing the dissolution medium from HCl to PBS was also conducted. Figure 5.22c shows that the release from alginate and pectin aerogel is not highly affected by their exposure to the low pH HCl medium. Even though the release of nifedipine from pectin aerogel is around 30% after 1 h in the HCl medium, the already swollen aerogel shows drug release characteristics similar to those of the dry one (Figure 5.22b). Complete release of nifedipine is achieved in 6 h (1 h in the HCl medium and 5 h in PBS).

Similar *in vitro* drug dissolution experiments were performed for guar and xanthan. Nifedipine release from both carriers in the HCl medium is shown in Figure 5.23a. These two drug release profiles are similar to those from alginate and pectin (Figure 5.22a). All polysaccharide aerogels seem to be resistant to the low pH of the HCl medium. After 24 hours of exposure to such conditions, all tablet-shaped aerogels still seem unaffected, just slightly swollen (Figure 5.24). However, the nifedipine release from xanthan and guar aerogels in PBS is drastically different from its release from the alginate and pectin aerogels. As is clear from Figure 5.23B, nifedipine release is very slow and lasts up for 14 days, which opens up the possibility for other applications.

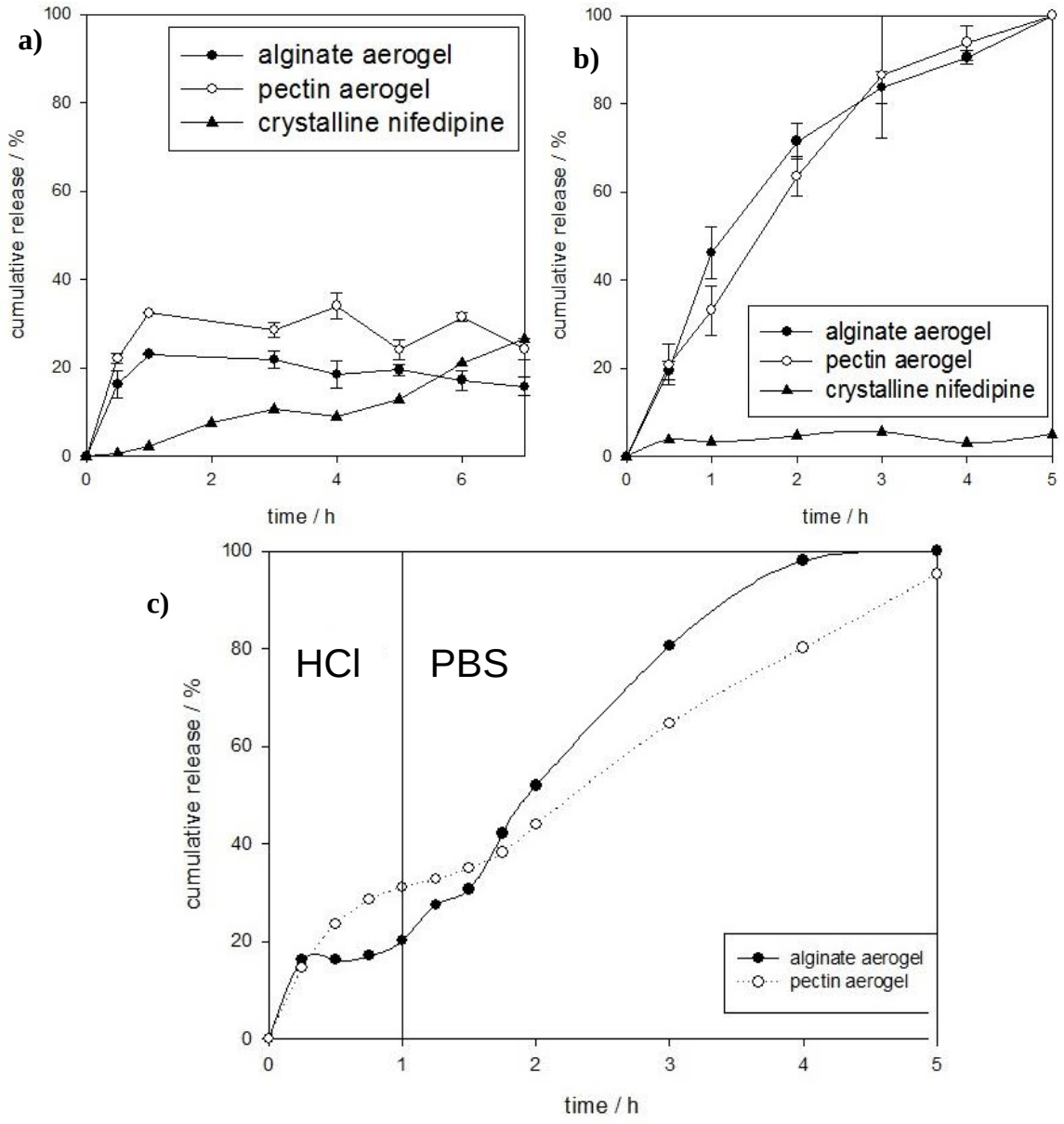

Figure 5.22. Nifedipine release from alginate and pectin aerogels in a) HCl medium, b) PBS and c) HCl medium-PBS.

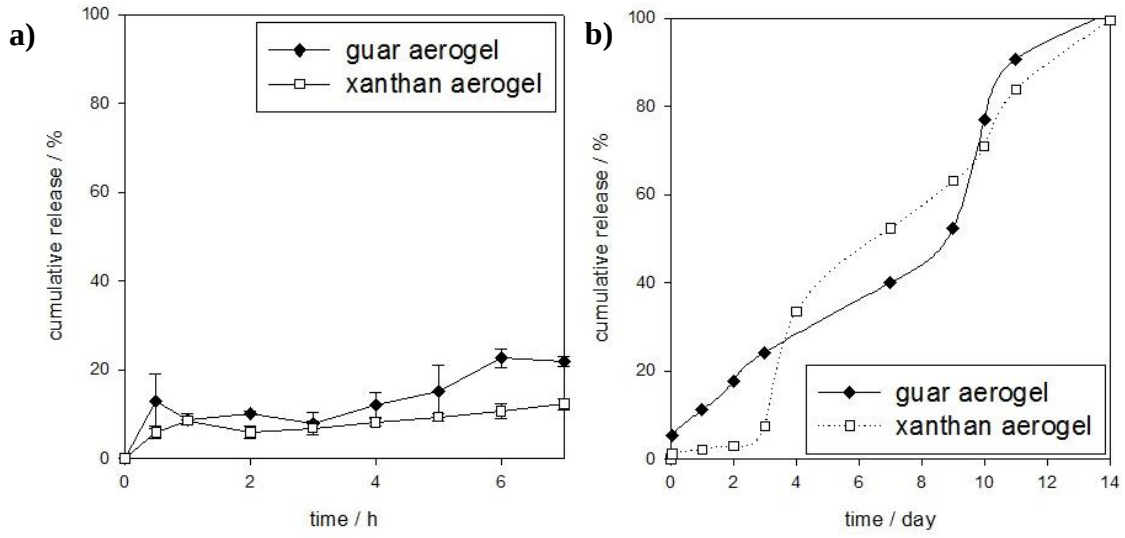

Figure 5.23. Nifedipine release from guar and xanthan aerogels in a) HCl media, b) PBS.

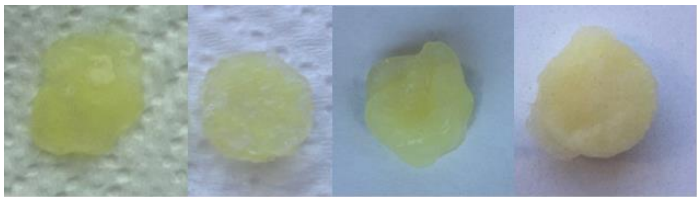

Figure 5.24. Dug loaded aerogels after 24 h contact with HCl media. From left to right: guar, pectin, xanthan and alginate.

Pectin-xanthan aerogel coatings for orthopedic applications

Total hip arthroplasty (THA) is a common procedure in orthopaedics that is subject to constant innovation. In order to improve the quality of life for patients suffering from hip fractures, novel materials and techniques are continuously studied and some have been introduced into clinical practice [179]. The most commonly used materials in THA are titanium alloys, various ceramics and stainless steel [180]. The material used must be biocompatible with body tissues and fluids, be able to withstand wear and corrosion, have or ideally exhibit mechanical properties similar to those of bone, etc. [181] Therefore, many studies now focus on developing coatings for base artificial hip materials in order to improve their functionality and durability. More recently, biomaterial-based coatings have been used as part of orthopedic implants in order to modulate the surrounding biological environment [182–185]. Among biomaterial-based coatings, polysaccharides were found to be especially promising as regards enhancing the respective implant integration [186]. Pectin, a polysaccharide commonly found in nature, has previously been used to increase the hydrophilicity of surfaces [187] and to enhance osteoblast-specific production [188]. Polysaccharide-based aerogels are interesting candidate materials for metal coatings in THA, especially considering the latest related research oriented towards drug-loaded coatings for local drug delivery [185,189,190]. NSAIDs and prophylactic radiotherapy can even prevent ectopic bone formation around the hip after total hip arthroplasty [191]. Therefore, two NSAID drugs, diclofenac sodium (DCF) and indomethacin (IND), a drug commonly used to prevent heterotopic ossification [192], were used in this study.

5.6 Experimental

5.6.1 Materials

The same medical-grade stainless steel samples (disc shape 15 mm in diameter) and the same preparation procedure as reported previously [185] were employed in this study. However, in contrast to the previous study, the samples were additionally passivated by immersion for 1 h in a 30 wt. % HNO_3 solution to simulate real artificial hip material. Afterwards, the samples were thoroughly rinsed with ultra-pure water, dried under nitrogen of high purity (99.999 wt. %) and stored in a desiccator for subsequent use.

High methoxyl pectin (hmP) (Pectin Classic CU-L 069/13; degree of esterification 78%) was provided by Herbstreith & Fox (Germany), and xanthan (Xa) (800–1200 cps) was obtained from Sigma Aldrich (USA). All polysaccharide solutions were prepared with ultra-pure water.

5.6.2 Aerogel coating formation

Both polysaccharides, hmP and Xa, were chosen based on their good gelation ability and proven drug release performance [147,178]. Various mass ratios of hmP and Xa solutions were prepared before the ratio 1:1 was ultimately found to provide the best adhesion on the medical-grade stainless steel. HmP (0.5 wt. %) was slowly poured into water while stirring and mixed until homogenization at 400 rpm for 30 min. Then, Xa (0.5 wt. %) was added to the hmP solution and again mixed until homogenization for about another 30 min. It is essential for this process that both polysaccharides are added to the water/solution very slowly in order to avoid the formation of clumps.

The prepared hmP:Xa solution was sonicated for 30 min in to remove any air bubbles formed during mixing. Then, a 300 µL hmP:Xa solution was precisely transferred onto medical-grade stainless steel in order to cover the whole disc evenly. Absolute ethanol (Sigma Aldrich, ACS reagent, ≥ 99.5) was poured onto the polysaccharide coating. It was previously reported by our group that gelation of both hmP and Xa can occur in the presence of ethanol [178]. This method

was therefore used to produce hmP:Xa alcogels (ethanol in the pores of a gel) on the surface of medical-grade stainless steel. The outer layer of the polysaccharide solution gelled quickly after contact with absolute ethanol. For the drying process, it is essential that all water in the pores be replaced by absolute ethanol. Therefore, the coated samples were placed in absolute ethanol for 3 h before supercritical drying.

5.6.3 Encapsulation of diclofenac sodium and indomethacin

DCF (analytical grade, ≥ 99.0% purity) was provided by Chemos (Germany). HmP:Xa solution (1:1) was prepared as described in Chapter 5.6.2. Since DCF is a water-soluble drug (with a solubility of 50 mg/mL [193]), this NSAID (1 wt.%) was added to the hmP:Xa solution while mixing. The hmP:Xa-DCF solution was sonicated in order to remove excess bubbles. Then, 300 µL of the homogenized solution was precisely transferred to the medical-grade stainless steel sample, followed by gelation in ethanol for 1 h. The ethanol solution was saturated with DCF in order to avoid the diffusion of this NSAID from the coating.

IND (analytical grade, ≥ 99% purity) was provided by Sigma Aldrich. IND has limited solubility in water, as it belongs to BCS Class II (highly permeable with low solubility) [194]. However, its solubility in ethanol is much greater than in water and can reach up to 50 mg/mL [195] upon stirring. Therefore, loading of this model drug had to be different than for DCF. IND was loaded into the hmP:Xa gel coating on medical-grade stainless steel samples by diffusion through IND-saturated ethanol for 5 h.

Drying was performed according to a method developed in our laboratory [66]. The supercritical drying was conducted at 314 K and 12 MPa. The chosen temperature and pressure allow the formation of a homogeneous phase of CO_2 and ethanol inside the hmP:Xa alcogels, in order to allow drying without the phase interface between the supercritical CO_2 and liquid phases and to preserve the adhesion of the coating. The drying was performed for 7 h at a CO_2 flow rate of approximately 200 L h^{-1}. After the supercritical drying, the system was depressurized at 0.2 MPa min^{-1}, after which white polysaccharide aerogel coatings on medical-

grade stainless steel were obtained. The samples were left to cool to room temperature and then stored in a desiccator.

5.6.4 Aerogel coating characterization

Specific surface area and porosity parameters were determined using the Brunauer-Emmett-Teller (BET) technique based on nitrogen gas adsorption (Micromeritics ASAP 2020) [196]. Prior to that, the hmP:Xa, hmP:Xa-IND, and hmP:Xa-DCF aerogel coatings were removed from the medical-grade stainless steel and outgassed.

Micrographs of the prepared aerogels were obtained by a field emission scanning electron microscope (FE-SEM) Sirion 400 NC. The aerogel coatings were scraped from the medical-grade stainless steel surface, sputter-coated with gold particles and fixed to aluminum sample holders with double-sided carbon tape. They were then scanned at an accelerating voltage of 10 kV using a TLD detector.

Ultra-pure water (with a resistivity of 18.2 MΩ cm at 25°C) produced by the Milli-Q® system was used to prepare a physiological body fluid of 0.9 wt. % NaCl used for the electrochemical analysis. NaCl (for analysis – ACS quality) and ethanol (for analysis – ACS quality) were provided by Carlo Erba Reagents (Italy).

Electrochemical impedance spectroscopy (EIS) and cyclic polarization (CP) techniques were employed for the electrochemical study, under stagnant conditions at 37°C, using a three-electrode cell system and the same equipment as reported before [185]. At least three replicate measurements were performed for each EIS experiment, where Grubbs' test [197] was used to check for outliers. The average values after the fitting procedure are presented for EIS measurements, while a representative CP curve was presented to describe each system studied.

ATR-FTIR spectra were recorded using an Agilent Cary 630 FTIR spectrometer with the diamond ATR module at a scan range of 4000–650 cm^{-1}. The scans were performed at three different spots on each sample surface (hmP:Xa, hmP:Xa-DCF, and hmP:Xa-IND) or using a

sufficient amount of pure drugs (IND, DCF) to perform the measurement. ATR-FTIR spectra were also measured after the *in vitro* release testing (after 24 h) to confirm that the whole amount of the respective incorporated drug had been released.

5.6.5 Drug loading and the *in vitro* dissolution test

About 10 mg of aerogel coating was removed from the surface of the sample and poured into 10 mL of phosphate buffer saline (pH = 7.4) for 24 h. Phosphate buffered saline (PBS) was prepared by dissolving 6.8 g of KH_2PO_4 (Ph. Eur., anhydrous, ≥ 98%, Sigma Aldrich) in 1 L of water, and the pH was adjusted to 7.4 with 1 M NaOH (Ph. Eur. ≥ 98%, Sigma Aldrich). After 10 min of sonicating and 6 h of stirring at 250 rpm and 37±1°C, the solution was filtered through a Teflon® 0.45 μm filter and the drug amount was determined spectrophotometrically (Varian, Cary 50 Probe UV spectrophotometer) at 276 nm for DCF and at 320 nm for IND. From the calibration curve, the mass of the drug (m_d) was then determined. The drug loading (DL) was calculated from Eq. (8).

The drug release experiments were performed as previously described in [198]. In order to determine the drug release as a function of time, we used 11 samples to represent individual time points (0.5, 1, 2, 3, 4, 5, 6, 7 12, 16, and 24 h) for each NSAID. Each sample was placed in 20 mL of PBS. At selected time intervals, 2 mL of solution was withdrawn, filtrated through a 0.45 μm PTFE filter and analyzed spectrophotometrically at 276 nm for DCF and at 320 nm for IND. The cumulative release was calculated by Eq (5). Three replicates were performed for each NSAID. The average values with standard deviations for the specific time point were calculated. The confidence interval was determined as $\pm ts/\sqrt{x}$, where t is a Student's t-distribution, s is the standard deviation, and x is the number of measurements. The dissolution curve was plotted as the cumulative release (%) vs. time with 95% confidence interval.

5.6.6 Cytotoxicity and cell cycle analysis

In order to perform biocompatibility testing, a human bone-derived osteoblast cell culture was used (ATCC CRL-11372, LGC Standards, UK). All testing was performed according to the

ISO 10993-5:2009 standard. The as-prepared samples (hmP:Xa, hmP:Xa-DCF, and hmP:Xa-IND) were incubated with 6 mL of cell culturing media. The resulting sample solutions were incubated with the osteoblast cell culture on P96 microtiter plates. Cell viability was determined after 24 h incubation via the reduction reaction of the tetrazolium salt according to Mosmann [199], using the standard reduction for tetrazolium salt MTT [200,201]. Absorbance was measured at 570 nm using a spectrophotometer (Varioskan, ThermoFisher Scientific, USA).

All prepared samples (hmP:Xa, hmP:Xa-DCF, and hmP:Xa-IND) were sterilized under UV for 30 minutes. These were then transferred to a centrifuge tube (50 mL) and filled with 6 mL of medium Advanced DMEM with 5 wt. % FBS. Prepared samples were applied to a culture of human osteoblasts hFOB (ATCC CRL-11372, LGC Standards, UK). Preparation of cells: the osteoblasts were plated on a P12 well plate at a density of 100,000 cells per well and were incubated overnight at 34°C, 5 wt. % CO_2. Then, the as-prepared samples were placed on cells in three replicates at a concentration of 1:2 in the medium Advanced DMEM with 5 wt. % FBS. As the control, a cell monolayer was prepared in the medium Advanced DMEM with 5 wt. % FBS. A further incubation step followed, and after 24 hours, the cells were trypsinized, strictly following the manufacturer's protocol for the use of Cell Cycle Kit (Catalog No. 100106 MCH). The analysis was performed using the MUSE Cell Analyzer (EMD Millipore, USA).

5.7 Results and discussion

5.7.1 Aerogel coating formation

The aim of this research was to produce novel advanced coatings on medical-grade stainless steel to investigate their potential use in THA. To the best of our knowledge, polysaccharide aerogels had never been prepared or investigated as coatings on any of the materials used in THA. Compared to other coating materials for THA reported in the literature [202], the advantage of an aerogel coating lies in its drying. After carefully choosing the drying conditions (314 K, 12 MPa), the initially prepared alcogels were dried in the absence of capillary forces. The extraction of a solvent (ethanol) in the alcogels was achieved by supercritical CO_2, and the

final aerogel showed good adhesion and great structural properties. The ratio between the two polysaccharides used in the research had to be precisely determined in order to achieve the coating adhesion on the passivated medical-grade stainless steel and good drug release performance at the same time. The optimum ratio of hmP and Xa was determined to be 1:1. After supercritical drying, the hmP:Xa aerogel coating was characterized by nitrogen adsorption, which confirmed its nanoporous structure. The specific surface area was 289 m^2g^{-1}, the pore volume was 0.11 cm^3g^{-1}, and the average pore size was 6.8 nm, as determined by the BJH adsorption method. The specific surface area for hmP:Xa-DCF was 183 $m^2\ g^{-1}$, and for hmP:Xa-IND 175 $m^2\ g^{-1}$, which are in the range of polysaccharide aerogels obtained by ethanol-induced gelation [178].

5.7.2 Aerogel coating characterization

Figure 5.25 shows SEM micrographs of the prepared aerogel coatings. The highly porous structure of the hmP:Xa aerogel coating is clearly evident from Figure 5.25a, which shows the surface of this sample. In order to gain more insight into the microstructure of the respective aerogel samples, cross-sections of all samples were prepared and observed using FE-SEM at magnifications of 10,000 and 100,000. Owing to the highly non-conductive nature of the materials, scanning at higher magnifications was not possible. The microstructure of the hmP:Xa, hmP:Xa-DCF and hmP:Xa-IND samples is quite similar (Figure 5.25b, c, d), and the morphological structure of the coating was not significantly affected by the addition of DCF and IND.

The latter could provide a good indication of the potential use for such aerogels, regardless of the drug chosen to be incorporated. This is even more important considering the different loading procedures for the hmP:Xa-DCF and hmP:Xa-IND. The FE-SEM micrographs show a highly compact, layered structure for all samples, confirming the low average pore size obtained by nitrogen adsorption.

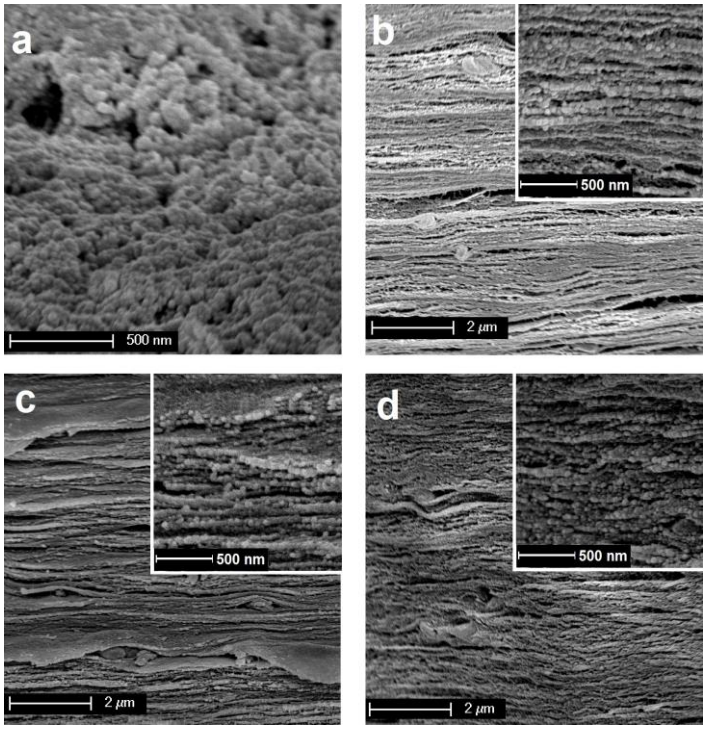

Figure 5.25. Scanning electron micrographs of (a) the surface of hmP:Xa coating, (b) cross-section of hmP:Xa coating, (c) cross-section of hmP:Xa-DCF coating, and (d) cross-section of hmP:Xa-IND coating.

In this study, corrosion susceptibility was investigated by electrochemical analysis based on EIS and CP measurements. The corrosion process of the medical-grade stainless steel in simulated physiological body fluid at 37°C is under kinetic control, as no diffusion was detected. The polarization resistance (Rp) values give an indication of the resistance of the steel samples to general corrosion. The higher the Rp value, the more resistive the sample. Rp values are calculated as Rp = R1 + R2. Figure 5.26 represents the polarization resistance (Rp) values for all the studied systems, i.e. passivated steel and both coated medical-grade stainless steel samples. For each system, the confidence interval was determined according to $\pm ts/\sqrt{x}$, where t is a Student's t-distribution, s is the standard deviation, and x is the number of measurements. For comparison, the Rp values for the uncoated, non-passivated medical-grade stainless steel samples (as previously reported in [185]) are presented in Figure 5.26. The Rp values of the uncoated, non-passivated samples were obtained using an EEC model that took into account

the diffusion process, which is not the case for all passivated systems in this study. From the results, it can be observed that all three passivated samples are more resistant to pitting corrosion compared to the uncoated, non-passivated sample. However, not all the studied samples have repassivation abilities. The same was previously concluded for the non-passivated uncoated samples [185].

CP measurements were performed on the three studied passivated systems (uncoated, hmP:Xa-IND, and hmP:Xa-DCF) after 11 h of immersion. The localized corrosion behavior of the uncoated and coated samples can be determined based on the potential differences [203]. The higher the potential difference, the slower the pitting process.

The hmP:Xa, hmP:Xa-DCF, hmP:Xa-IND aerogel samples on stainless steel discs were studied using ATR-FTIR spectroscopy before and after *in vitro* drug release testing (Figure 5.27). Figure 5.27a shows the spectra of the hmP:Xa aerogel coating, the respective drugs (DCF and IND), as well as both aerogels with the incorporated drugs (hmP:Xa-DCF and hmP:Xa-IND). From the several peaks that can be observed for the spectra of hmP:Xa-DCF and hmP:Xa-IND that can be assigned to the peaks of the pure NSAID drugs (IND, DCF), and their comparison with the hmP:Xa aerogel, it can be confirmed that the drug was indeed incorporated into the aerogels.

A broad peak between 3700 and 3000 cm^{-1}, which corresponds to O–H vibration, is observed in the spectra of all aerogel samples (blank and with incorporated drugs). For the hmP:Xa-DCF aerogel coating, several new peaks can be observed, namely the HC–N–CH bending vibration at 1376 cm^{-1}, the R=C=O stretching vibration at 1577 cm^{-1}, and the CH_2 bending at 1462 cm^{-1} [204,205]. For the hmP:Xa-IND aerogel coating, the newly observed peaks include the R-C=O stretching vibration at 1717 cm^{-1}, the indole ring deformation at around ~1600 cm^{-1}, the HC-N-CH stretching at 1316 cm^{-1}, and the CH_2 bending vibration at 1288 cm^{-1} [206,207].

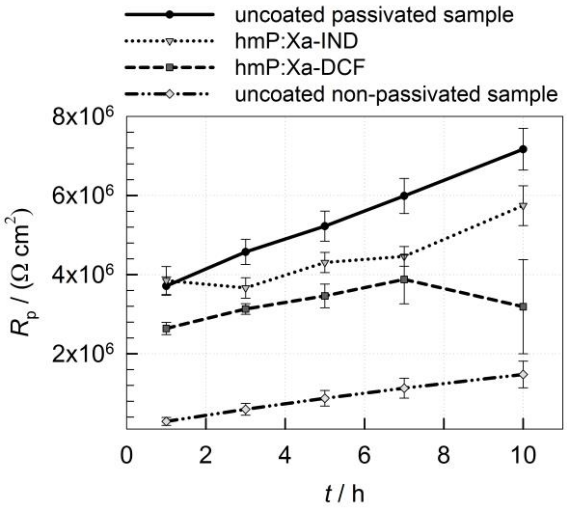

Figure 5.26. R_p values obtained from impedance fitting and the corresponding 95% confidence intervals for medical-grade stainless steel samples passivated (uncoated, hmP:Xa-IND, and hmP:Xa-DCF) and non-passivated, measured after 1, 3, 5, 7, and 10 h of immersion in simulated physiological body fluid at 37 °C.

Since ATR-FTIR was successfully used as a method to confirm the presence of the incorporated NSAID drugs, the same method was used to confirm the completeness of their release after 24 h (Figure 5.27 b and c). The suitability of such an approach is also in agreement with previous findings [204]. Figure 5.27 b and c show the spectra of samples originating from the respective NSAID-aerogel combinations. These include the spectra after the *in vitro* drug release. The latter are in agreement with the release analysis, which showed no drug leftovers in the respective samples after 24 h. Since the aerogel samples had almost completely dissolved in this time and in the given release media, the IR spectra after the release no longer show the same structural properties as found in the as-prepared aerogels.

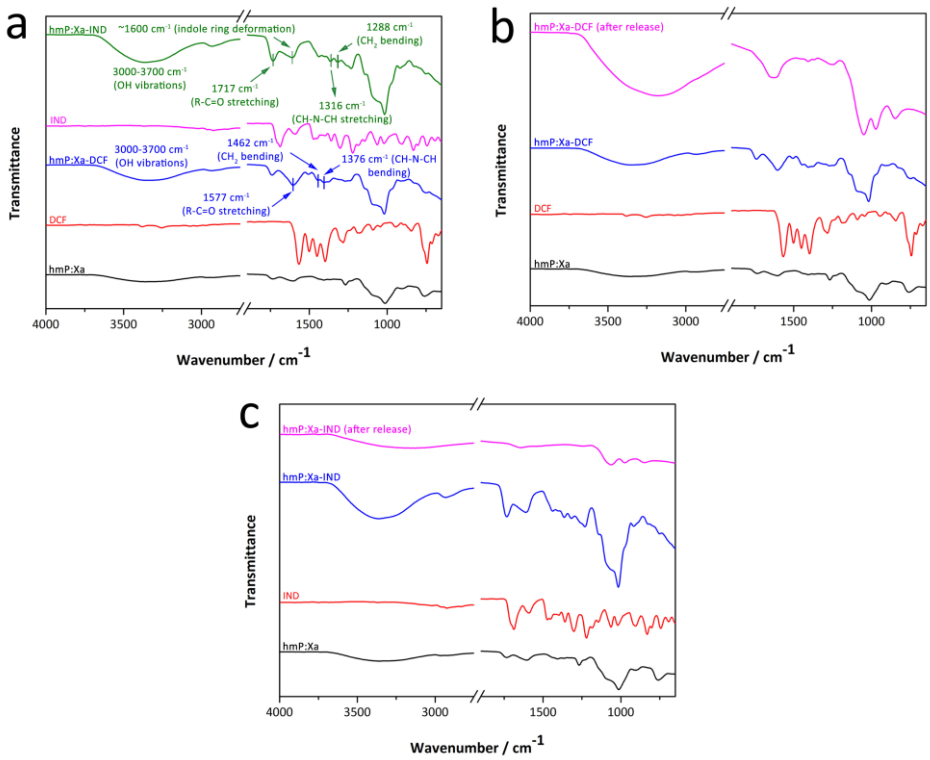

Figure 5.27. ATR-FTIR spectra of the sample before and after release.

5.7.3 Drug loading and the *in vitro* dissolution test

In order to evaluate the potential of aerogel coatings on artificial medical-grade stainless steel-based hips to relieve pain by administering drugs locally, NSAID-loaded coatings (IND and DCF) were prepared in this research, and the release profile was carefully evaluated. Local drug delivery has many advantages in comparison to systemic administration, e.g. fewer side effects and the absence of intravenous drug administration. Local delivery can lead to a locally excessive concentration, but these absolute drug amounts are far lower compared to systemic administration, which often has a yield below 50% (depending on the respective drug pharmacokinetic and pharmacodynamics properties). Finally, locally administered DCF or IND also provide a local anti-inflammatory effect and lower the possibility of an immune response [208].

Drug content was determined as the ratio between the amount of the NSAID and the total amount of coating. Similar results were obtained for both drugs, 4.5 ± 0.2% and 4.2 ± 0.3% for DCF and IND, respectively. Owing to its higher water solubility, DCF was incorporated in the first step of the gelation process while preparing a polysaccharide aqueous solution [178]. In contrast, IND was incorporated by means of diffusion through ethanol. The similar loadings are most likely a consequence of the characteristics of the prepared aerogel and its available surface area [209].

Figure 5.28 shows the results of the respective NSAID release testing as a percentage of the release of DCF or IND as a function of time. The release was calculated as the ratio between the NSAID concentration at a selected time and the final released NSAID concentration. Both types of samples were exposed to PBS for an extended period of time, and the concentration variation was monitored. The completeness of the NSAID release was confirmed by the prolonged exposure of all samples to PBS, which led to no additional increase in the respective NSAID concentration. This is also in agreement with the FTIR analysis after 24 h, which showed no NSAID peaks. The release profiles of the two NSAIDs were different, as had been expected, given the different nature of the drugs loaded on the same carrier. DCF release is slower at the beginning compared to IND, while it surpasses the latter after 5 h. When hmP:Xa-DCF aerogel coating on medical-grade stainless steel comes into contact with PBS, PBS starts to diffuse into the pores of the aerogel, dissolving the DCF and also partially the aerogel. The dissolved DCF is released from the pores in the aerogel and slowly diffuses into the release media. If the intrusion of the PBS into the aerogel is faster than the DCF diffusion, the release profile is initially slower. In contrast, IND release was faster in the initial 3 h of the *in vitro* drug release experiment. Since IND is a lipophilic drug incorporated into a hydrophilic carrier, an initial burst release may occur [210]. Upon contact with PBS, the IND is dissolved and released from the coating. However, since IND solubility in water is lower than that of DCF, the release of IND from the porous aerogel coating is delayed. It is important to point out that all of the incorporated respective drugs were completely released from the aerogels, as can be seen in the IR spectroscopy measurement (Figure 5.27 b and c). Thus, no peaks can be observed in the spectra of the material leftovers after the release that could be assigned to the respective

drugs (or were present in the spectra of the respective aerogels with the incorporated drugs). Considering the high cost of drugs, this is important for the possible future commercial potential of such material-drug combinations.

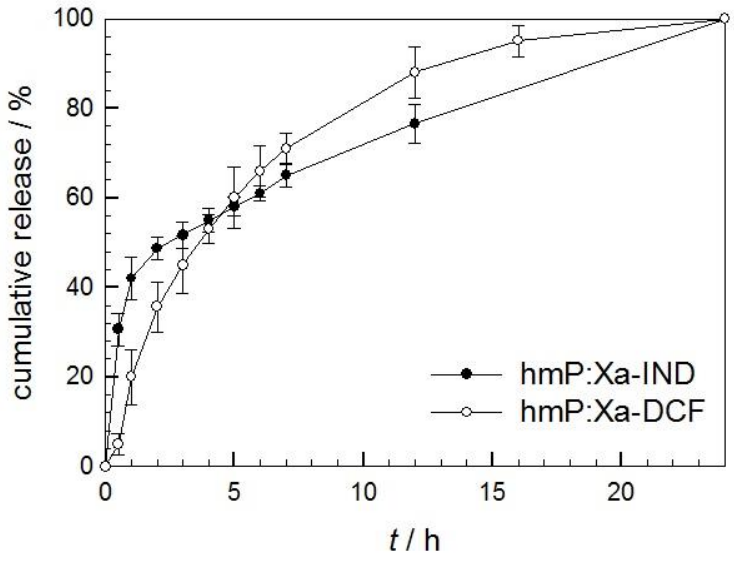

Figure 5.28. Cumulative release of DCF and IND from hmP:Xa aerogel coatings on medical-grade stainless steel. The results are shown with the corresponding 95% confidence intervals.

5.7.4 Cytotoxicity and cell cycle analysis

In order to evaluate the potential of the prepared samples for osteointegration, which is critical in patient acceptance of an artificial hip after THA, biocompatibility testing was performed using human bone-derived osteoblasts. The main objective of this testing was therefore to assess if the proposed aerogels with incorporated drugs degrade to or release any toxic products that could affect cell growth. Additionally, we were interested in the potential increase in cell viability, since the drugs used have already been proven safe for other clinical applications, and because we used natural polysaccharide materials for preparing the aerogels. The second

objective was therefore to determine whether the proposed materials show any measurable effect on the growth of the osteoblast cells when compared to the control measurement (Advanced DMEM + 5 wt. % FBS). Three different dilutions of the dissolved sample solutions were incubated with the cells to evaluate the different physiological scenarios to which an artificial hip can be exposed in the body (different volumes and concentrations of body fluids with growth factors and other biomolecules) [211,212].

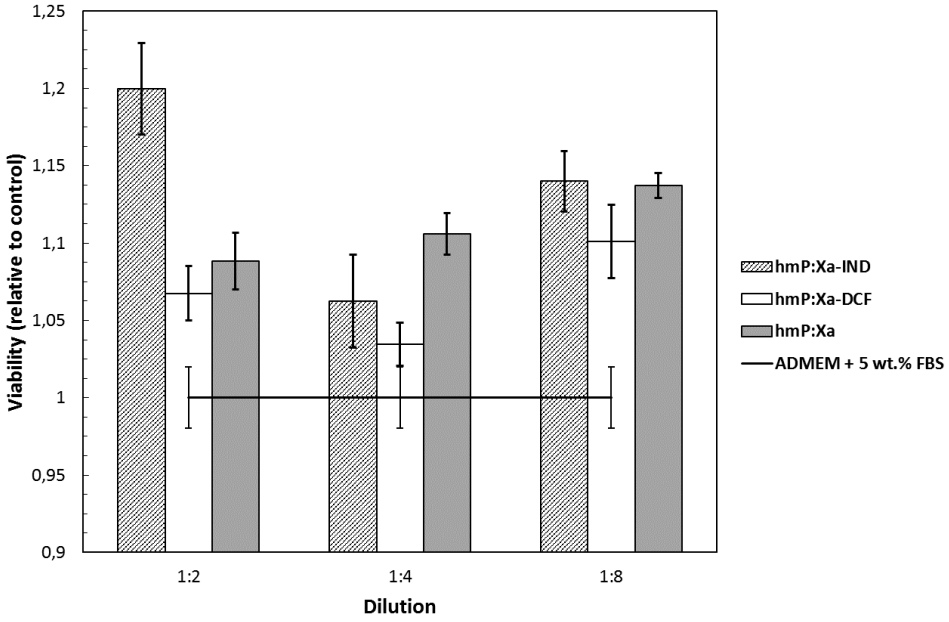

Figure 5.29. The cell viability of the aerogel samples. The results are shown with the corresponding 95% confidence intervals.

Regardless of the time, all three aerogel samples (hmP:Xa, hmP:Xa-IND, and hmP:Xa-DCF) show a higher viability compared to the control sample. It is worth noting that the hmP:Xa aerogel sample even outperforms the hmP:Xa-DCF sample, while the hmP:Xa-IND still exhibits a higher cell viability. For all curves shown in Figure 5.29, the confidence interval was determined as $\pm ts/\sqrt{x}$, where t is a Student's t-distribution, s is the standard deviation, and x is

the number of measurements (in our case 3). Increased cell viability in comparison with the control means potentially better osteointegration, hence a promising direction for future testing and development in bone tissue engineering. The improved cell viability of all three aerogel samples (hmP:Xa, hmP:Xa-IND, and hmP:Xa-DCF) compared to the control sample means that, regardless of the drug incorporation, these samples are not only biocompatible, but even increase the number of osteoblast cells grown in the same period of time when compared to the control. This result is important in two regards. Firstly, the as-prepared samples are biocompatible regardless of the polysaccharide combination used (and other components used in the preparation of the aerogels) and the respective drug, and regardless of possible aerogel degradation products that could occur during the exposure of tissue to these materials. And secondly, these results are very promising with regard to our desire to prepare coatings on medical-grade stainless steel that would promote osteointegration. We can also conclude that eventually the aerogels will degrade/dissolve in the body, were such products to be used in a clinical setting. And when this happens, osteoblasts would still also attach to the bare substrates (medical-grade stainless steel), possibly increasing the suitability of such materials for orthopaedic applications even further.

6 CONCLUSIONS

The last, sixth chapter summarizes the work during and results of this PhD research.

The main objective of this dissertation was the preparation of natural polysaccharide aerogels, the development of a novel gelation method and application of such aerogels as carriers for drug delivery. The supercritical technology was used to preserve the morphological structure of the resulting wet materials in order to obtain stable dry carriers. The purpose of the research work in the third chapter was to optimise a well-known method for the preparation of pectin and alginate aerogels and then in the chapter four to develop the method for the gelation of various polysaccharide gels. In chapter five, the aim was to prepare carriers for controlled drug release – to slow down the release of high water-soluble drugs and enhance the release of low-soluble drugs for enhancing bioavailability. The last part of the research was the preparation of novel aerogel coatings for local drug delivery in medical applications.

The first chapter forms the background of the study. Briefly, the structure and function of natural polysaccharides is described with a focus on pectin, alginate, guar and xanthan, which were later used in the study. The main focus of the first chapter is on the gelation of those polysaccharides, such as the familiar mechanisms of gelation and a review of published results in the field. The last part is about the transformation from wet gel to dry gel.

The thesis continues with the methods used in the later research work. Supercritical drying is the most critical step for obtaining highly sophisticated materials – aerogels. Some characterisation methods are then described and briefly explained in order to understand and accordingly discuss the results later in the thesis. Drug encapsulation is another critical step in the production of aerogels as drug carriers. Supercritical impregnation and *in vitro* dissolution tests are thus described in this section.

The third chapter is the beginning of the experimental part of the thesis. Low-methoxyl pectin, alginate and their composite aerogels were prepared first by cross-linking with different divalent ions. The impact of calcium ions had been previously investigated and published. The aim of this research was to investigate the impact of different divalent ions on final aerogel characteristics and subsequently on the release of active substances. Zinc and strontium ions were used as a comparison to calcium ions. The aerogels were prepared in a spherical form of approx. 2 mm in diameter. All prepared materials were mesoporous with large surface areas.

Calcium cross-linked aerogels provided the largest surface areas and zinc cross-linked, the least. All the samples were stable in the HCl medium over a period of 7 h and started to swell in contact with PBS. Undoubtedly, all samples show pH-dependent swelling. It was shown that zinc cross-linked aerogels (low-methoxyl pectin, alginate and a composite of these two polysaccharides) yielded the highest swelling ratio, but the lowest erosion in phosphate buffer solution. Aerogels cross-linked with calcium ions behave in the opposite manner. This characteristic is important for the later investigation of the release of model drugs.

The fourth chapter describes the newly developed method for the preparation of various polysaccharide aerogels, including high-methoxyl pectin, low-methoxyl pectin, alginate, xanthan and guar. This method proposes the increase in hydrophobic interactions between polysaccharide units by the addition of ethanol alone. The method was first developed on high-methoxyl pectin. By the addition of ethanol, stable monolithic alcogels were formed. After supercritical drying, the structure remained the same. The concentration of high-methoxyl pectin on the shrinkage during supercritical drying was investigated. It was observed that the highest pectin concentration (4%) gave the lowest shrinkage. The lower shrinkage then resulted in a larger surface area. Wet gels were dried under two different pressures, 150 bar and 200 bar, and no major difference could be observed in the structural properties of the resulting materials. Thus, it was assumed that higher pressures during the drying process do not influence the structure of the gel. Concentrations of hmP aqueous solutions higher than 4% wt could not be obtained, owing to the high viscosity of the solution. The same method was then applied to other polysaccharides, lmP, Xa, Gu and Al. Different shape monoliths could be prepared, from small tablet-like shaped monoliths, to larger cylindrical or membrane shaped monoliths. Conventionally, those polysaccharides are prepared by dissolution in water, cross-linking by various cross-linkers, and then prior to supercritical drying, the water in the gel has to be exchanged with organic solvent. Since in this research, the gelation occurred directly in ethanol without additional cross-linkers, there was also no need for the solvent exchange step. The total production time was thus reduced. The time of gelation strongly depends on the size of the monoliths, mainly on account of the diffusion governed gelation. All the polysaccharide aerogels obtained were prepared from 4% polysaccharide solution. Monoliths with large

surface areas and high porosities were obtained. The largest yet reported surface area of monolithic aerogels was obtained for lmP (510 m^2g^{-1}), hmP (384 m^2g^{-1}), Xa (363 m^2g^{-1}) and Gu (111 m^2g^{-1}). The total production time was lower compared to conventional polysaccharide aerogel synthesis, since in this process, no solvent-exchange or washing was needed prior to supercritical drying. In addition, to the best of our knowledge this is the first report on the preparation of pure xanthan and guar aerogels. To date, these gels have been prepared with the addition of other polysaccharides. Xanthan gum aerogels also possessed comparably high specific surface areas. All the samples had also very low thermal conductivity, which corresponded to specific surface areas and porosity. Namely, by increasing the surface area and porosity, the thermal conductivity decreased. Therefore, pectin aerogels were the ones with the lowest thermal conductivity, which is in the range of the best insulating materials.

Since Al aerogels prepared by the novel gelation method did not provide comparable results with the conventional method (surface area of only 147 m^2g^{-1}), further research was focused on the optimization of the novel method for this particular polysaccharide. We investigated the influence of process parameters during alginate aerogel production. The parameters investigated were the time of gelation (1h vs 24 h), the viscosity of alginic acid and the alcohol used for the gelation. It was observed that 1h gelation time does not provide samples with surface areas significantly lower than samples prepared using 24 h gelation time. The difference is only 30 m^2g^{-1}. However, the visual appearance is completely different; after 24 h of gelation, the resulting aerogels had polished surfaces compared to the coarse surfaces of aerogels obtained after 1 h of gelation. The viscosity of alginate indeed influences the structural properties of aerogels. Highly viscous alginate provided a denser structure with a higher surface area. Indeed, the most important parameter in alginate aerogel production was the type of alcohol. The results show that the best option for the gelation of alginate is methanol, as the obtained surface areas of those materials are twice as large as for those gelled in ethanol. Also, the N_2 adsorption capacity is better. Headspace GC results confirmed the presence of methanol after supercritical drying; however, the amount is low, and those materials could also be safely used in pharmaceutical or medical applications. Gelation in propanol and butanol was unsuccessful. Since the resulting materials possessed very small specific surface areas, the

adsorption capacities were near zero. It is assumed that the propanol and butanol molecules are too big to interact with the alginate chains, and complete gelation does not occur. The alcohol chain's length seemed to have the greatest impact on the gelation ability of alginate. The smaller the molecule, the closer the alginate chains, which resulted in increased interactions. The thermal conductivity of aerogels prepared in ethanol was high and was expectedly lower with methanol-obtained aerogels. However, thermal conductivity is still not within the range of some other published results on polysaccharide aerogels. Further research is thus needed in order to obtain even better properties of alginate aerogels.

The fifth chapter of the thesis reports the results on aerogels developed and optimised for pharmaceutical or medical applications. Issues with optimal drug delivery are first discussed in the introduction. Then the aerogels described in the third chapter of this thesis were used for the encapsulation of water-soluble diclofenac sodium (DCF). DCF was added to a polysaccharide solution in the first step of the sol-gel process, mixed into the polysaccharide aqueous solution. Spherical aerogels, cross-linked with zinc, strontium and calcium were prepared to investigate the impact of these ions on drug release. Extremely high loading was achieved--around 70%. The *in vitro* dissolution test for pure DCF showed very high solubility within the buffer solution. Thus, a proper carrier should be obtained in order to prolong the release of this drug. The prepared mesoporous aerogels have been shown to be suitable for prolonging the release of diclofenac sodium. Aerogels are stable in dry air conditions; therefore, for the final drug product, they are way more suitable than hydrogels. These matrices are also biodegradable and biocompatible and thus suitable for use in pharmaceutical applications. The drug loading was the highest in the case of zinc cross-linked aerogels. In this research we showed that calcium ions are indeed not proper cross-linkers for preparing a controlled release drug carrier. By using zinc as a cross-linker, the drug release was much more controlled. Comparing all the experimental work from *in vitro* dissolution studies, and drug loading to swelling and erosion, pectin aerogels cross-linked with zinc are considered the most promising carriers for the controlled release of DCF. Calcium cross-linking is useful only in the case where immediate drug release is desired. The final controlled release drug formulation containing pectin-zinc aerogels within a gelatine capsule was compared with two commercial drugs of

DCF. No similarity was found among the three controlled release products. 80% of the drug was released from the aerogel-based carrier in 7 h. In this period, the whole carrier was degraded. In contrast, the remains of the carrier of both commercial drugs were present after 72 h in PBS. To conclude, the drug release kinetics from the spherical core, cross-linked by calcium, was rapid, but it was successfully prolonged by changing the cross-linking ion. According to those results, pectin aerogels cross-linked with zinc are the most suitable and can be safely used as sustained drug carriers.

The polysaccharide monolithic aerogels developed and optimized in Chapter Four were then used for the encapsulation of the low water-soluble drug, nifedipine. Polysaccharide aerogels were prepared by ethanol-induced gelation, and their swelling and erosion were investigated in simulated body fluids. Swelling in the lower pH of the HCl medium was high, but erosion did not occur. Rapid swelling of pectin and alginate aerogels was observed in the higher pH of PBS, followed by rapid erosion. ATR-IR analysis confirmed the presence of nifedipine in the aerogel. The highest drug loadings were achieved by the pectin and xanthan aerogels, 37.4% and 34.9%, respectively. Lower drug loadings for alginate and guar are likely the result of their structure, namely smaller surface area and pore volume. *In vitro* drug release experiments showed improved nifedipine release from pectin and alginate aerogels. In contrast, the nifedipine release from xanthan and guar aerogels was prolonged, owing to the greater stability of those two aerogels in simulated body fluids. Nifedipine release was prolonged for up to 14 days, leaving these two carriers as inappropriate for oral drug release. Nevertheless, prolonged drug release from these two carriers opens up new possibilities for using such carriers as other drug delivery devices, e.g. for local drug delivery or even as implants. In any case, these results show great prospects for further research on those particular aerogels.

The final section of the thesis describes the development of novel coating materials on medical-grade stainless steel, prepared from two polysaccharides, xanthan and high-methoxyl pectin. Additionally, two NSAIDs (DCF and IND) were incorporated into coatings, and their release was investigated *in vitro*. Such systems are very interesting for postoperative orthopaedic applications in order to reduce pain and prevent local inflammation, and hence to reduce

potential artificial material rejection. The corrosion of all passivated medical-grade stainless steel samples, coated and uncoated, is under a kinetic-controlled process, and all passivated samples are highly resistant to general corrosion. The resistance towards localized corrosion follows the trend hmP:Xa-DCF, passivated uncoated, hmP:Xa-IND, and non-passivated uncoated medical-grade stainless steel samples. Intravenous or oral administration of drugs right after surgery may cause unwanted side effects; therefore, the proposed system for local administration of NSAIDs is of high value to improve the patient's quality of postoperative life. Since the carrier was the same for both drugs, the final drug loading was comparable for both model drugs: around 4.5% and 4.2% for DCF and IND, respectively. The drug release profile of DCF was different from that of IND, and it could be described by a first-order release model. In contrast, Fickian diffusion governs the release rate of IND from hmP:Xa aerogel coatings. This indicates the potential of the prepared aerogel coatings for tuning the release of other drugs for similar applications. Both NSAIDs were completely released after 24 h, as confirmed by the plateau reached in the release profiles, as well as through post-release IR spectroscopy. All samples were shown to be biocompatible with human bone-derived osteoblasts. The osteoblast viability of all samples was higher when compared to the control, indicating a possible major potential for further research on their use in orthopaedic applications, in addition to their general application in bone tissue engineering.

7 REFERENCES

[1] A.M. Stephen, G.O. Phillips, Food Polysaccharides and Their Applications, CRC Press, 2014.

[2] J.N. BeMiller, An Introduction to Pectins: Structure and Properties, in: Chem. Funct. Pectins, American Chemical Society, 1986: pp. 2–12. http://dx.doi.org/10.1021/bk-1986-0310.ch001 (accessed March 30, 2016).

[3] B.L. Ridley, M.A. O'Neill, D. Mohnen, Pectins: structure, biosynthesis, and oligogalacturonide-related signaling, Phytochemistry. 57 (2001) 929–967.

[4] G.A. Morris, J. Castile, A. Smith, G.G. Adams, S.E. Harding, The effect of different storage temperatures on the physical properties of pectin solutions and gels, Polym. Degrad. Stab. 95 (2010) 2670–2673.

[5] M.B. Sticklen, Plant genetic engineering for biofuel production: towards affordable cellulosic ethanol, Nat. Rev. Genet. 9 (2008) 433–443. doi:10.1038/nrg2336.

[6] P. Srivastava, R. Malviya, Sources of pectin, extraction and its applications in pharmaceutical industry - An overview, Indian J. Nat. Prod. Resour. (2011) 10–18.

[7] M.L. Fishman, J.J. Jen, A.C.S.D. of A. and F. Chemistry, Chemistry and Function of Pectins, American Chemical Society, 1986.

[8] K.Y. Lee, D.J. Mooney, Alginate: properties and biomedical applications, Prog. Polym. Sci. 37 (2012) 106–126. doi:10.1016/j.progpolymsci.2011.06.003.

[9] F. García-Ochoa, V.E. Santos, J.A. Casas, E. Gómez, Xanthan gum: production, recovery, and properties, Biotechnol. Adv. 18 (2000) 549–579. doi:10.1016/S0734-9750(00)00050-1.

[10] E.D. Bartzoka, C. Crestini, H. Lange, Biomass Derived and Biomass Inspired Polymers in Pharmaceutical Applications, in: V.K. Thakur, M.K. Thakur (Eds.), Handb. Polym. Pharm. Technol., John Wiley & Sons, Inc., Hoboken, NJ, USA, 2015: pp. 127–203. doi:10.1002/9781119041450.ch5.

[11] H. Kono, H. Hara, H. Hashimoto, Y. Shimizu, Nonionic gelation agents prepared from hydroxypropyl guar gum, Carbohydr. Polym. 117 (2015) 636–643. doi:10.1016/j.carbpol.2014.09.085.

[12] M. George, T.E. Abraham, pH sensitive alginate–guar gum hydrogel for the controlled delivery of protein drugs, Int. J. Pharm. 335 (2007) 123–129. doi:10.1016/j.ijpharm.2006.11.009.

[13] H. Kono, F. Otaka, M. Ozaki, Preparation and characterization of guar gum hydrogels as carrier materials for controlled protein drug delivery, Carbohydr. Polym. 111 (2014) 830–840. doi:10.1016/j.carbpol.2014.05.050.

[14] Y.S.R. Krishnaiah, R.S. Karthikeyan, V. Satyanarayana, A three-layer guar gum matrix tablet for oral controlled delivery of highly soluble metoprolol tartrate, Int. J. Pharm. 241 (2002) 353–366. doi:10.1016/S0378-5173(02)00273-9.

[15] I. Gliko-Kabir, B. Yagen, A. Penhasi, A. Rubinstein, Low Swelling, Crosslinked Guar and Its Potential Use as Colon-Specific Drug Carrier, Pharm. Res. 15 (1998) 1019–1025. doi:10.1023/A:1011921925745.

[16] I. Gliko-Kabir, B. Yagen, A. Penhasi, A. Rubinstein, Phosphated crosslinked guar for colon-specific drug delivery: I. Preparation and physicochemical characterization, J. Controlled Release. 63 (2000) 121–127. doi:10.1016/S0168-3659(99)00179-0.

[17] M.H. Abo-Shosha, N.A. Ibrahim, E. Allam, E. El-Zairy, Preparation and characterization of polyacrylic acid/karaya gum and polyacrylic acid/tamarind seed gum adducts and utilization in textile printing, Carbohydr. Polym. 74 (2008) 241–249. doi:10.1016/j.carbpol.2008.02.011.

[18] C.J. Brinker, G.W. Scherer, Sol-gel Science: The Physics and Chemistry of Sol-gel Processing, Gulf Professional Publishing, 1990.

[19] S. Sakka, Handbook of sol-gel science and technology. 1. Sol-gel processing, Springer, 2005.

[20] A.C. Pierre, Introduction to Sol-Gel Processing, Springer Science & Business Media, 1998.

[21] S. Sakka, Handbook of sol-gel science and technology. 2. Characterization and properties of sol-gel materials and products, Springer Science & Business Media, 2005.

[22] S. Sakka, Handbook of sol-gel science and technology. 3. Applications of sol-gel technology, Springer Science & Business Media, 2005.

[23] A. Martucci, Sol-Gel Nanocomposites, Springer, 2014.

[24] C.J. Brinker, A.J. Hurd, P.R. Schunk, G.C. Frye, C.S. Ashley, Review of sol-gel thin film formation, J. Non-Cryst. Solids. 147–148 (1992) 424–436. doi:10.1016/S0022-3093(05)80653-2.

[25] L.P. Singh, S.K. Bhattacharyya, R. Kumar, G. Mishra, U. Sharma, G. Singh, S. Ahalawat, Sol-Gel processing of silica nanoparticles and their applications, Adv. Colloid Interface Sci. 214 (2014) 17–37. doi:10.1016/j.cis.2014.10.007.

[26] J. Livage, Sol-gel processes, Curr. Opin. Solid State Mater. Sci. 2 (1997) 132–138. doi:10.1016/S1359-0286(97)80057-5.

[27] H. Reuter, Sol–gel processes, Adv. Mater. 3 (1991) 258–259. doi:10.1002/adma.19910030510.

[28] N. Hüsing, U. Schubert, Aerogels—Airy Materials: Chemistry, Structure, and Properties, Angew. Chem. Int. Ed. 37 (1998) 22–45. doi:10.1002/(SICI)1521-3773(19980202)37:1/2<22::AID-ANIE22>3.0.CO;2-I.

[29] J. Dennis, H.K. Henisch, Nucleation and Growth of Crystals in Gels, J. Electrochem. Soc. 114 (1967) 263. doi:10.1149/1.2426564.

[30] S. Banerjee, S. Bhattacharya, Food Gels: Gelling Process and New Applications, Crit. Rev. Food Sci. Nutr. 52 (2012) 334–346. doi:10.1080/10408398.2010.500234.

[31] B. Posocco, E. Dreussi, J. de Santa, G. Toffoli, M. Abrami, F. Musiani, M. Grassi, R. Farra, F. Tonon, G. Grassi, B. Dapas, Polysaccharides for the Delivery of Antitumor Drugs, Materials. 8 (2015) 2569–2615. doi:10.3390/ma8052569.

[32] A.G. Olsen, Pectin Studies. III. General Theory of Pectin Jelly Formation., J. Phys. Chem. 38 (1933) 919–930. doi:10.1021/j150358a007.

[33] R.H. Walter, The Chemistry and Technology of Pectin, Academic Press, 2012.

[34] P. Sriamornsak, Chemistry of pectin and its pharmaceutical uses: A review, Silpakorn Univ. Int. J. 3 (2003) 206–228.

[35] S. Dumitriu, Polysaccharides: Structural Diversity and Functional Versatility, Second Edition, CRC Press, 2012.

[36] T. Gotoh, K. Matsushima, K.-I. Kikuchi, Adsorption of Cu and Mn on covalently cross-linked alginate gel beads, Chemosphere. 55 (2004) 57–64. doi:10.1016/j.chemosphere.2003.10.034.

[37] S. Zhao, M. Cao, H. Li, L. Li, W. Xu, Synthesis and characterization of thermo-sensitive semi-IPN hydrogels based on poly(ethylene glycol)-co-poly(epsilon-caprolactone) macromer, N-isopropylacrylamide, and sodium alginate, Carbohydr. Res. 345 (2010) 425–431. doi:10.1016/j.carres.2009.11.014.

[38] K. y. Lee, H. j. Kong, R. g. Larson, D. j. Mooney, Hydrogel Formation via Cell Crosslinking, Adv. Mater. 15 (2003) 1828–1832. doi:10.1002/adma.200305406.

[39] T. Lund, O. Smidsrød, B. Torger Stokke, A. Elgsaeter, Controlled gelation of xanthan by trivalent chronic ions, Carbohydr. Polym. 8 (1988) 245–256. doi:10.1016/0144-8617(88)90064-1.

[40] M. Tako, T. Nagahama, D. Nomura, Non-Newtonian Flow and Dynamic Viscoelasticity of Xanthan Gum, Nippon Nōgeikagaku Kaishi. 51 (1977) 513–518. doi:10.1271/nogeikagaku1924.51.8_513.

[41] M.S. Shobha, R.N. Tharanathan, Rheological behaviour of pullulanase-treated guar galactomannan on co-gelation with xanthan, Food Hydrocoll. 23 (2009) 749–754. doi:10.1016/j.foodhyd.2008.04.006.

[42] M. Tako, T. Teruya, Y. Tamaki, K. Ohkawa, Co-gelation mechanism of xanthan and galactomannan, Colloid Polym. Sci. 288 (2010) 1161–1166. doi:10.1007/s00396-010-2242-6.

[43] A. Abbaszadeh, W. MacNaughtan, G. Sworn, T.J. Foster, New insights into xanthan synergistic interactions with konjac glucomannan: A novel interaction mechanism proposal, Carbohydr. Polym. 144 (2016) 168–177. doi:10.1016/j.carbpol.2016.02.026.

[44] P. Fitzpatrick, J. Meadows, I. Ratcliffe, P.A. Williams, Control of the properties of xanthan/glucomannan mixed gels by varying xanthan fine structure, Carbohydr. Polym. 92 (2013) 1018–1025. doi:10.1016/j.carbpol.2012.10.049.

[45] S.M. Fitzsimons, J.T. Tobin, E.R. Morris, Synergistic binding of konjac glucomannan to xanthan on mixing at room temperature, Food Hydrocoll. 22 (2008) 36–46. doi:10.1016/j.foodhyd.2007.01.023.

[46] S.K. Gulrez, S. Al-Assaf, G.O. Phillips, Hydrogels: Methods of preparation, characterisation and applications, Prog. Mol. Environ. Bioeng. Anal. Model. Technol. Appl. (2011) 117–150.

[47] D. Bellet, L. Canham, Controlled drying: The key to better quality porous semiconductors, Adv. Mater. 10 (1998) 487–490.

[48] M.J. van Bommel, A.B. de Haan, Drying of silica aerogel with supercritical carbon dioxide, J. Non-Cryst. Solids. 186 (1995) 78–82. doi:10.1016/0022-3093(95)00072-0.

[49] C.A. García-González, M.C. Camino-Rey, M. Alnaief, C. Zetzl, I. Smirnova, Supercritical drying of aerogels using CO2: Effect of extraction time on the end material textural properties, J. Supercrit. Fluids. 66 (2012) 297–306. doi:10.1016/j.supflu.2012.02.026.

[50] A. Michels, C. Michels, Isotherms of CO2 between 0 degrees and 150 degrees and Pressures from 16 to 250 Atm (Amagat Densities 18-206), Proc. R. Soc. Math. Phys. Eng. Sci. 153 (1935) 201–214. doi:10.1098/rspa.1935.0231.

[51] A. Michels, C. Michels, H. Wouters, Isotherms of CO2 between 70 and 3000 Atmospheres (Amagat Densities between 200 and 600), Proc. R. Soc. Math. Phys. Eng. Sci. 153 (1935) 214–224. doi:10.1098/rspa.1935.0232.

[52] J.L. Kendall, D.A. Canelas, J.L. Young, J.M. DeSimone, Polymerizations in Supercritical Carbon Dioxide, Chem. Rev. 99 (1999) 543–564. doi:10.1021/cr9700336.

[53] S.S. Kistler, Coherent Expanded Aerogels and Jellies., Nature. 127 (1931) 741–741. doi:10.1038/127741a0.

[54] M.A. Aegerter, N. Leventis, M.M. Koebel, Aerogels Handbook, Springer, 2011.

[55] A. Berg, M.W. Droege, J.D. Fellmann, J. Klaveness, P. Rongved, Medical use of organic aerogels and biodegradable organic aerogels, EP 0707474 A1, 1996. http://www.google.com/patents/EP0707474A1?cl=en.

[56] Y.K. Akimov, Fields of application of aerogels (Review), Instrum. Exp. Tech. 46 (2003) 287–299. doi:10.1023/A:1024401803057.

[57] R.J. Contolini, L.W. Hrubesh, A.F. Bernhardt, Aerogels for Microelectronic Applications: Fast, Inexpensive, and Light as Air, Lawrence Livermore National Lab., CA (United States), 1993. http://www.osti.gov/scitech/biblio/10175075 (accessed May 22, 2014).

[58] G.M. Pajonk, Aerogel catalysts, Appl. Catal. 72 (1991) 217–266. doi:10.1016/0166-9834(91)85054-Y.

[59] R. Baetens, B.P. Jelle, A. Gustavsen, Aerogel insulation for building applications: A state-of-the-art review, Energy Build. 43 (2011) 761–769. doi:10.1016/j.enbuild.2010.12.012.

[60] L. Ling, M. Qing-Han, Electrochemical properties of mesoporous carbon aerogel electrodes for electric double layer capacitors, J. Mater. Sci. 40 (2005) 4105–4107.

[61] S.J. Kim, S.W. Hwang, S.H. Hyun, Preparation of carbon aerogel electrodes for supercapacitor and their electrochemical characteristics, J. Mater. Sci. 40 (2005) 725–731. doi:10.1007/s10853-005-6313-x.

[62] Z. Ulker, C. Erkey, An emerging platform for drug delivery: Aerogel based systems, J. Controlled Release. 177 (2014) 51–63. doi:10.1016/j.jconrel.2013.12.033.

[63] J.S. Lim, Y.Y. Lee, H.S. Chun, Phase equilibria for carbon dioxide-ethanol-water system at elevated pressures, J. Supercrit. Fluids. 7 (1994) 219–230. doi:10.1016/0896-8446(94)90009-4.

[64] A.C. Pierre, G.M. Pajonk, Chemistry of aerogels and their applications, Chem. Rev. 102 (2002) 4243–4266. doi:10.1021/cr0101306.

[65] N. Job, A. Théry, R. Pirard, J. Marien, L. Kocon, J.-N. Rouzaud, F. Béguin, J.-P. Pirard, Carbon aerogels, cryogels and xerogels: Influence of the drying method on the textural properties of porous carbon materials, Carbon. 43 (2005) 2481–2494. doi:10.1016/j.carbon.2005.04.031.

[66] Z. Novak, Ž. Knez, Diffusion of methanol–liquid CO2 and methanol–supercritical CO2 in silica aerogels, J. Non-Cryst. Solids. 221 (1997) 163–169.

[67] A.F. Benton, T.A. White, The sorption of gases by iron, J. Am. Chem. Soc. 54 (1932) 1820–1830.

[68] S. Brunauer, P.H. Emmett, E. Teller, Adsorption of Gases in Multimolecular Layers, J. Am. Chem. Soc. 60 (1938) 309–319.

[69] J.C. Echeverria, M.T. Morera, C. Mazkiaran, J.J. Garrido, Characterization of the porous structure of soils: adsorption of nitrogen (77 K) and carbon dioxide (273 K), and mercury porosimetry, Eur. J. Soil Sci. 50 (1999) 497–503.

[70] K. Sing, The use of nitrogen adsorption for the characterisation of porous materials, Colloids Surf. Physicochem. Eng. Asp. 187–188 (2001) 3–9. doi:10.1016/S0927-7757(01)00612-4.

[71] K.S.W. Sing, D.H. Everett, R.A.W. Haul, L. Moscou, R.A. Pierotti, J. Rouquerol, T. Siemieniewska, Reporting physisorption data for gas/solid systems with special reference to the determination of surface area and porosity, Pure Appl Chem. 57 (1985) 603–619.

[72] P.A. Webb, C. Orr, Analytical methods in fine particle technology, Micromeritics Instrument Corporation, 1997.

[73] P. Echlin, Handbook of Sample Preparation for Scanning Electron Microscopy and X-Ray Microanalysis, Springer, 2011.

[74] J.I. Goldstein, D.E. Newbury, P. Echlin, D.C. Joy, C.E. Lyman, E. Lifshin, L. Sawyer, J.R. Michael, Scanning Electron Microscopy and X-ray Microanalysis, Springer US, Boston, MA, 2003. doi:10.1007/978-1-4615-0215-9.

[75] H. Menzel, DSC, Inst. Für Tech. Chem. (2010). http://www.itc.tu-bs.de/Abteilungen/Makro/Methods/dsc3.gif (accessed March 23, 2017).

[76] K. Czerwinski, TG, Instrum. Anal. (2005). http://radchem.nevada.edu/classes/chem455/lecture_22__thermal_methods.htm (accessed March 23, 2017).

[77] A. Berge, P. Johansson, Literature Review of High Performance Thermal Insulation, Chalmers University of Technology, Gothenburg, Sweden, 2012.

[78] A. Franco Júnior, D.J. Shanafield, Thermal conductivity of polycrystalline aluminum nitride (AlN) ceramics, Cerâmica. 50 (2004) 247–253. doi:10.1590/S0366-69132004000300012.

[79] C. Effting, S. Güths, O.E. Alarcon, Evaluation of the thermal comfort of ceramic floor tiles, Mater. Res. 10 (2007) 301–306. doi:10.1590/S1516-14392007000300016.

[80] E. Cohen, L. Glicksman, Thermal properties of silica aerogel formula, J. Heat Transf. 137 (2015). doi:10.1115/1.4028901.

[81] E. Cohen, L. Glicksman, Analysis of the transient hot-wire method to measure thermal conductivity of silica aerogel: Influence of wire length, and radiation properties, J. Heat Transf. 136 (2014). doi:10.1115/1.4025921.

[82] C. Rudaz, R. Courson, L. Bonnet, S. Calas-Etienne, H. Sallée, T. Budtova, Aeropectin: Fully Biomass-Based Mechanically Strong and Thermal Superinsulating Aerogel, Biomacromolecules. 15 (2014) 2188–2195. doi:10.1021/bm500345u.

[83] R. Sescousse, R. Gavillon, T. Budtova, Aerocellulose from cellulose–ionic liquid solutions: Preparation, properties and comparison with cellulose–NaOH and cellulose–NMMO routes, Carbohydr. Polym. 83 (2011) 1766–1774. doi:10.1016/j.carbpol.2010.10.043.

[84] P. Gurikov, S.P. Raman, D. Weinrich, M. Fricke, I. Smirnova, A novel approach to alginate aerogels: carbon dioxide induced gelation, RSC Adv. 5 (2015) 7812–7818. doi:10.1039/C4RA14653K.

[85] S.P. Raman, P. Gurikov, I. Smirnova, Organic and Biopolymer Aerogels for Thermal Superinsulation: Synthesis and Processing Routes, Chem. Ing. Tech. 86 (2014) 1503–1503. doi:10.1002/cite.201450460.

[86] A. Demilecamps, C. Beauger, C. Hildenbrand, A. Rigacci, T. Budtova, Cellulose–silica aerogels, Carbohydr. Polym. 122 (2015) 293–300. doi:10.1016/j.carbpol.2015.01.022.

[87] P.S. Gaal, M.-A. Thermitus, D.E. Stroe, Thermal conductivity measurements using the flash method, J. Therm. Anal. Calorim. 78 (2004) 185–189. doi:10.1023/B:JTAN.0000042166.64587.33.

[88] G. Hakvoort, L.L. van Reijen, A.J. Aartsen, Measurement of the thermal conductivity of solid substances by DSC, Thermochim. Acta. 93 (1985) 317–320. doi:10.1016/0040-6031(85)85081-4.

[89] S.M. Marcus, R.L. Blaine, Thermal conductivity of polymers, glasses and ceramics by modulated DSC, Thermochim. Acta. 243 (1994) 231–239. doi:10.1016/0040-6031(94)85058-5.

[90] D. Sánchez-Rodríguez, J.P. López-Olmedo, J. Farjas, P. Roura, Determination of thermal conductivity of powders in different atmospheres by differential scanning calorimetry, J. Therm. Anal. Calorim. 121 (2015) 469–473. doi:10.1007/s10973-015-4429-z.

[91] Simple determination of the thermal conductivity of polymers by DSC, UserCom. 2 (2005) 19–23.

[92] M.E.M. Braga, M.T.V. Pato, H.S.R.C. Silva, E.I. Ferreira, M.H. Gil, C.M.M. Duarte, H.C. de Sousa, Supercritical solvent impregnation of ophthalmic drugs on chitosan derivatives, J. Supercrit. Fluids. 44 (2008) 245–257. doi:10.1016/j.supflu.2007.10.002.

[93] T. Mehling, I. Smirnova, U. Guenther, R.H.H. Neubert, Polysaccharide-based aerogels as drug carriers, J. Non-Cryst. Solids. 355 (2009) 2472–2479.

[94] I. Smirnova, S. Suttiruengwong, W. Arlt, Aerogels: Tailor-made carriers for immediate and prolonged drug release, KONA Powder Part. J. 23 (2005) 86–97. doi:10.14356/kona.2005012.

[95] S. Üzer, U. Akman, Ö. Hortaçsu, Polymer swelling and impregnation using supercritical CO2: A model-component study towards producing controlled-release drugs, J. Supercrit. Fluids. 38 (2006) 119–128.

[96] S. Kazarian, Supercritical Fluid Impregnation of Polymers for Drug Delivery, in: Supercrit. Fluid Technol. Drug Prod. Dev., Informa Healthcare, 2004. http://www.crcnetbase.com/doi/abs/10.1201/9780203021378.ch8 (accessed May 22, 2014).

[97] A. López-Periago, A. Argemí, J.M. Andanson, V. Fernández, C.A. García-González, S.G. Kazarian, J. Saurina, C. Domingo, Impregnation of a biocompatible polymer aided by supercritical CO2: Evaluation of drug stability and drug–matrix interactions, J. Supercrit. Fluids. 48 (2009) 56–63. doi:10.1016/j.supflu.2008.09.015.

[98] P. Colombo, R. Bettini, P. Santi, N.A. Peppas, Swellable matrices for controlled drug delivery: gel-layer behaviour, mechanisms and optimal performance, Pharm. Sci. Technol. Today. 3 (2000) 198–204. doi:10.1016/S1461-5347(00)00269-8.

[99] P. Sriamornsak, N. Thirawong, Y. Weerapol, J. Nunthanid, S. Sungthongjeen, Swelling and erosion of pectin matrix tablets and their impact on drug release behavior, Eur. J. Pharm. Biopharm. 67 (2007) 211–219. doi:10.1016/j.ejpb.2006.12.014.

[100] G. Lamberti, I. Galdi, A.A. Barba, Controlled release from hydrogel-based solid matrices. A model accounting for water up-take, swelling and erosion, Int. J. Pharm. 407 (2011) 78–86. doi:10.1016/j.ijpharm.2011.01.023.

[101] K. Huanbutta, K. Terada, P. Sriamornsak, J. Nunthanid, Advanced technologies for assessment of polymer swelling and erosion behaviors in pharmaceutical aspect, Eur. J. Pharm. Biopharm. 83 (2013) 315–321. doi:10.1016/j.ejpb.2012.10.002.

[102] C. Kim, Advanced Pharmaceutics: Physicochemical Principles, CRC Press, 2004.

[103] D. Sinha Roy, B.D. Rohera, Comparative evaluation of rate of hydration and matrix erosion of HEC and HPC and study of drug release from their matrices, Eur. J. Pharm. Sci. 16 (2002) 193–199. doi:10.1016/S0928-0987(02)00103-3.

[104] R. Uddin, N. Saffoon, K. Sutradhar Bishwajit, Dissolution and Dissolution Apparatus: A Review, Int. J. Curr. Biomed. Pharm. Res. 1(4) (2011) 201–207.

[105] F. Acartürk, S. Takka, Calcium alginate microparticles for oral administration: II. Effect of formulation factors on drug release and drug entrapment efficiency, J. Microencapsul. 16 (1999) 291–301. doi:10.1080/026520499289022.

[106] G. Fundueanu, E. Esposito, D. Mihai, A. Carpov, J. Desbrieres, M. Rinaudo, C. Nastruzzi, Preparation and characterization of Ca-alginate microspheres by a new emulsification method, Int. J. Pharm. 170 (1998) 11–21. doi:10.1016/S0378-5173(98)00063-5.

[107] M.. González-Rodríguez, M.. Holgado, C. Sánchez-Lafuente, A.. Rabasco, A. Fini, Alginate/chitosan particulate systems for sodium diclofenac release, Int. J. Pharm. 232 (2002) 225–234. doi:10.1016/S0378-5173(01)00915-2.

[108] Y. Murata, M. Miyashita, K. Kofuji, E. Miyamoto, S. Kawashima, Drug release properties of a gel bead prepared with pectin and hydrolysate, J. Controlled Release. 95 (2004) 61–66. doi:10.1016/j.jconrel.2003.10.026.

[109] P. Sriamornsak, J. Nunthanid, Calcium pectinate gel beads for controlled release drug delivery:: I. Preparation and in vitro release studies, Int. J. Pharm. 160 (1998) 207–212. doi:10.1016/S0378-5173(97)00310-4.

[110] A. Veronovski, G. Tkalec, Ž. Knez, Z. Novak, Characterisation of biodegradable pectin aerogels and their potential use as drug carriers, Carbohydr. Polym. 113 (2014) 272–278. doi:10.1016/j.carbpol.2014.06.054.

[111] Y. Zhao, F. Hu, J.J. Evans, M.T. Harris, Study of sol–gel transition in calcium alginate system by population balance model, Chem. Eng. Sci. 66 (2011) 848–858. doi:10.1016/j.ces.2010.11.025.

[112] K. Potter, B.J. Balcom, T.A. Carpenter, L.D. Hall, The gelation of sodium alginate with calcium ions studied by magnetic resonance imaging (MRI), Carbohydr. Res. 257 (1994) 117–126. doi:10.1016/0008-6215(94)84112-8.

[113] P. Aslani, R.A. Kennedy, Studies on diffusion in alginate gels. I. Effect of cross-linking with calcium or zinc ions on diffusion of acetaminophen, J. Controlled Release. 42 (1996) 75–82. doi:10.1016/0168-3659(96)01369-7.

[114] I. El-Gibaly, Oral delayed-release system based on Zn-pectinate gel (ZPG) microparticles as an alternative carrier to calcium pectinate beads for colonic drug delivery, Int. J. Pharm. 232 (2002) 199–211. doi:10.1016/S0378-5173(01)00903-6.

[115] G. Dupuis, O. Chambin, C. Génelot, D. Champion, Y. Pourcelot, Colonic drug delivery: influence of cross-linking agent on pectin beads properties and role of the shell capsule type, Drug Dev. Ind. Pharm. 32 (2006) 847–855. doi:10.1080/03639040500536718.

[116] K.S. Khairou, W.M. Al-Gethami, R.M. Hassan, Kinetics and mechanism of sol–gel transformation between sodium alginate polyelectrolyte and some heavy divalent metal ions with formation of capillary structure polymembranes ionotropic gels, J. Membr. Sci. 209 (2002) 445–456. doi:10.1016/S0376-7388(02)00353-8.

[117] A. Assifaoui, A. Lerbret, H.T.D. Uyen, F. Neiers, O. Chambin, C. Loupiac, F. Cousin, Structural behaviour differences in low methoxy pectin solutions in the presence of divalent cations (Ca2+ and Zn2+): a process driven by the binding mechanism of the cation with the galacturonate unit, Soft Matter. 11 (2014) 551–560. doi:10.1039/C4SM01839G.

[118] G.A. Paredes Juárez, M. Spasojevic, M.M. Faas, P. de Vos, Immunological and technical considerations in application of alginate-based microencapsulation systems, Front. Bioeng. Biotechnol. 2 (2014) 26. doi:10.3389/fbioe.2014.00026.

[119] Ý.A. Mørch, I. Donati, B.L. Strand, Effect of Ca2+, Ba2+, and Sr2+ on Alginate Microbeads, Biomacromolecules. 7 (2006) 1471–1480. doi:10.1021/bm060010d.

[120] M.R.A. A. Akhgari, Evaluation of swelling, erosion and drug release from polysaccharide matrix tablets based on pectin and inulin, Jundishapur J. Nat. Pharm. Prod. 6 (2011) 51–58.

[121] C.-Y. Yu, B.-C. Yin, W. Zhang, S.-X. Cheng, X.-Z. Zhang, R.-X. Zhuo, Composite microparticle drug delivery systems based on chitosan, alginate and pectin with improved pH-sensitive drug release property, Colloids Surf. B Biointerfaces. 68 (2009) 245–249. doi:10.1016/j.colsurfb.2008.10.013.

[122] J. Siepmann, A. Göpferich, Mathematical modeling of bioerodible, polymeric drug delivery systems, Adv. Drug Deliv. Rev. 48 (2001) 229–247. doi:10.1016/S0169-409X(01)00116-8.

[123] J. Siepmann, F. Siepmann, Mathematical modeling of drug delivery, Int. J. Pharm. 364 (2008) 328–343. doi:10.1016/j.ijpharm.2008.09.004.

[124] R.S. Harland, R.K. Prud'homme, eds., Polyelectrolyte gels: properties, preparation, and applications, American Chemical Society, Washington, DC, 1992.

[125] A. Veronovski, G. Tkalec, Ž. Knez, Z. Novak, Characterisation of biodegradable pectin aerogels and their potential use as drug carriers, Carbohydr. Polym. 113 (2014) 272–278. doi:10.1016/j.carbpol.2014.06.054.

[126] H.-B. Chen, B.-S. Chiou, Y.-Z. Wang, D.A. Schiraldi, Biodegradable pectin/clay aerogels, ACS Appl. Mater. Interfaces. 5 (2013) 1715–1721. doi:10.1021/am3028603.

[127] C.A. García-González, E. Carenza, M. Zeng, I. Smirnova, A. Roig, Design of biocompatible magnetic pectin aerogel monoliths and microspheres, RSC Adv. 2 (2012) 9816–9823.

[128] R.J. White, V.L. Budarin, J.H. Clark, Pectin-Derived Porous Materials, Chem. - Eur. J. 16 (2010) 1326–1335.

[129] P.D. Gaudio, G. Auriemma, T. Mencherini, G.D. Porta, E. Reverchon, R.P. Aquino, Design of alginate-based aerogel for nonsteroidal anti-inflammatory drugs controlled delivery systems using prilling and supercritical-assisted drying, J. Pharm. Sci. 102 (2013) 185–194. doi:10.1002/jps.23361.

[130] A. Veronovski, Ž. Knez, Z. Novak, Preparation of multi-membrane alginate aerogels used for drug delivery, J. Supercrit. Fluids. 79 (2013) 209–215. doi:10.1016/j.supflu.2013.01.025.

[131] A. Veronovski, Ž. Knez, Z. Novak, Comparison of ionic and non-ionic drug release from multi-membrane spherical aerogels, Int. J. Pharm. 454 (2013) 58–66. doi:10.1016/j.ijpharm.2013.06.074.

[132] H.H. Tønnesen, J. Karlsen, Alginate in drug delivery systems, Drug Dev. Ind. Pharm. 28 (2002) 621–630.

[133] L. Wang, D.A. Schiraldi, M. Sánchez-Soto, Foamlike Xanthan Gum/Clay Aerogel Composites and Tailoring Properties by Blending with Agar, Ind. Eng. Chem. Res. 53 (2014) 7680–7687. doi:10.1021/ie500490n.

[134] D. Bilanovic, J. Starosvetsky, R.H. Armon, Cross-linking xanthan and other compounds with glycerol, Food Hydrocoll. 44 (2015) 129–135. doi:10.1016/j.foodhyd.2014.09.024.

[135] K.S. Mikkonen, K. Parikka, J.-P. Suuronen, A. Ghafar, R. Serimaa, M. Tenkanen, Enzymatic oxidation as a potential new route to produce polysaccharide aerogels, RSC Adv. 4 (2014) 11884–11892. doi:10.1039/C3RA47440B.

[136] T. Mehling, I. Smirnova, U. Guenther, R.H.H. Neubert, Polysaccharide-based aerogels as drug carriers, J. Non-Cryst. Solids. 355 (2009) 2472–2479. doi:10.1016/j.jnoncrysol.2009.08.038.

[137] R. Valentin, R. Horga, B. Bonelli, E. Garrone, F. Di Renzo, F. Quignard, Acidity of Alginate Aerogels Studied by FTIR Spectroscopy of Probe Molecules, Macromol. Symp. 230 (2005) 71–77. doi:10.1002/masy.200551144.

[138] R. Valentin, R. Horga, B. Bonelli, E. Garrone, F. Di Renzo, F. Quignard, FTIR Spectroscopy of NH3 on Acidic and Ionotropic Alginate Aerogels, Biomacromolecules. 7 (2006) 877–882. doi:10.1021/bm050559x.

[139] F. Liebner, E. Haimer, M. Wendland, M.-A. Neouze, K. Schlufter, P. Miethe, T. Heinze, A. Potthast, T. Rosenau, Aerogels from Unaltered Bacterial Cellulose: Application of scCO2 Drying for the Preparation of Shaped, Ultra-Lightweight Cellulosic Aerogels, Macromol. Biosci. 10 (2010) 349–352. doi:10.1002/mabi.200900371.

[140] R. Gavillon, T. Budtova, Aerocellulose: New Highly Porous Cellulose Prepared from Cellulose−NaOH Aqueous Solutions, Biomacromolecules. 9 (2008) 269–277. doi:10.1021/bm700972k.

[141] Y. Kobayashi, T. Saito, A. Isogai, Aerogels with 3D Ordered Nanofiber Skeletons of Liquid-Crystalline Nanocellulose Derivatives as Tough and Transparent Insulators, Angew. Chem. Int. Ed. 53 (2014) 10394–10397. doi:10.1002/anie.201405123.

[142] M. Robitzer, A. Tourrette, R. Horga, R. Valentin, M. Boissière, J.M. Devoisselle, F. Di Renzo, F. Quignard, Nitrogen sorption as a tool for the characterisation of polysaccharide aerogels, Carbohydr. Polym. 85 (2011) 44–53. doi:10.1016/j.carbpol.2011.01.040.

[143] D. Oakenfull, A. Scott, Hydrophobic Interaction in the Gelation of High Methoxyl Pectins, J. Food Sci. 49 (1984) 1093–1098. doi:10.1111/j.1365-2621.1984.tb10401.x.

[144] J.P. Soares, J.E. Santos, G.O. Chierice, E.T.G. Cavalheiro, Thermal behavior of alginic acid and its sodium salt, Eclética Quím. 29 (2004) 57–64. doi:10.1590/S0100-46702004000200009.

[145] A. Imeson, Food Stabilisers, Thickeners and Gelling Agents, John Wiley & Sons, 2011.

[146] C.A. García-González, M. Alnaief, I. Smirnova, Polysaccharide-based aerogels—Promising biodegradable carriers for drug delivery systems, Carbohydr. Polym. 86 (2011) 1425–1438.

[147] G. Tkalec, Ž. Knez, Z. Novak, Fast production of high-methoxyl pectin aerogels for enhancing the bioavailability of low-soluble drugs, J. Supercrit. Fluids. 106 (2015) 16–22. doi:10.1016/j.supflu.2015.06.009.

[148] K. Grodowska, A. Parczewski, Organic solvents in the pharmaceutical industry, Acta Pol. Pharm. 67 (2010) 3–12.

[149] R.H. Marchessault, F. Ravenelle, X.X. Zhu, eds., Polysaccharides for Drug Delivery and Pharmaceutical Applications, American Chemical Society, Washington, DC, 2006. doi:10.1021/bk-2006-0934.

[150] L. Liu, M.L. Fishman, K.B. Hicks, Pectin in controlled drug delivery – a review, Cellulose. 14 (2007) 15–24.

[151] H. Kim, Natural products to improve quality of life targeting for colon drug delivery, Curr. Drug Deliv. 9 (2012) 132–147.

[152] L. Pachuau, B. Mazumder, Colonic drug delivery systems based on natural polysaccharides and their evaluation, Mini Rev. Med. Chem. 13 (2013) 1982–1991.

[153] K. Yu, D. Wong, J. Parasrampuria, D. Friend, H.G. Brittain, Guar Gum, in: Anal. Profiles Drug Subst. Excip. Vol. 24, Academic Press, San Diego; New York; Boston, 1996.

[154] M. Szekalska, Puci&#x142, A. Owska, Szyma&#x144, E. Ska, P. Ciosek, K. Winnicka, Alginate: Current Use and Future Perspectives in Pharmaceutical and Biomedical Applications, Int. J. Polym. Sci. 2016 (2016) e7697031. doi:10.1155/2016/7697031.

[155] H. Fabek, S. Messerschmidt, V. Brulport, H.D. Goff, The effect of in vitro digestive processes on the viscosity of dietary fibres and their influence on glucose diffusion, Food Hydrocoll. 35 (2014) 718–726. doi:10.1016/j.foodhyd.2013.08.007.

[156] M. Fuwa, Y. Nakanishi, H. Moritaka, Effect of Xanthan Gum on Blood Sugar Level after Cooked Rice Consumption, Food Sci. Technol. Res. 22 (2016) 117–126. doi:10.3136/fstr.22.117.

[157] J. Siepmann, R.A. Siegel, M.J. Rathbone, eds., Fundamentals and Applications of Controlled Release Drug Delivery, Springer US, Boston, MA, 2012. http://link.springer.com/10.1007/978-1-4614-0881-9 (accessed April 23, 2014).

[158] L.V.J. Allen, N.G. Popovich, H.C. Ansel, Ansel's pharmaceutical dosage forms and drug delivery systems, Ninth edition, LWW, Philadelphia, 2010.

[159] R. Dubey, Microencapsulation Technology and Applications, Def. Sci. J. 59 (2009) 82–95. doi:10.14429/dsj.59.1489.

[160] Z.-Z. Piao, J.-S. Choe, K.T. Oh, Y.-S. Rhee, B.-J. Lee, Formulation and in vivo human bioavailability of dissolving tablets containing a self-nanoemulsifying itraconazole solid dispersion without precipitation in simulated gastrointestinal fluid, Eur. J. Pharm. Sci. Off. J. Eur. Fed. Pharm. Sci. 51 (2014) 67–74. doi:10.1016/j.ejps.2013.08.037.

[161] H. Park, K. Park, W.S.W. Shalaby, Biodegradable Hydrogels for Drug Delivery, CRC Press, 2011.

[162] M.. Fernández-Hervás, M.. Holgado, A. Fini, J.. Fell, In vitro evaluation of alginate beads of a diclofenac salt, Int. J. Pharm. 163 (1998) 23–34. doi:10.1016/S0378-5173(97)00333-5.

[163] P.A. Todd, E.M. Sorkin, Diclofenac Sodium, Drugs. 35 (1988) 244–285. doi:10.2165/00003495-198835030-00004.

[164] R.N. Brogden, R.C. Heel, G.E. Pakes, T.M. Speight, G.S. Avery, Diclofenac sodium: a review of its pharmacological properties and therapeutic use in rheumatic diseases and pain of varying origin, Drugs. 20 (1980) 24–48.

[165] D.W. Scholer, E.C. Ku, I. Boettcher, A. Schweizer, Pharmacology of diclofenac sodium, Am. J. Med. 80 (1986) 34–38.

[166] A.A. AL-Kahtani, B.S. Sherigara, Semi-interpenetrating network of acrylamide-grafted-sodium alginate microspheres for controlled release of diclofenac sodium, preparation and characterization, Colloids Surf. B Biointerfaces. 115 (2014) 132–138. doi:10.1016/j.colsurfb.2013.11.040.

[167] P. Costa, J.M. Sousa Lobo, Modeling and comparison of dissolution profiles, Eur. J. Pharm. Sci. 13 (2001) 123–133. doi:10.1016/S0928-0987(01)00095-1.

[168] P. Patil, D. Chavanke, M. Wagh, A review on ionotropic gelation method: novel approach for controlled gastroretentive gelispheres, Int J Pharm Pharm Sci. 4 (2012) 27–32.

[169] H.K. Makadia, S.J. Siegel, Poly Lactic-co-Glycolic Acid (PLGA) as Biodegradable Controlled Drug Delivery Carrier, Polymers. 3 (2011) 1377–1397. doi:10.3390/polym3031377.

[170] S.K. Prajapati, C.P. Jain, Variables influencing the drug entrapment efficiency of microspheres: A pharmaceutical review, Int. Res. J. Pharm. Appl. Sci. 3 (2013) 24–28.

[171] E. Galia, E. Nicolaides, D. Hörter, R. Löbenberg, C. Reppas, J.B. Dressman, Evaluation of various dissolution media for predicting in vivo performance of class I and II drugs, Pharm. Res. 15 (1998) 698–705.

[172] M. Siewert, J. Dressman, C.K. Brown, V.P. Shah, J.-M. Aiache, N. Aoyagi, D. Bashaw, C. Brown, W. Brown, D. Burgess, others, FIP/AAPS guidelines to dissolution/in vitro release testing of novel/special dosage forms, AAPS PharmSciTech. 4 (2003) 43–52.

[173] V. Pillay, M.P. Danckwerts, Z. Muhidinov, R. Fassihi, Novel Modulation of Drug Delivery Using Binary Zinc-Alginate-Pectinate Polyspheres for Zero-Order Kinetics Over Several Days: Experimental Design Strategy to Elucidate the Crosslinking Mechanism, Drug Dev. Ind. Pharm. 31 (2005) 191–207. doi:10.1081/DDC-200047806.

[174] C. Romanini, A.L. Tranquilli, Calcium Antagonists in the Treatment of Hypertension in Pregnancy, CRC Press, 1999.

[175] Ž. Knez, M. Škrget, P. Senčar-Božič, A. Rižner, Solubility of Nifedipine and Nitrendipine in Supercritical CO2, 40 (1995) 216–220.

[176] G. Tkalec, M. Pantić, Z. Novak, Ž. Knez, Supercritical impregnation of drugs and supercritical fluid deposition of metals into aerogels, J. Mater. Sci. 50 (2015) 1–12. doi:10.1007/s10853-014-8626-0.

[177] J. Della Rocca, D. Liu, W. Lin, Are high drug loading nanoparticles the next step forward for chemotherapy?, Nanomed. 7 (2012) 303–305. doi:10.2217/nnm.11.191.

[178] G. Tkalec, Ž. Knez, Z. Novak, Formation of polysaccharide aerogels in ethanol, RSC Adv. 5 (2015) 77362–77371. doi:10.1039/C5RA14140K.

[179] X.-W. Liu, Y. Zi, L.-B. Xiang, Y. Wang, Total hip arthroplasty: A review of advances, advantages and limitations, Int. J. Clin. Exp. Med. 8 (2015) 27–36.

[180] P.A. Revell, Joint Replacement Technology, Elsevier, 2014.

[181] R.K. Silverwood, P.G. Fairhurst, T. Sjöström, F. Welsh, Y. Sun, G. Li, B. Yu, P.S. Young, B. Su, R.M.D. Meek, M.J. Dalby, P.M. Tsimbouri, Analysis of Osteoclastogenesis/Osteoblastogenesis on Nanotopographical Titania Surfaces, Adv. Healthc. Mater. 5 (2016) 947–955. doi:10.1002/adhm.201500664.

[182] S.B. Goodman, Z. Yao, M. Keeney, F. Yang, The future of biologic coatings for orthopaedic implants, Biomaterials. 34 (2013) 3174–3183. doi:10.1016/j.biomaterials.2013.01.074.

[183] A.M. Peterson, H. Möhwald, D.G. Shchukin, pH-Controlled Release of Proteins from Polyelectrolyte-Modified Anodized Titanium Surfaces for Implant Applications, Biomacromolecules. 13 (2012) 3120–3126. doi:10.1021/bm300928s.

[184] A. Elyada, N. Garti, H. Füredi-Milhofer, Polyelectrolyte Multilayer-Calcium Phosphate Composite Coatings for Metal Implants, Biomacromolecules. 15 (2014) 3511–3521. doi:10.1021/bm5006245.

[185] M. Finšgar, A.P. Uzunalić, J. Stergar, L. Gradišnik, U. Maver, Novel chitosan/diclofenac coatings on medical grade stainless steel for hip replacement applications, Sci. Rep. 6 (2016) 26653. doi:10.1038/srep26653.

[186] A. Travan, E. Marsich, I. Donati, M.-P. Foulc, N. Moritz, H.T. Aro, S. Paoletti, Polysaccharide-coated thermosets for orthopedic applications: from material characterization to in vivo tests, Biomacromolecules. 13 (2012) 1564–1572. doi:10.1021/bm3002683.

[187] K. Gurzawska, R. Svava, N.R. Jørgensen, K. Gotfredsen, Nanocoating of titanium implant surfaces with organic molecules. Polysaccharides including glycosaminoglycans, J. Biomed. Nanotechnol. 8 (2012) 1012–1024.

[188] H.E. Kokkonen, J.M. Ilvesaro, M. Morra, H.A. Schols, J. Tuukkanen, Effect of Modified Pectin Molecules on the Growth of Bone Cells, Biomacromolecules. 8 (2007) 509–515. doi:10.1021/bm060614h.

[189] M. Taha, F. Chai, N. Blanchemain, C. Neut, M. Goube, M. Maton, B. Martel, H.F. Hildebrand, Evaluation of sorption capacity of antibiotics and antibacterial properties of a cyclodextrin-polymer functionalized hydroxyapatite-coated titanium hip prosthesis, Int. J. Pharm. 477 (2014) 380–389. doi:10.1016/j.ijpharm.2014.10.026.

[190] D. Neut, R.J.B. Dijkstra, J.I. Thompson, C. Kavanagh, der M. van, H.J. Busscher, A biodegradable gentamicin-hydroxyapatite-coating for infection prophylaxis in cementless hip prostheses, Eur. Cell. Mater. 29 (2015) 42–56.

[191] R. Fijn, R.T. Koorevaar, J.R.B.J. Brouwers, Prevention of heterotopic ossification after total hip replacement with NSAIDs, Pharm. World Sci. 25 (2003) 138–145. doi:10.1023/A:1024830213832.

[192] A. Bedi, R.M. Zbeda, V.F. Bueno, B. Downie, M. Dolan, B.T. Kelly, The Incidence of Heterotopic Ossification After Hip Arthroscopy, Am. J. Sports Med. 40 (2012) 854–863. doi:10.1177/0363546511434285.

[193] Sigma Aldrich, Diclofenac sodium salt, Properties, (2016). http://www.sigmaaldrich.com/catalog/product/sigma/d6899?lang=en&region=SI.

[194] FDA, The Biopharmaceutics Classification System (BCS) Guidance, (2016). http://www.fda.gov/AboutFDA/CentersOffices/OfficeofMedicalProductsandTobacco/CDER/ucm128219.htm.

[195] Sigma-Aldrich, Indomethacin ≥99.0% (TLC), (2016). http://www.sigmaaldrich.com/catalog/product/sial/57413?lang=en&region=SI.

[196] A. Veronovski, G. Tkalec, Ž. Knez, Z. Novak, Characterisation of biodegradable pectin aerogels and their potential use as drug carriers, Carbohydr. Polym. 113 (2014) 272–278. doi:10.1016/j.carbpol.2014.06.054.

[197] D.L. Massart, B.G. Vandeginste, L.M.C. Buydens, P.J. Lewi, J. Smeyers-Verbeke, S.D. Jong, Handbook of Chemometrics and Qualimetrics: Part A, Elsevier Science Inc., New York, NY, USA, 1997.

[198] M. Stigter, J. Bezemer, K. de Groot, P. Layrolle, Incorporation of different antibiotics into carbonated hydroxyapatite coatings on titanium implants, release and antibiotic efficacy, J. Controlled Release. 99 (2004) 127–137. doi:10.1016/j.jconrel.2004.06.011.

[199] T. Mosmann, Rapid colorimetric assay for cellular growth and survival: application to proliferation and cytotoxicity assays, J. Immunol. Methods. 65 (1983) 55–63.

[200] A.A. van de Loosdrecht, R.H. Beelen, G.J. Ossenkoppele, M.G. Broekhoven, M.M. Langenhuijsen, A tetrazolium-based colorimetric MTT assay to quantitate human monocyte mediated cytotoxicity against leukemic cells from cell lines and patients with acute myeloid leukemia, J. Immunol. Methods. 174 (1994) 311–320.

[201] M. Ferrari, M.C. Fornasiero, A.M. Isetta, MTT colorimetric assay for testing macrophage cytotoxic activity in vitro, J. Immunol. Methods. 131 (1990) 165–172.

[202] R. Sonntag, J. Reinders, J.P. Kretzer, What's next? Alternative materials for articulation in total joint replacement, Acta Biomater. 8 (2012) 2434–2441. doi:10.1016/j.actbio.2012.03.029.

[203] M. Finšgar, I. Milošev, Corrosion behaviour of stainless steels in aqueous solutions of methanesulfonic acid, Corros. Sci. 52 (2010) 2430–2438. doi:10.1016/j.corsci.2010.04.001.

[204] T. Maver, S. Hribernik, T. Mohan, D.M. Smrke, U. Maver, K. Stana-Kleinschek, Functional wound dressing materials with highly tunable drug release properties, RSC Adv. 5 (2015) 77873–77884. doi:10.1039/c5ra11972c.

[205] T. Maver, U. Maver, F. Mostegel, T. Griesser, S. Spirk, D.M. Smrke, K. Stana-Kleinschek, Cellulose based thin films as a platform for drug release studies to mimick wound dressing materials, Cellulose. 22 (2015) 749–761. doi:10.1007/s10570-014-0515-9.

[206] K. Löbmann, R. Laitinen, H. Grohganz, C. Strachan, T. Rades, K.C. Gordon, A theoretical and spectroscopic study of co-amorphous naproxen and indomethacin, Int. J. Pharm. 453 (2013) 80–87. doi:10.1016/j.ijpharm.2012.05.016.

[207] L.S. Taylor, G. Zografi, Spectroscopic Characterization of Interactions Between PVP and Indomethacin in Amorphous Molecular Dispersions, Pharm. Res. 14 (1997) 1691–1698. doi:10.1023/A:1012167410376.

[208] K. Yamaki, H. Uchida, Y. Harada, R. Yanagisawa, H. Takano, H. Hayashi, Y. Mori, S. Yoshino, Effect of the nonsteroidal anti-inflammatory drug indomethacin on Th1 and Th2 immune responses in mice, J. Pharm. Sci. 92 (2003) 1723–1729. doi:10.1002/jps.10380.

[209] D. Preisig, D. Haid, F.J.O. Varum, R. Bravo, R. Alles, J. Huwyler, M. Puchkov, Drug loading into porous calcium carbonate microparticles by solvent evaporation, Eur. J. Pharm. Biopharm. 87 (2014) 548–558. doi:10.1016/j.ejpb.2014.02.009.

[210] J. Zeng, L. Yang, Q. Liang, X. Zhang, H. Guan, X. Xu, X. Chen, X. Jing, Influence of the drug compatibility with polymer solution on the release kinetics of electrospun fiber formulation, J. Controlled Release. 105 (2005) 43–51. doi:10.1016/j.jconrel.2005.02.024.

[211] S.M. Fröhlich, V. Dorrer, V.-M. Archodoulaki, G. Allmaier, M. Marchetti-Deschmann, Synovial fluid protein adsorption on polymer-based artificial hip joint material investigated by MALDI-TOF mass spectrometry imaging, EuPA Open Proteomics. 4 (2014) 70–80. doi:10.1016/j.euprot.2014.05.001.

[212] M. Roba, M. Naka, E. Gautier, N.D. Spencer, R. Crockett, The adsorption and lubrication behavior of synovial fluid proteins and glycoproteins on the bearing-surface materials of hip replacements, Biomaterials. 30 (2009) 2072–2078. doi:10.1016/j.biomaterials.2008.12.062.

8 SCIENTIFIC BIBLIOGRAPHY OF THE CANDIDATE

ČLANKI IN DRUGI SESTAVNI DELI

1.01 Izvirni znanstveni članek

1. HORVAT, Gabrijela, PANTIČ, Milica, KNEZ, Željko, NOVAK, Zoran. Encapsulation and drug release of poorly water soluble nifedipine from bio-carriers. Journal of Non-Crystalline Solids, 2018, 481, 486-493

2. HORVAT, Gabrijela, XHANARI, Klodian, FINŠGAR, Matjaž, GRADIŠNIK, Lidija, MAVER, Uroš, KNEZ, Željko, NOVAK, Zoran. Novel ethanol-induced pectin-xanthan aerogel coatings for orthopedic applications. Carbohydrate polymers, ISSN 0144-8617. [Print ed.], 15 June 2017, vol. 166, str. 365-376, ilustr., doi: 10.1016/j.carbpol.2017.03.008. [COBISS.SI-ID 20354838], [JCR, SNIP, WoS do 19. 5. 2017: št. citatov (TC): 0, čistih citatov (CI): 0, Scopus do 25. 3. 2017: št. citatov (TC): 0, čistih citatov (CI): 0]

3. HORVAT, Gabrijela, KRANVOGL, Roman, PERVA-UZUNALIĆ, Amra, KNEZ, Željko, NOVAK, Zoran. Optimisation of critical parameters during alginate aerogels' production. Journal of non-crystalline solids, ISSN 0022-3093. [Print ed.], 1 July 2016, vol. 443, str. 112-117, doi: 10.1016/j.jnoncrysol.2016.04.014. [COBISS.SI-ID 19535382], [JCR, SNIP, WoS do 26. 3. 2017: št. citatov (TC): 1, čistih citatov (CI): 0, Scopus do 31. 8. 2017: št. citatov (TC): 1, čistih citatov (CI): 0]

4. HORVAT, Gabrijela, FAJFAR, Tanja, PERVA-UZUNALIĆ, Amra, KNEZ, Željko, NOVAK, Zoran. Thermal properties of polysaccharide aerogels. Journal of thermal analysis and calorimetry, ISSN 1388-6150. [Print ed.], Published online: 17 September 2016, str. 1-8, doi: 10.1007/s10973-016-5814-y. [COBISS.SI-ID 19878422], [JCR, SNIP, WoS do 24. 12. 2017: št. citatov (TC): 2, čistih citatov (CI): 2, Scopus do 29. 11. 2017: št. citatov (TC): 1, čistih citatov (CI): 1]

5. HORVAT, Gabrijela, KNEZ, Željko, NOVAK, Zoran. PH sensitive mesoporous materials for immediate or controlled release of NSAID. Microporous and mesoporous materials : zeolites, clays, carbons and related materials, ISSN 1387-1811, April 2016, vol. 224, str. 190-200, doi: 10.1016/j.micromeso.2015.11.048. [COBISS.SI-ID 19247638], [JCR, SNIP, WoS do 1. 11. 2016: št. citatov (TC): 1, čistih citatov (CI): 0, Scopus do 1. 10. 2016: št. citatov (TC): 1, čistih citatov (CI): 0]

6. HORVAT, Gabrijela, KNEZ, Željko, NOVAK, Zoran. Encapsulation of pharmaceuticals into pectin aerogels for controlled drug release. Advanced technologies, ISSN 2406-3037. [Online ed.], 2015, vol. 4, iss. 2, str. 49-52. http://www.tf.ni.ac.rs/casopis/sveska4vol2/C8.pdf. [COBISS.SI-ID 19245590]

7. HORVAT, Gabrijela, KNEZ, Željko, NOVAK, Zoran. Fast production of high-methoxyl pectin aerogels for enhancing the bioavailability of low-soluble drugs. The Journal of supercritical fluids, ISSN 0896-8446. [Print ed.], Nov./Dec. 2015, vol. 106, str. 16-22, doi: 10.1016/j.supflu.2015.06.009. [COBISS.SI-ID 18831126], [JCR, SNIP, WoS do 26. 11. 2017: št. citatov (TC): 3, čistih citatov (CI): 1, Scopus do 28. 12. 2017: št. citatov (TC): 3, čistih citatov (CI): 1]

8. HORVAT, Gabrijela, KNEZ, Željko, NOVAK, Zoran. Formation of polysaccharide aerogels in ethanol. RSC advances, ISSN 2046-2069, 2015, vol. 5, iss. 94, str. 77362-77371, doi: 10.1039/C5RA14140K. [COBISS.SI-ID 18923286], [JCR, SNIP, WoS do 28. 5. 2017: št. citatov (TC): 5, čistih citatov (CI): 3, Scopus do 28. 12. 2017: št. citatov (TC): 6, čistih citatov (CI): 4]

9. VERONOVSKI, Anja, HORVAT, Gabrijela, KNEZ, Željko, NOVAK, Zoran. Characterisation of biodegradable pectin aerogels and their potential use as drug carriers. Carbohydrate polymers, ISSN 0144-8617. [Print ed.], 26 Nov. 2014, vol. 113, str. 272-278, doi: 10.1016/j.carbpol.2014.06.054. [COBISS.SI-ID 18000150], [JCR, SNIP, WoS do 24. 9. 2017: št. citatov (TC): 18, čistih citatov (CI): 12, Scopus do 27. 12. 2017: št. citatov (TC): 21, čistih citatov (CI): 16]

1.02 Pregledni znanstveni članek

10. HORVAT, Gabrijela, PANTIĆ, Milica, NOVAK, Zoran, KNEZ, Željko. Supercritical impregnation of drugs and supercritical fluid deposition of metals into aerogels. *Journal of Materials Science*, ISSN 0022-2461, Jan. 2015, vol. 50, iss. 1, str. 1-12, doi: 10.1007/s10853-014-8626-0. [COBISS.SI-ID 18137110], [JCR, SNIP, WoS do 24. 9. 2017: št. citatov (TC): 13, čistih citatov (CI): 11, Scopus do 28. 11. 2017: št. citatov (TC): 14, čistih citatov (CI): 12]

1.08 Objavljeni znanstveni prispevek na konferenci

11. HORVAT, Gabrijela, KRANVOGL, Roman, PERVA-UZUNALIĆ, Amra, FAJFAR, Tanja, BRUMEC, Daša, KNEZ, Željko, NOVAK, Zoran. Optimizacija procesnih parametrov pri pripravi alginatnih aerogelov z novo metodo geliranja = Optimization of processing parameters for the preparation of alginate aerogels by novel gellation method. V: KAUČIČ, Venčeslav (ur.), BEŠTER-ROGAČ, Marija (ur.), GANTAR, Marjana (ur.). *Zbornik referatov in povzetkov*, 22. Slovenski kemijski dnevi, Portorož, 28.-30. september 2016 = 22. Slovenian Chemical Days Portorož, September 28-30, 2016. Ljubljana: Slovensko kemijsko društvo. 2016, str. 1-5, ilustr. [COBISS.SI-ID 19907350]

12. NOVAK, Zoran, HORVAT, Gabrijela, KNEZ, Željko. Polisaharidni aerogeli in njihove farmacevtske aplikacije = Polysaccharide aerogels and their pharmaceutical application. V: KAUČIČ, Venčeslav (ur.), BEŠTER-ROGAČ, Marija (ur.), GANTAR, Marjana (ur.). *Zbornik referatov in povzetkov*, 22. Slovenski kemijski dnevi, Portorož, 28.-30. september 2016 = 22. Slovenian Chemical Days Portorož, September 28-30, 2016. Ljubljana: Slovensko kemijsko društvo. 2016, str. 1-5, ilustr. [COBISS.SI-ID 19915286]

13. HORVAT, Gabrijela, KNEZ, Željko, NOVAK, Zoran. Z geliranjem polisaharidov v etanolu do naprednih materialov - aerogelov = Gelation of polysaccharides in ethanol for production of advanced materials - aerogels. V: KAUČIČ, Venčeslav (ur.), et al. *Zbornik referatov in povzetkov*, Slovenski kemijski dnevi 2015, Ljubljana, 24. - 25. september 2015 = Slovenian Chemical Days 2015, Ljubljana, September 24 - 25, 2015. Ljubljana: Slovensko kemijsko društvo. 2015, str. [1-5]. [COBISS.SI-ID 18974998]

14. HORVAT, Gabrijela, KNEZ, Željko, NOVAK, Zoran. Biodegradable pectin aerogels for potential drug delivery systems. V: *Proceedings*, Seminar on aerogels, 6th - 7th October 2014, Hamburg, Germany. [Hamburg]: ISASF. 2014, str. 73-81, ilustr. [COBISS.SI-ID 18156054]

15. HORVAT, Gabrijela, KNEZ, Željko, NOVAK, Zoran. Pektinski aerogeli za potencialne farmacevtske aplikacije. V: KRAVANJA, Zdravko (ur.), BOGATAJ, Miloš (ur.), NOVAK-PINTARIČ, Zorka (ur.). *Slovenski kemijski dnevi 2014, Maribor, 11. - 12. september 2014*, Slovenski kemijski dnevi 2014, Maribor, 11.-12. september 2014. Maribor: Fakulteta za kemijo in kemijsko tehnologijo. 2014, str. 1-6, ilustr. [COBISS.SI-ID 18083862]

1.12 Objavljeni povzetek znanstvenega prispevka na konferenci

16. HORVAT, Gabrijela, PANTIĆ, Milica, KNEZ, Željko, NOVAK, Zoran. Low-soluble drugs release from bio-aerogels. V: *16th European meeting on Supercritical fluids, EMSF 2017, 25-28 April 2017, Lisbon : [book of abstracts]*. [S. l.: s. n. 2017], str. 225. [COBISS.SI-ID 20621334]

17. HORVAT, Gabrijela, KNEZ, Željko, NOVAK, Zoran. Polysaccharide aerogels : formation, characterization and application. V: MLAKAR, Damir (ur.). *1st AARC PhD Students Conference on Environment and Sustainable Energy, November 24th - 25th 2016, Maribor, Slovenia*. Maribor: University. 2016, str. 59. [COBISS.SI-ID 20060438]

18. HORVAT, Gabrijela, KNEZ, Željko, NOVAK, Zoran. Bio-aerogels for controlled and prolonged release of low-soluble drugs. V: *Book of abstracts*, 15th European meeting on Supercritical fluids, EMSF 2016, 8-11 May 2016, Essen, Germany. [S. l.: s. n. 2016], str. 182. [COBISS.SI-ID 19914006]

19. HORVAT, Gabrijela, GRAČNAR, Maja, KNEZ, Željko, NOVAK, Zoran. Polysaccharide-silica aerogels. V: *Proceedings*, Third international seminar on aerogels, synthesis-properties-applications, 22-23 September 2016, Sophia Antipolis (France). [S. l.: ISASF. 2016], str. 78. [COBISS.SI-ID 20011286]

20. HORVAT, Gabrijela, FAJFAR, Tanja, KNEZ, Željko, NOVAK, Zoran. DSC as a tool for determination of extremely low thermal conductivities of aerogels. V: ROTARU, Andrei (ur.), CERC KOROŠEC, Romana (ur.). *Book of abstracts : CEEC-TAC3*, 3rd Central and Eastern European Conference on Thermal Analysis and Calorimetry, 25-28 August 2015, Ljubljana, Slovenia. [S. l.]: Central and Eastern European Committee for Thermal Analysis and Calorimetry. cop. 2015, str. 367. [COBISS.SI-ID 18915350]

21. HORVAT, Gabrijela, KNEZ, Željko, NOVAK, Zoran. The encapulation of pharmaceuticals into pectin aerogels for the controlles drug release. V: LAZIĆ, Miodrag (ur.). *Zbornik izvoda radova = Book of abstracts*. Leskovac: Tehnološki fakultet: = Faculty of Technology. 2015, str. 124. [COBISS.SI-ID 19212822]

MONOGRAFIJE IN DRUGA ZAKLJUČENA DELA

2.11 Diplomsko delo

22. HORVAT, Gabrijela. *Priprava pektinskih aerogelov za oralno dostavo aktivnih učinkovin : diplomsko delo univerzitetnega študijskega programa*. Maribor: [G. Tkalec], 2013. XIV, 61 f., ilustr. http://dkum.uni-mb.si/IzpisGradiva.php?id=41403. [COBISS.SI-ID 17495830]

IZVEDENA DELA (DOGODKI)

3.15 Prispevek na konferenci brez natisa

23. HORVAT, Gabrijela, KNEZ, Željko, NOVAK, Zoran. Synthesis of high-methoxyl pectin aerogels for enchancing the dissolution of low-soluble drugs : lecture at ISSF 2015, 11th International symposium on supercritical fluids, October 11-14 2015, Seoul, Korea. 2015. [COBISS.SI-ID 19086102]

SEKUNDARNO AVTORSTVO

Intervjuvanec

24. RITUPER RODEŽ, A. Nana. Znanje imamo, zdaj ga moramo še uporabiti : domači raziskovalci so dosegli pomembne uspehe, vendar je zanimanje zanje slabo, možnosti za zaposlitev pa malo. *Vestnik*, ISSN 0351-6407. [Tiskana izd.], 5. jun. 2014, let. 66, št. 23, str. 26, ilustr. [COBISS.SI-ID 17901078]

NERAZPOREJENO

25. FRAS, Maja, HORVAT, Katja, HORVAT, Gabrijela. *Ekološko pridelana hrana : raziskovalna naloga*. Ljutomer: Gimnazija Franca Miklošiča, 2006. 43 f., ilustr. [COBISS.SI-ID 7653683]

9 CURRICULUM VITAE

GABRIJELA HORVAT


Srednja Bistrica 87b, SI-9232 Črenšovci, Slovenia


gabi.tkalec@gmail.com / gabrijela.horvat@um.si


00386-31-497-123

WORKING EXPERIENCES

2014 - **Assistant**

Faculty of Chemistry and Chemical Engineering, University of Maribor

2013 - 2018 **Young researcher**

Faculty of Chemistry and Chemical Engineering, University of Maribor

2011-2013 **Vice dean for student's affairs**

Faculty of Chemistry and Chemical Engineering, University of Maribor

2009-2011 **Student tutor** (physical chemistry)

Faculty of Chemistry and Chemical Engineering, University of Maribor

EDUCATION

2013 - **PhD**

Faculty of Chemistry and Chemical Engineering, University of Maribor

2011-2012 **Measurement Science in Chemistry, Euromaster**

Measurement Science in Chemistry is a master's programme jointly delivered by a consotrium of 9 universities.

The programme offers thorough knowledge and skills in the field of basics of measurement science in chemistry (analitical chemistry). The joint programme has been awarded Euromaster quality label by the ECTN.

AWARDS

2018	L'oreal UNESCO For Women in Science Slovenia
2014	Pomurje Research Award. Best diploma thesis in 2013 in the fields of natural sciences.PIF
2013	Golden Dean's Award for the best diploma thesis in 2013 at Faculty of Chemistry and Chemical Engineering, University of Maribor
2006	*Golden Cankar's award* – highest national *award* in *Slovenian language*